MINISTRY OF EDUCATION AND RESEARCH

THE ANNALS OF "DUNAREA DE JOS" UNIVERSITY OF GALATI

Fascicle IX
METALLURGY AND MATERIALS SCIENCE

YEAR XLIV (XLIX)
September 2026, no. 3

ISSN 2668-4748; e-ISSN 2668-4756

GALATI UNIVERSITY PRESS

2026

EDITORIAL BOARD

THE ANNALS OF "DUNAREA DE JOS" UNIVERSITY OF GALATI
FASCICLE IX. METALLURGY AND MATERIALS SCIENCE
Nº. 3 - 2026, ISSN 2668-4748; e-ISSN 2668-4756
Volume DOI: https://doi.org/10.35219/mms.2026.3

Table of Contents

THE ANNALS OF "DUNAREA DE JOS" UNIVERSITY OF GALATI
FASCICLE IX. METALLURGY AND MATERIALS SCIENCE
Nº. 3 - 2026, ISSN 2668-4748; e-ISSN 2668-4756
Volume DOI: https://doi.org/10.35219/mms.2026.3

THE ANNALS OF "DUNAREA DE JOS" UNIVERSITY OF GALATI
FASCICLE IX. METALLURGY AND MATERIALS SCIENCE
N°. 3 - 2026, ISSN 2668-4748; e-ISSN 2668-4756
Article DOI: https://doi.org/10.35219/mms.2026.3.01

ASSESSMENT OF NUTRIENTS IN THE DANUBE RIVER AND THEIR IMPACT ON WATER QUALITY IN THE BRĂILA SECTOR

Nicoleta CIOBOTARU
"Dunarea de Jos" University of Galati, Faculty of Engineering and Agronomy,
Calarasi Street, 29, RO-810017, Braila, Romania
e-mail: nicoleta.ciobotaru@ugal.ro

ABSTRACT

This study analyses the water quality of the Danube River in the Brăila sector by evaluating key nutrients and relevant physicochemical parameters. The concentrations of nitrogen compounds (nitrates, nitrites, ammonium) and phosphorus compounds (phosphates) were determined, along with parameters such as pH, total dissolved solids (TDS), dissolved oxygen, and biochemical oxygen demand (BOD_5). For a more comprehensive assessment of water quality, chloride and sulphate ions were additionally analysed as indicators of mineralization and anthropogenic influences. The obtained results were compared with the reference values established by current national legislation. The analysed parameters indicate good water quality, with no major signs of organic pollution; however, the presence of nutrients may, under certain conditions, promote eutrophication processes. The findings contribute to the assessment of the ecological status of the water and highlight the importance of continuous monitoring of quality parameters in order to prevent the degradation of aquatic ecosystems and to ensure sustainable water resource management.

KEYWORDS: Danube, nutrients, nitrates, phosphates, eutrophication, water quality

1. Introduction

The Danube River has a particular importance at the European level, as it flows through numerous countries and represents a key element in regional development and biodiversity conservation. Surface water quality is an essential indicator of the health status of aquatic ecosystems, and its monitoring is necessary for the prevention and control of pollution.

Among the main parameters used in water quality assessment are nutrients, especially nitrogen and phosphorus compounds. These are essential for the growth of aquatic organisms; however, at high concentrations, they may lead to significant ecological imbalances [1]. The increase in nutrient concentrations in surface waters is frequently associated with anthropogenic activities, such as intensive agriculture and industrial activities [2].

Agricultural activities within the Danube River Basin, particularly through the use of chemical fertilizers whose components (nitrogen and phosphorus) are transported into surface waters via diffuse runoff and leaching processes, represent a major source of nutrient input. Domestic wastewater constitutes another important source of nutrients in surface waters, due to its nitrogen and phosphorus content originating from organic matter and household products, including detergents and cleaning agents. In particular, phosphates used in detergent formulations contribute to the nutrient loading of receiving waters, intensifying eutrophication processes under conditions of insufficient or inefficient urban wastewater treatment [3]. The eutrophication process is characterized by excessive growth of phytoplankton and algae, reduced water transparency, and consequently a decrease in dissolved oxygen concentration [4]. This phenomenon can have severe consequences for aquatic ecosystems, leading to the mortality of aquatic organisms and the degradation of water quality [5].

In addition, navigation along the Danube River represents another anthropogenic factor that may influence the physicochemical parameters of water. Shipping activities can locally contribute to sediment resuspension, increased turbidity, and potential inputs of pollutants (oils, hydrocarbons, residual

THE ANNALS OF "DUNAREA DE JOS" UNIVERSITY OF GALATI
FASCICLE IX. METALLURGY AND MATERIALS SCIENCE
N°. 3 - 2026, ISSN 2668-4748; e-ISSN 2668-4756
Article DOI: https://doi.org/10.35219/mms.2026.3.01

compounds), which may cause localized changes in ion concentrations and water quality indicators, particularly in areas with intense river traffic [6].

Throughout its European course, the Danube River flows through numerous countries and capital cities, progressively accumulating various natural and anthropogenic loads from the river basins it traverses. Although rivers exhibit a natural self-purification capacity through physical, chemical, and biological processes, these do not lead to a complete reduction of the pollutant load [7].

Consequently, the Danube River is subjected to significant pressures generated by human activities within its extensive catchment area, which includes agricultural, urban, and industrial regions. Monitoring these quality indicators is essential for assessing the ecological status of water and for implementing appropriate management measures.

The aim of the present study is to evaluate the nutrient levels in the Danube River, in the Brăila sector, by determining the main nitrogen compounds (nitrates, nitrites, ammonium) and phosphorus compounds (phosphates), as well as analysing their impact on water quality. The obtained results are interpreted in relation to the limits established by the current legislation, in order to determine the water quality status and to identify potential sources of pollution. This analysis aims to highlight the importance of nutrient monitoring in surface waters and to contribute to a better understanding of the processes influencing water quality in the Danube River.

2. Materials and methods

2.1. Study area

Throughout its European course, the Danube River flows through numerous countries and capital cities, progressively accumulating various natural and anthropogenic loads from the river basins it traverses. Located near its discharge into the Black Sea, the lower sector represents a final stage of integration and transformation of the river's water composition [8].

In the Brăila sector, the Danube River forms a complex fluvial ecosystem, characterized by a wide floodplain, secondary channels, and wetlands with high biodiversity.

In this region, the river significantly influences sediment dynamics and the local hydrological regime, playing an essential role in landscape formation. At the same time, the river sector in the Brăila area is of both ecological and socio-economic importance, being used for water supply, fishing, and adjacent agricultural activities.

2.2. Sampling

Water samples were collected from a representative point of the Danube River, located near the riverbank, in a sector with moderate anthropogenic influence, namely the riverside promenade area (Figure 1). Sampling was carried out in spring, during the month of May, and the water temperature at the time of collection was 16 °C.

The samples were collected in clean glass containers, previously rinsed with water from the sampling site to avoid contamination. The samples were transported under controlled conditions and analysed as soon as possible in order to minimize physicochemical changes.

Fig. 1. *Sampling area* [9]

2.3. Analytical parameters

Within the study, a set of parameters was determined in order to assess both the eutrophication status of the water and its overall physicochemical quality.

The experimental determinations were carried out using standard laboratory methods, as follows:

- pH was determined using the potentiometric method;
- total dissolved solids (TDS) were determined using the conductometric method;
- dissolved oxygen was determined using the Winkler method;
- biochemical oxygen demand (BOD_5) was determined by incubation at 20 °C for 5 days;

THE ANNALS OF "DUNAREA DE JOS" UNIVERSITY OF GALATI
FASCICLE IX. METALLURGY AND MATERIALS SCIENCE
N°. 3 - 2026, ISSN 2668-4748; e-ISSN 2668-4756
Article DOI: https://doi.org/10.35219/mms.2026.3.01

- nitrates, nitrites, ammonium, phosphates, chlorides, and sulphates were determined spectrophotometrically.

2.4. Results interpretation

The obtained results were interpreted in accordance with the provisions of Order 161/2006, which establishes the classification of surface waters into five quality classes based on physicochemical and biological parameter values.

The classification of each parameter was carried out by comparing the experimental values with the corresponding limits of the quality classes presented in Table 1, in order to assess the ecological status of the water (Class I represents the highest quality and Class V the lowest quality).

Table 1. *Permitted quality classes for surface waters (mg/L)* [10]

Indicator	Class I	Class II	Class III	Class IV	Class V
pH	6.5–8.5	6.0–9.0	5.5–9.5	5.0–10.0	<5 or >10
Dissolved oxygen	≥ 9	≥ 7	≥ 5	≥ 4	< 4
BOD_5	≤ 3	≤ 5	≤ 7	≤ 20	> 20
Nitrates (NO_3^-–N)	≤ 1.0	≤ 3.0	≤ 5.6	≤ 11.2	> 11.2
Nitrites (NO_2^-–N)	≤ 0.01	≤ 0.03	≤ 0.06	≤ 0.30	> 0.30
Ammonium (NH_4^+–N)	≤ 0.40	≤ 0.80	≤ 1.20	≤ 3.2	> 3.2
Phosphates (PO_4^{3-}–P)	≤ 0.10	≤ 0.20	≤ 0.40	≤ 0.90	> 0.90
Chlorides (Cl^-)	≤ 25	≤ 50	≤ 250	≤ 300	> 300
Sulfates (SO_4^{2-})	≤ 60	≤ 120	≤ 250	≤ 300	> 300
Total dissolved solids (TDS)	≤ 500	≤ 750	≤ 1000	≤ 1500	> 1500

3. Results and Discussion

The results of the performed analyses are presented in Table 2, both for the physicochemical parameters and for the nutrients in the sampled Danube water.

Table 2. *Variation of the studied water quality indicators in the Danube River (mg/L)*

Indicator	Obtained values
pH	7.21
Dissolved oxygen	12.8
BOD_5	2.8
Nitrates (NO_3^-–N)	1.67
Nitrites (NO_2^-–N)	0.02
Ammonium (NH_4^+–N)	1.25
Phosphates (PO_4^{3-}–P)	0.2
Chlorides (Cl^-)	38
Sulfates (SO_4^{2-})	20
Total dissolved solids (TDS)	332

3.1. Physicochemical parameters

The results obtained from the physicochemical analyses of the Danube River water in the Brăila sector revealed variations in the main investigated parameters. The measured pH value was 7.21, indicating a slightly alkaline reaction, characteristic of natural surface waters [11]. This range falls within the permissible limits for good-quality waters according to Order 161/2006 (6.5-8.5), suggesting the absence of significant acidification or excessive alkalinization processes (Figure 2).

The total dissolved solids (TDS) concentration was 332 mg/L, indicating a moderate level of water mineralization (Figure 3). This value is below the 500 mg/L threshold specific to very good and good-quality waters, suggesting a limited anthropogenic influence on the ionic composition of the water in the studied sector [12].

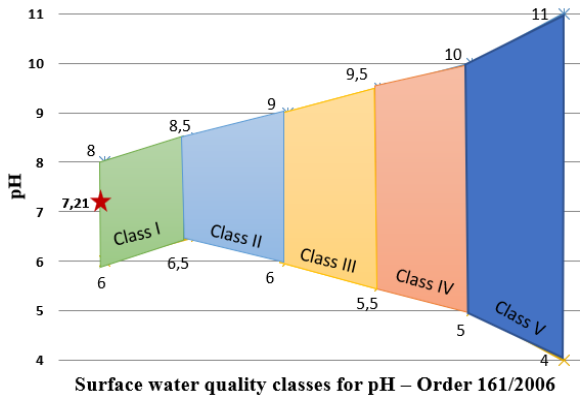

Fig. 2. *The pH concentration in relation to the permissible limits*

THE ANNALS OF "DUNAREA DE JOS" UNIVERSITY OF GALATI
FASCICLE IX. METALLURGY AND MATERIALS SCIENCE
Nº. 3 - 2026, ISSN 2668-4748; e-ISSN 2668-4756
Article DOI: https://doi.org/10.35219/mms.2026.3.01

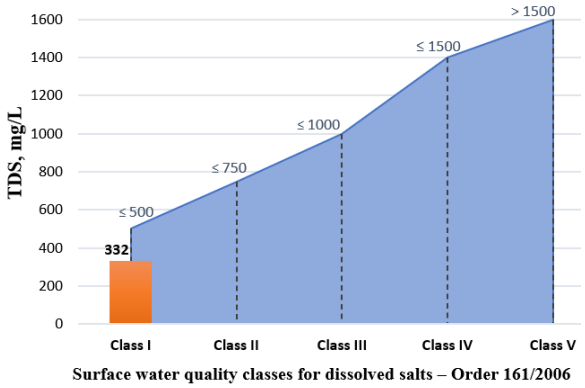

Fig. 3. *The TDS concentration in relation to the permissible limits*

At a water temperature of approximately 16 °C, the solubility of oxygen in water is relatively high (around 9-10 mg/L at saturation); however, the measured value (12.8 mg/L) indicates oxygen supersaturation of the water (Figure 4). This phenomenon is commonly observed in the spring season and may be associated both with intense phytoplanktonic and macrophyte photosynthesis processes and with enhanced aeration due to the hydrodynamic regime (increased discharge, turbulence) [13]. The high level of dissolved oxygen reflects good oxygenation conditions and favourable environments for aquatic organisms, suggesting the absence of significant excessive biological oxygen consumption processes [14].

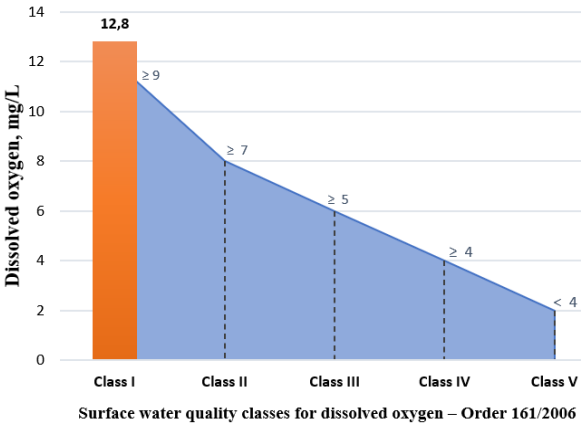

Fig. 4. *Dissolved oxygen concentration in relation to the permissible limits*

The 5-day biochemical oxygen demand value falls within the range characteristic of surface waters with low levels of biodegradable organic matter (Figure 5). At a temperature of 16 °C, microbiological activity is moderate, and the relatively low BOD_5 value indicates that biological degradation processes do not exert significant pressure on the dissolved oxygen reservoir [15]. Correlated with the high dissolved oxygen concentration, this confirms good water quality in terms of organic pollution and a favourable balance between oxygen production and consumption [16].

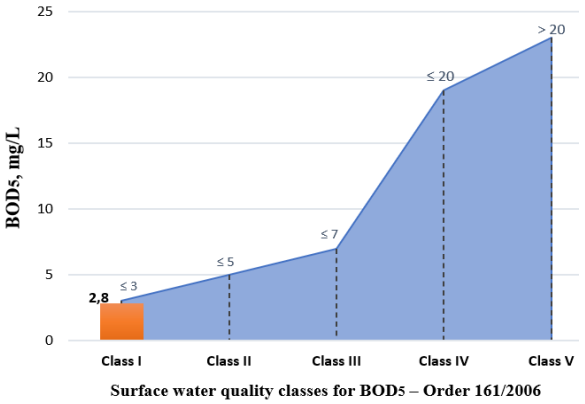

Fig. 5. *BOD_5 concentration in relation to the permissible limits*

The chloride concentration, shown in Fig. 6, falls within the typical range for surface waters in the lower sector of the Danube River, reflecting mainly a natural mineral background, to which moderate anthropogenic contributions may be added (urban wastewater, runoff from anthropized surfaces) [16]. At relatively high discharges, characteristic of May, dilution processes limit the excessive accumulation of this ion; thus, the measured value does not indicate significant pollution pressure.

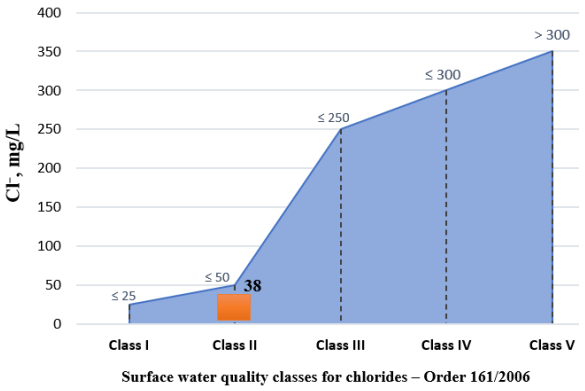

Fig. 6. *Chlorides concentration in relation to the permissible limits*

The low sulphate concentration suggests a limited influence of industrial pollution sources or inputs derived from intense mineralization processes. Under the hydrological conditions specific to spring (increased discharge, precipitation input), low values can also be explained by the dilution effect [11].

THE ANNALS OF "DUNAREA DE JOS" UNIVERSITY OF GALATI
FASCICLE IX. METALLURGY AND MATERIALS SCIENCE
N°. 3 - 2026, ISSN 2668-4748; e-ISSN 2668-4756
Article DOI: https://doi.org/10.35219/mms.2026.3.01

From a qualitative perspective, this level is characteristic of good-quality waters and indicates the absence of major sources of sulphur compound contamination (Figure 7).

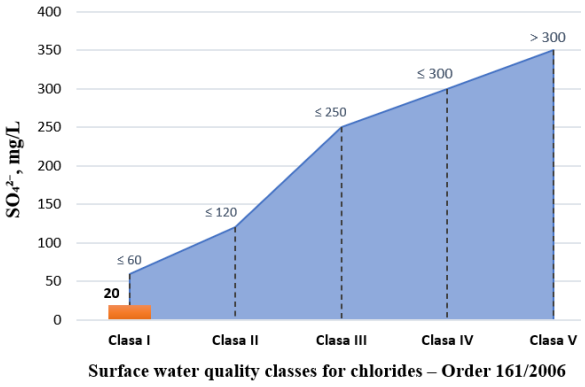

Fig. 7. *Sulphates concentration in relation to the permissible limits*

The overall set of analysed parameters indicates well-oxygenated water, with low organic loading and moderate mineralization, characteristic of spring conditions in the lower sector of the Danube River. The correlation between oxygen supersaturation and low BOD_5 values suggests the predominance of primary production processes over biological consumption processes, while the low concentrations of the analysed ions indicate a limited anthropogenic influence during the sampling period.

3.2. Nutrient analysis

With regard to nitrogen compounds (Figure 8), the nitrate concentration ($N–NO_3^-$ = 1.67 mg/L) falls within the range characteristic of good-quality surface waters, indicating a moderate presence of nutrients mainly originating from diffuse catchment activities, such as the use of nitrogen-based fertilizers in agriculture. This value reflects nitrogen mineralization and oxidation processes without suggesting severe contamination; however, it still highlights a basin-scale anthropogenic influence [17]. The obtained result for nitrate nitrogen corresponds to Class II surface water quality [10].

The ammonium nitrogen concentration ($N–NH_4^+$ = 1.25 mg/L) indicates the presence of recent organic matter in the aquatic system, being a sensitive indicator of inputs from domestic wastewater or biological decomposition processes (Figure 9). At this level, ammonium nitrogen suggests a moderate anthropogenic influence, but not of high intensity, particularly under well-oxygenated water conditions that favour its transformation into oxidized forms (nitrites and nitrates). The obtained value falls within Class III water quality according to the official classification [10]. This result may indicate inputs of decomposing organic matter or the influence of insufficiently treated wastewater, representing a sensitive indicator of recent organic pollution [18].

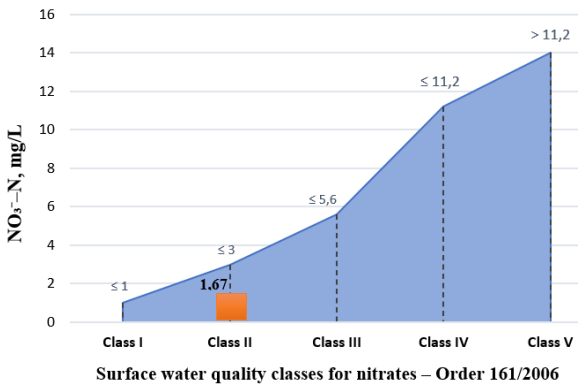

Fig. 8. *Nitrates concentration in relation to the permissible limits*

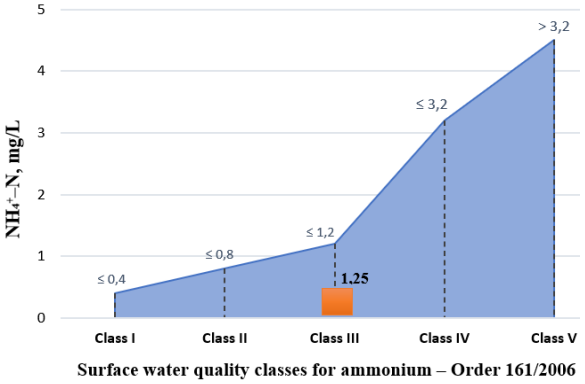

Fig. 9. *Ammonium concentration in relation to the permissible limits*

The nitrite concentration ($N–NO_2^-$) was 0.02 mg/L, a low value characteristic of well-oxygenated surface waters (Figure 10). From a water quality classification perspective, this concentration falls within Class II according to Order 161/2006. The low nitrite level indicates efficient oxidation of intermediate nitrogen compounds towards more stable forms (nitrates), a process favoured by the observed aerobic conditions and the high dissolved oxygen concentration [12]. Thus, the obtained values suggest reduced recent sources of organic pollution and a rapid transformation of nitrogen species within the aquatic system. The phosphate concentration (PO_4^{3-}) was 0.2 mg/L (Figure 11), a value corresponding to Class II water quality according to Order 161/2006.

This concentration may reflect a moderate influence of anthropogenic sources, such as domestic wastewater or diffuse agricultural runoff, as phosphates are commonly associated with detergents

THE ANNALS OF "DUNAREA DE JOS" UNIVERSITY OF GALATI
FASCICLE IX. METALLURGY AND MATERIALS SCIENCE
N°. 3 - 2026, ISSN 2668-4748; e-ISSN 2668-4756
Article DOI: https://doi.org/10.35219/mms.2026.3.01

and fertilizers [19]. Although the value does not indicate severe pollution, the presence of this nutrient above natural background levels may contribute, under favourable conditions, to the intensification of eutrophication processes, particularly during periods of elevated temperatures and reduced water flow.

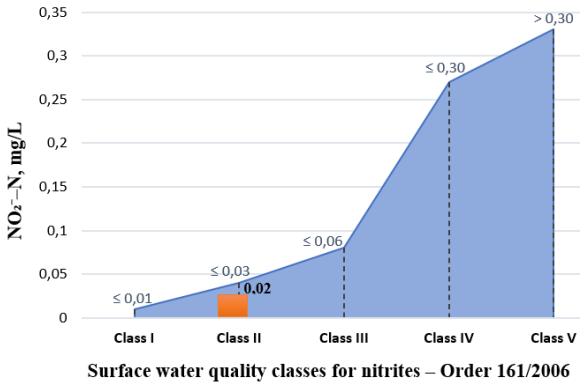

Fig. 10. *Nitrites concentration in relation to the permissible limits*

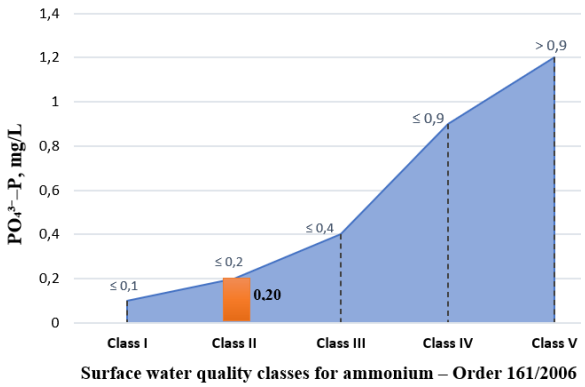

Fig. 11. *Phosphates concentration in relation to the permissible limits*

An important aspect is the existence of a wastewater treatment plant serving the municipality, which significantly contributes to the reduction of organic and nutrient loads discharged into the receiving water body. The obtained results suggest that the efficiency of the treatment processes, combined with the dilution and self-purification capacity of the Danube River, ensures the maintenance of a good ecological status in the studied sector, with no indications of advanced eutrophication or significant water quality degradation in the analysed area [20].

However, downstream of the municipality of Brăila and other urban settlements in the lower sector, the river flows in proximity to the Great Island of Brăila, an area of intensive agricultural use that contributes substantially to diffuse nutrient loading (nitrogen and phosphorus) through fertilizer application. In the context of continuous river transport, these inputs accumulate and are further transferred towards the coastal zone of the Black Sea [21].

Under favourable summer conditions (high temperature, intense solar radiation, and thermal stratification), accumulated nutrients may support intensive phytoplankton development and the occurrence of algal blooms, a phenomenon associated with riverine eutrophication [19].

Excessive and uncontrolled proliferation of marine algae has devastating effects on the environment: it leads to changes in the structure of marine animal populations, the occurrence of algal accumulations along the shoreline, and massive oxygen depletion in water, which can result in the suffocation of benthic organisms [4].

Overall, the correlation of all analysed parameters indicates water of good ecological status, characterized by moderate mineralization, high oxygenation, and low organic loading. Nutrient values suggest a present but limited anthropogenic influence, typical for a downstream river sector where dilution, transformation, and self-purification processes contribute to maintaining a relatively stable chemical balance. These results are consistent with the natural dynamics of the Danube River in its lower sector, where the river integrates inputs from the entire catchment area while still maintaining a significant capacity to attenuate pollution.

The interpretation of the results highlights the need for continuous monitoring of nutrients in the Danube River, especially in sectors influenced by agricultural and urban activities, in order to prevent the deterioration of water ecological quality.

4. Conclusions

Based on the results obtained within the study, the following conclusions regarding water quality in the Danube River in the Brăila sector can be formulated:

• The analysis of physicochemical parameters indicates an overall good water status, characterized by slightly alkaline pH (7.21) and a moderate level of mineralization (TDS = 332 mg/L), values falling within the range specific to very good-quality natural surface waters according to Order 161/2006. These results suggest the absence of significant chemical degradation processes and a relatively low anthropogenic influence on ionic composition.

• The oxygen regime indicates well-oxygenated water, with high dissolved oxygen concentrations (12.8 mg/L) and low biochemical oxygen demand (2.8 mg/L), suggesting reduced organic loading and a good self-purification capacity of the fluvial system under the analysed conditions (water temperature of

16 °C, May). This balance reflects favourable hydrodynamic conditions and controlled biological activity.

• The low concentrations of nitrites and sulphates, as well as the moderate level of chlorides, confirm the absence of major point-source pollution, while the phosphate concentration (0.2 mg/L) indicates a moderate anthropogenic influence, mainly associated with diffuse inputs.

Overall, the study highlights that the Brăila sector of the Danube River exhibits adequate water quality, locally influenced by anthropogenic activities but mitigated by natural transformation processes and the existing wastewater treatment infrastructure.

References

[1]. Carpenter S. R., *et al.*, *Nonpoint pollution of surface waters with phosphorus and nitrogen*, Ecological Applications, 8(3), p. 559-568, 1998.
[2]. Perera M. K., *et. al.*, *Technologies for recovering nutrients from wastewater: A critical review*, Environmental Engineering Science, 36(5), p. 558-574, 2019.
[3]. Correll D. L., *The role of phosphorus in the eutrophication of receiving waters: A review*, Journal of Environmental Quality, 27(2), p. 261-266, 1998.
[4]. Diaz R. J., Rosenberg R., *Spreading dead zones and consequences for marine ecosystems*, Science, 321(5891), p. 926-929, 2008.
[5]. Smith V. H., Tilman G. D., Nekola J. C., *Eutrophication: impacts of excess nutrient inputs on freshwater, marine, and terrestrial ecosystems*, Environmental Pollution, 100(1-3), p. 179-196, 1999.
[6]. Schipper M., *et al.*, *River traffic and its impact on water quality in large European rivers*, Science of the Total Environment, 758, p. 143-152, 2021.
[7]. Schiller D., *et al.*, *Rivers as bioreactors: nutrient retention and transformation in fluvial systems*, Freshwater Biology, 56(12), p. 2302-2320, 2011.
[8]. Billen G., *et al.*, *Modelling the transfer and retention of nutrients in the drainage network of the Danube River*, Estuarine, Coastal Shelf Science, 54(3), p. 285-308, 2002.
[9]. ***, *Braila City Map*, https://braila-city.map2web.eu/?mtk=1&location= 3113310,5665060,13.
[10]. ***, *Ordinul 161/2006, privind clasificarea calității apelor de suprafață în România și stabilirea normelor pentru evaluarea stării ecologice a corpurilor de apă*.
[11]. Stumm W., Morgan J. J., *Aquatic Chemistry: Chemical Equilibria and Rates in Natural Waters*, 3rd ed., Wiley, 1996.
[12]. Wetzel R. G., *Limnology: Lake and River Ecosystems*, 3rd ed., Academic Press, 2001.
[13]. Calmuc M., *et al.*, *Assessment of nutrients and oxygen regime in the Lower Danube water*, Annals of "Dunărea de Jos" University of Galați, 43(1), p. 68-74, 2020.
[14]. Chapra S. C., *Surface Water-Quality Modeling*, Waveland Press, 2008.
[15]. Metcalf & Eddy, *Wastewater Engineering: Treatment and Resource Recovery*, 5th ed., McGraw-Hill, 2014.
[16]. Griga M., *Evaluation of chemical indicators of anthropogenic influence in the lower Danube basin*, Hydrology, Hydrochemistry and Hydroecology, 1(71), p. 74-84, 2024.
[17]. Halder J., *et al.*, *Nitrate sources and mixing in the Danube watershed*, Scientific Reports, 12, 2150, 2022.
[18]. Tran Y. B., *et al.*, *Predicting high-frequency nutrient dynamics in the Danube River*, Frontiers in Water, 4:894548, 2022.
[19]. Seitzinger S., *et al.*, *Global River nutrient export and eutrophication trends*, Global Biogeochemical Cycles, 24(4), 2020.
[20]. Kirschner A., *et al.*, *Long-term impact of wastewater management on the Danube River*, Environmental Science and Pollution Research, 31, p. 45697-45710, 2024.
[21]. Garnier J., *et al.*, *Biogeochemical transformations of inorganic nutrients in the mixing zone between the Danube River and the north-western Black Sea*, Estuarine, Coastal and Shelf Science, 54(3), p. 321-336, 2002.

THE ANNALS OF "DUNAREA DE JOS" UNIVERSITY OF GALATI
FASCICLE IX. METALLURGY AND MATERIALS SCIENCE
N°. 3 - 2026, ISSN 2668-4748; e-ISSN 2668-4756
Article DOI: https://doi.org/10.35219/mms.2026.3.02

CAD/CAE WORKFLOW FOR THE TOPOLOGY OPTIMIZATION AND GEOMETRIC RECONSTRUCTION OF A STRUCTURAL COMPONENT

Florin-Bogdan MARIN, Mihaela MARIN
"Dunarea de Jos" University of Galati, Romania,
Interdisciplinary Research Centre in the Field of Eco-Nano Technology and Advanced Materials CC-ITI,
Faculty of Engineering, "Dunarea de Jos" University of Galati, Romania, 47 Domnească Street, RO-800008, Galaţi, Romania
e-mail: flmarin@ugal.ro

ABSTRACT

This paper presents a study on the topological optimization of a structural component and the conversion of the optimized result into a manufacturable geometric model. The initial model was developed in a CAD environment and imported into the finite element analysis software, where boundary conditions and loading constraints were applied. The optimization process aimed to minimize structural compliance while reducing material usage and maintaining adequate stiffness. Different volume fractions and design parameters were investigated to identify a suitable optimized configuration. The obtained topology optimization results were analysed in terms of structural continuity, manufacturability, and clarity of the load-bearing features. Since the raw optimized geometry often contains irregular surfaces and complex shapes that are difficult to manufacture directly, the result was further reconstructed using NURBS and PolyNURBS modelling techniques. This stage allowed the creation of a smoother, continuous, and closed geometric model suitable for further analysis and production. Lattice structures are also integrated inside the reconstructed model to reduce mass while maintaining mechanical performance. The proposed workflow shows how CAD/CAE tools can transform an optimized conceptual design into a manufacturable structural component. The results emphasize the importance of post-processing, geometric reconstruction, and manufacturability checks in topology optimization.

KEYWORDS: topology optimization, PolyNURBS, lattice structure, CAD/CAE

1. Introduction

The development of lightweight, efficient and manufacturable structural components represents an important objective in modern mechanical engineering. In fields such as automotive engineering, aerospace, robotics and additive manufacturing, structural components must meet increasingly complex requirements regarding stiffness, strength, mass reduction and technological feasibility. Conventional design methods are usually based on the gradual modification of an initial geometry, which may limit the possibility of obtaining an efficient material distribution. In contrast, topology optimization provides a numerical design method that determines the most effective distribution of material within a predefined design domain, according to the applied loads, boundary conditions and design constraints [1-2].

Topology optimization has become strongly connected with additive manufacturing, which allows complex and lightweight geometries to be fabricated more easily than by conventional manufacturing. The integration of topology optimization and additive manufacturing can lead to improved stiffness-to-weight ratios, reduced material consumption and increased design freedom [2-4]. However, raw optimization outputs may contain irregular surfaces, discontinuities, thin members or geometrical details that are difficult to manufacture directly. Therefore,

THE ANNALS OF "DUNAREA DE JOS" UNIVERSITY OF GALATI
FASCICLE IX. METALLURGY AND MATERIALS SCIENCE
N°. 3 - 2026, ISSN 2668-4748; e-ISSN 2668-4756
Article DOI: https://doi.org/10.35219/mms.2026.3.02

manufacturability constraints, minimum feature size control and post-processing operations are essential for transforming numerical optimization results into practical engineering components [5-7].

The integration of manufacturing constraints into topology optimization has been widely investigated. Mhapsekar *et al.* [5] proposed additive manufacturing constraints in topology optimization to improve manufacturability, especially by reducing support-related limitations. Other studies have considered overhang constraints, build direction limitations, distortion control and process-related restrictions to obtain designs that are more suitable for additive manufacturing [6, 7]. Another important aspect is the conversion of the optimized topology into a clean and manufacturable CAD model. Reconstruction methods, including feature-based approaches, NURBS-based modelling and automated CAD reconstruction, can generate smoother and editable models suitable for further analysis and manufacturing [8-10]. NURBS and PolyNURBS modelling techniques are relevant because they allow rough topology-optimized geometries to be converted into smoother closed CAD models while preserving the main structural load paths.

Lattice structures represent another important direction in lightweight structural design. Due to their cellular architecture, lattice structures can reduce mass while maintaining or improving mechanical performance, especially when combined with additive manufacturing technologies [11-15]. In topology-optimized components, internal lattice structures can be introduced to further reduce mass while preserving the main load-bearing regions of the optimized geometry.

The main objective of this paper is to demonstrate how CAD/CAE tools can be combined to transform a topology-optimized conceptual design into a practical, continuous and manufacturable structural component.

2. Experimental procedure

The experimental research was carried out to define a CAD/CAE workflow for the topology optimization of a structural component and for the reconstruction of the optimized result into a manufacturable geometric model. The workflow included finite element analysis, topology optimization, NURBS/PolyNURBS reconstruction and lattice structure generation. The initial component was designed in a CAD environment and imported into the finite element analysis software. The geometry was checked before analysis to ensure proper meshing. The component was fixed at the cylindrical mounting interface, while a vertical force corresponding to a mass of 7.70 kg, approximately 75.5 N, was applied to the free region of the model. The initial finite element analysis was used to determine the displacement and von Mises stress distributions. These results allowed the identification of the main deformation zones, stress concentration regions and load transfer paths. They were then used as a reference for defining and interpreting the topology optimization process.

Topology optimization was performed using a density-based method, with the objective of minimizing compliance and increasing structural stiffness. Several volume fractions were investigated to identify a suitable compromise between material reduction, structural continuity and manufacturability. Based on the comparison of the investigated volume fractions, the 40% volume fraction was selected for further reconstruction because it provided clearer and more continuous load-bearing paths.

The optimized geometry selected from the volume-fraction comparison was imported as an STL model and used as a reference for CAD reconstruction. NURBS and PolyNURBS tools were applied to rebuild the main structural surfaces, smooth the geometry and obtain a closed solid model. The cylindrical mounting interface was preserved as a functional region and integrated into the reconstructed body.

After reconstruction, an internal tetrahedral lattice structure was generated to further reduce mass while maintaining adequate stiffness. The lattice members were assigned a uniform thickness of 1.5 mm, selected as a compromise between manufacturability, stiffness and lightweight design.

3. Results and discussion

The results obtained in this study are grouped into four main stages: the initial finite element analysis, the topology optimization results, the reconstruction of the optimized geometry, and the generation of the internal lattice structure.

The initial finite element analysis was performed to evaluate the structural response of the original component before topology optimization. A vertical force corresponding to a mass of 7.70 kg, approximately 75.5 N, was applied to the model. The analysis focused mainly on the displacement distribution and the von Mises stress distribution, because these results indicate the critical regions and the main load transfer paths. The displacement results show that the highest deformation appears in the regions located farther from the fixed support. This behaviour is expected, since the fixed mounting area restricts movement, while the free regions of the structure are more affected by the applied vertical load. The stress distribution indicates the zones where the material is more intensively loaded and therefore

THE ANNALS OF "DUNAREA DE JOS" UNIVERSITY OF GALATI
FASCICLE IX. METALLURGY AND MATERIALS SCIENCE
Nº. 3 - 2026, ISSN 2668-4748; e-ISSN 2668-4756
Article DOI: https://doi.org/10.35219/mms.2026.3.02

must be preserved during the optimization process. These results were used as a basis for defining the topology optimization problem and for interpreting the optimized material distribution. Figure 1 shows the displacement distribution of the initial component under the applied vertical load. The figure is included to identify the regions with the highest deformation before topology optimization. Figure 2 shows the von Mises stress distribution of the initial component. This result is important because it identifies the highly stressed regions that must be preserved during the topology optimization process.

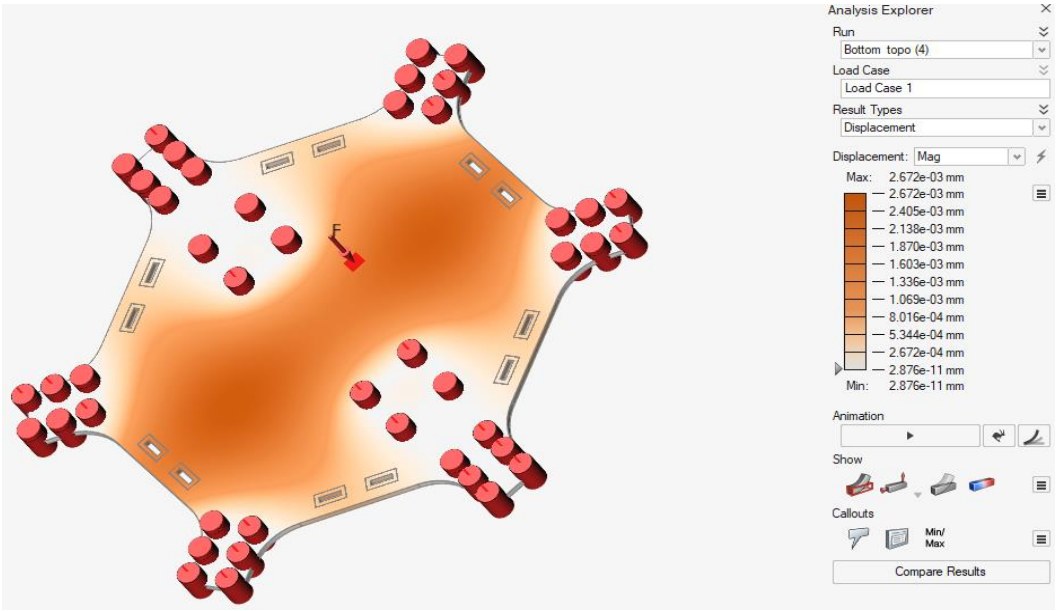

Fig. 1. *The displacement distribution of the initial component*

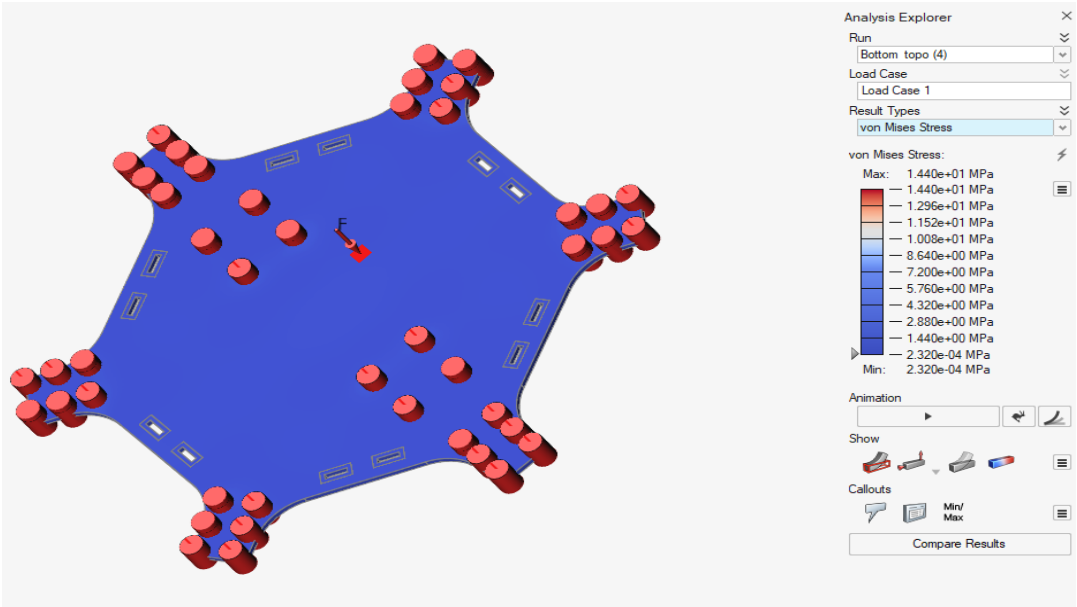

Fig. 2. *Von Mises stress distribution of the initial component*

The topology optimization results indicate that material is mainly retained along the principal load paths between the applied load region and the fixed mounting interface.

Low-density regions indicate material that can be removed without significantly affecting the global stiffness of the component. However, not all optimized configurations are suitable for manufacturing. Some volume fractions produced

THE ANNALS OF "DUNAREA DE JOS" UNIVERSITY OF GALATI
FASCICLE IX. METALLURGY AND MATERIALS SCIENCE
Nº. 3 - 2026, ISSN 2668-4748; e-ISSN 2668-4756
Article DOI: https://doi.org/10.35219/mms.2026.3.02

discontinuous or poorly defined structural members, which could not be directly converted into a reliable CAD model.

The results obtained for lower volume fractions showed a higher level of material reduction, but also a greater risk of discontinuities and weak structural regions. In contrast, higher volume fractions produced more continuous geometries, but with a smaller mass reduction.

Therefore, the selection of the final topology was based not only on material saving, but also on the clarity of the structural members and the possibility of reconstructing the geometry into a manufacturable model. Figure 3 compares two topology optimization results obtained for different volume fractions. The comparison shows that the 40% volume fraction provides clearer and more continuous structural members than the 20% volume fraction, which is more prone to discontinuities.

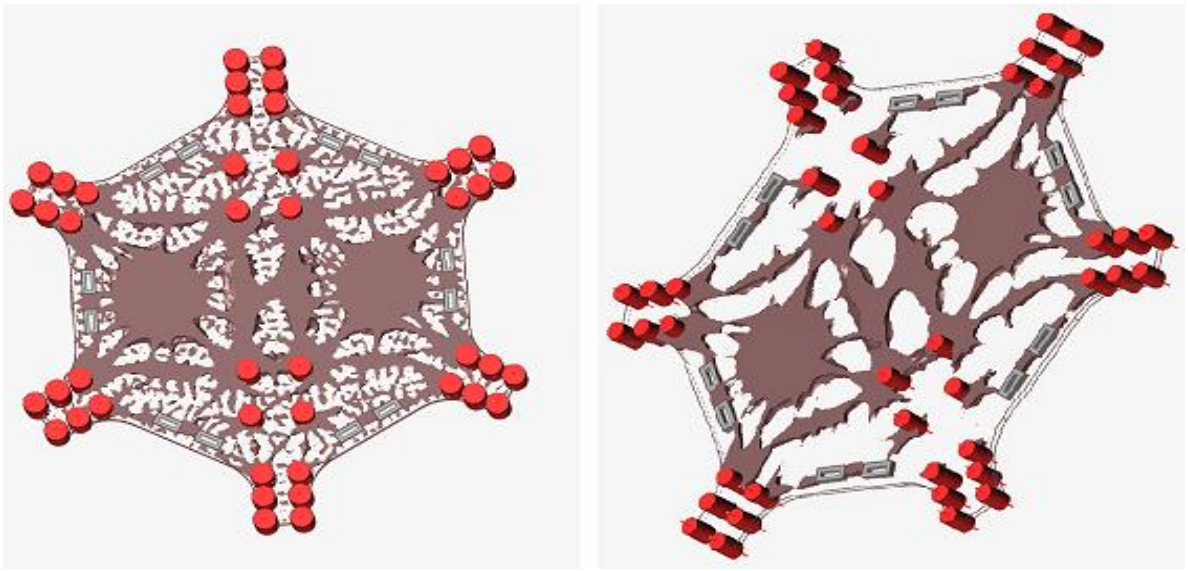

a b

Fig. 3. *Comparison of topology optimization results for different volume fractions: (a) 40% VF and (b) 20% VF*

The optimized geometry was selected by considering three main criteria: structural continuity, manufacturability, and preservation of the main load-bearing paths. The selected topology presents a continuous material distribution and clearly defined structural members. The density distribution indicates that the optimized shape follows the main force transmission directions. This confirms that the optimization process successfully identified the regions where material contributes most effectively to stiffness. The surface of the optimized STL model was rough and contained irregular features. For this reason, the optimized result was used as a design guide for the reconstruction stage rather than as a directly manufacturable part.

The reconstruction stage was necessary to transform the rough topology optimization result into a smooth and closed CAD geometry. The optimized STL model was imported into the modeling environment, where NURBS and PolyNURBS tools were used to create a manufacturable free-form shape. The reconstruction began by creating sections through the optimized model. These sections were used as references for generating NURBS surfaces along the main structural paths. Since the model was symmetrical, only half of the geometry was initially reconstructed. This reduced modelling time and allowed better control of the central region. The half-model was then mirrored, and the coincident vertices were welded to obtain a continuous geometry.

Figure 4 presents the reconstructed PolyNURBS model obtained after smoothing and correction operations. The figure is used to demonstrate that the rough topology optimization result was converted into a continuous and closed manufacturable geometry.

During reconstruction, several geometric issues were observed, including overlapping faces, hidden surfaces, non-welded vertices, and local discontinuities. These defects were corrected by editing vertices, edges, and faces, since a non-closed model cannot be reliably used for additive manufacturing or further finite element analysis. The cylindrical mounting interface was reconstructed separately using a PolyDisk feature and then integrated into the main body to obtain a continuous

THE ANNALS OF "DUNAREA DE JOS" UNIVERSITY OF GALATI
FASCICLE IX. METALLURGY AND MATERIALS SCIENCE
No. 3 - 2026, ISSN 2668-4748; e-ISSN 2668-4756
Article DOI: https://doi.org/10.35219/mms.2026.3.02

transition between the functional region and the optimized structure.

The final PolyNURBS model was checked using tolerance verification tools to ensure that the reconstructed geometry represented a closed solid. One of the main difficulties encountered during reconstruction was the integration of the cylindrical mounting interface with the optimized design region. The original topology result did not provide a clean transition between the structural body and the mounting cylinder. Therefore, the cylindrical region was reconstructed separately using a PolyDisk feature. The PolyDisk was extruded to the required length and then combined with the main reconstructed body. Several faces were removed, and the remaining edges were connected manually to create a continuous transition. This operation was necessary because the mounting interface is a functional region and must be preserved in the final geometry. The successful integration of the mounting interface is important because discontinuities in this region could generate stress concentrations or manufacturing problems. A single continuous body is preferable to the simple combination of separate design and non-design regions, because the connection zones may otherwise become mechanically weak. After obtaining the closed PolyNURBS geometry, the model was prepared for lattice structure generation. The purpose of the lattice structure was to reduce the mass of the component while maintaining adequate stiffness. The reconstructed geometry was imported as an STL file, and a surface mesh was generated.

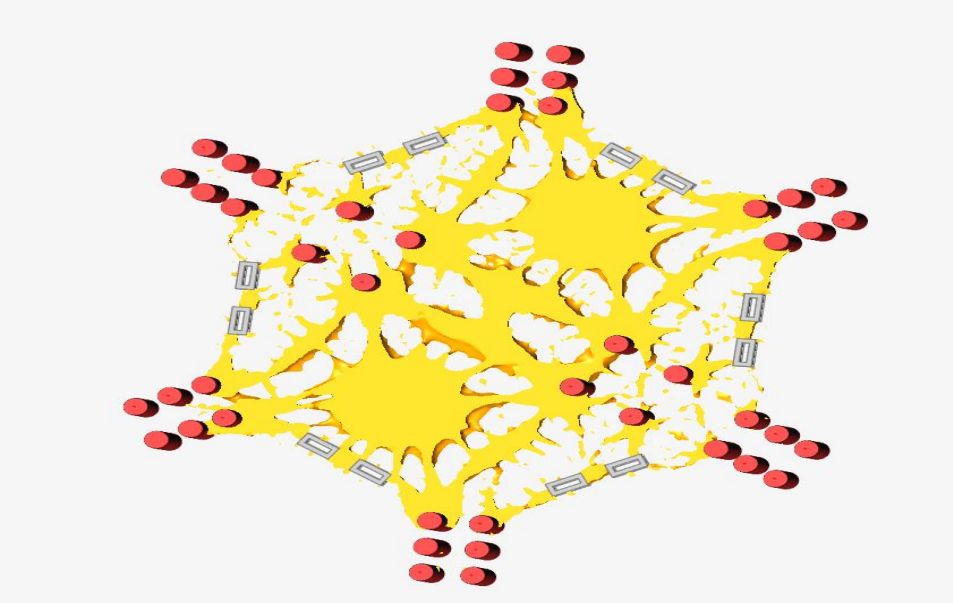

Fig. 4. *Reconstructed PolyNURBS model obtained after smoothing and correction operations*

Before lattice generation, the reconstructed geometry was meshed and remeshed to improve the regularity of the internal lattice. Mesh quality was important because an irregular surface mesh could lead to non-uniform lattice distribution. A tetrahedral lattice structure was selected because it provides good stiffness and is suitable for internal reinforcement. The lattice rule was defined and then applied inside the reconstructed geometry. The internal volume lattice was adjusted so that the members remained inside the component boundary. The lattice members were assigned a uniform thickness of 1.5 mm. This value was chosen to obtain a balance between manufacturability, stiffness and mass reduction. The final lattice-reinforced model was exported for further analysis. Figure 5 presents a detail of the final lattice-reinforced component obtained after applying the tetrahedral lattice inside the reconstructed geometry. This figure highlights the internal lightweight structure prepared for further analysis or additive manufacturing.

The obtained results show that topology optimization is an efficient method for identifying the main load-bearing regions of a structural component. The NURBS/PolyNURBS reconstruction stage proved to be essential for converting the optimized concept into a smooth and manufacturable model. This stage allowed the preservation of the main structural load paths while eliminating surface irregularities and geometric errors. The final reconstructed geometry was more suitable for finite element analysis, STL export and additive manufacturing preparation.

THE ANNALS OF "DUNAREA DE JOS" UNIVERSITY OF GALATI
FASCICLE IX. METALLURGY AND MATERIALS SCIENCE
No. 3 - 2026, ISSN 2668-4748; e-ISSN 2668-4756
Article DOI: https://doi.org/10.35219/mms.2026.3.02

The integration of lattice structures further improved the lightweight design concept. By replacing part of the internal volume with a

tetrahedral lattice, the component can achieve additional mass reduction while maintaining internal support. Nevertheless, the lattice generation process depends strongly on mesh quality. A non-uniform surface mesh can lead to irregular lattice distribution, while excessive remeshing may alter the external geometry. Therefore, mesh control is an important factor in obtaining reliable lattice-reinforced components.

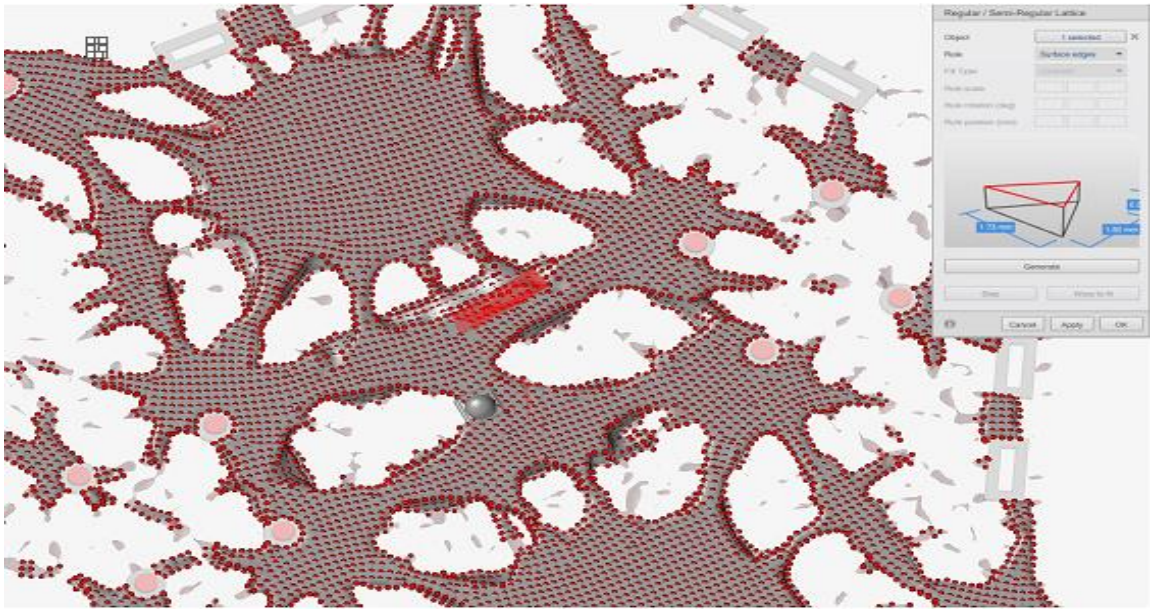

Fig. 5. *Detail of the final reconstructed component with internal tetrahedral lattice structure*

The proposed CAD/CAE workflow transforms a numerical optimization result into a practical structural component that can be further analysed or manufactured.

The topology optimization results obtained for different volume fractions are summarized in Table 1. The results show that lower volume fractions lead to higher material reduction, but they also increase the risk of discontinuities and poorly defined members. The configuration corresponding to a 40% volume fraction was selected because it provided a more continuous geometry and a better basis for NURBS/PolyNURBS reconstruction.

Table 1. *Comparison of topology optimization results for different volume fractions*

Volume fraction [%]	Material reduction [%]	Relative remaining material [%]	Structural continuity	Manufacturability assessment
20	80	20	Low	Discontinuous members and poorly defined geometry
25	75	25	Medium	Some load paths are visible, but several regions are difficult to reconstruct
30	70	30	Medium	Improved material distribution, but local discontinuities are still present
35	65	35	Medium-High	More continuous members, but some structural features remain unclear
40	60	40	High	Continuous geometry and clearer load-bearing paths

THE ANNALS OF "DUNAREA DE JOS" UNIVERSITY OF GALATI
FASCICLE IX. METALLURGY AND MATERIALS SCIENCE
Nº. 3 - 2026, ISSN 2668-4748; e-ISSN 2668-4756
Article DOI: https://doi.org/10.35219/mms.2026.3.02

4. Conclusions

This paper presented a CAD/CAE workflow for the topology optimization of a structural component and for the conversion of the optimized result into a manufacturable geometric model. The proposed approach included finite element analysis, topology optimization, NURBS/PolyNURBS reconstruction, geometry verification, and lattice structure generation.

The initial finite element analysis allowed the identification of the main displacement and von Mises stress regions, which were used to define and interpret the topology optimization process. The comparison of different volume fractions showed that lower volume fractions can increase material reduction but may also lead to discontinuous or poorly defined structural members. Therefore, the final optimized configuration was selected based on both mass reduction and manufacturability.

The reconstruction stage proved to be essential, since the raw topology optimization result could not be used directly as a final CAD model. By using NURBS and PolyNURBS tools, the optimized geometry was transformed into a smoother, continuous, and closed model while preserving the main load-bearing paths and the functional mounting interface.

The integration of an internal tetrahedral lattice structure provided an additional lightweight design solution. The results also showed that mesh quality and geometric continuity are important factors for obtaining a reliable lattice-reinforced model. The research confirms that topology optimization should be combined with geometric reconstruction and manufacturability verification to obtain a practical engineering component suitable for further analysis and additive manufacturing.

References

[1]. El Khadiri I., *et al.*, *Topology optimization methods for additive manufacturing: a review*, International Journal for Simulation and Multidisciplinary Design Optimization, vol. 14, article 12, 2023.

[2]. Zhu J., *et al.*, *A review of topology optimization for additive manufacturing: Status and challenges*, Chinese Journal of Aeronautics, vol. 34, no. 1, p. 91-110, 2021.

[3]. Prathyusha A. L. R., Kumar B. V. S. R. N., *A review on additive manufacturing and topology optimization process for weight reduction studies in various industrial applications*, Materials Today: Proceedings, vol. 62, p. 109-117, 2022.

[4]. Anh N. T., *et al.*, *Study on Topology Optimization Design for Additive Manufacturing*, Engineering, Technology & Applied Science Research, vol. 14, no. 3, p. 14437-14441, 2024.

[5]. Mhapsekar K., *et al.*, *Additive Manufacturing Constraints in Topology Optimization for Improved Manufacturability*, Journal of Manufacturing Science and Engineering, vol. 140, no. 5, article 051017, 2018.

[6]. Rosnitschek T., *et al.*, *Manufacturing Constraints in Topology Optimization for the Direct Extrusion-Based Additive Manufacturing of Parts*, Designs, vol. 7, no. 1, article 8, 2023.

[7]. Misiun G., *et al.*, *Topology optimization for additive manufacturing with distortion constraints*, Computer Methods in Applied Mechanics and Engineering, vol. 386, article 114095, 2021.

[8]. Liu S., *et al.*, *A realization method for transforming a topology optimization design into additive manufacturing structures*, Engineering, vol. 4, no. 2, p. 277-285, 2018.

[9]. Montemurro M., Refai K., *A Topology Optimization Method Based on Non-Uniform Rational Basis Spline Hyper-Surfaces for Heat Conduction Problems*, Symmetry, vol. 13, no. 5, article 888, 2021.

[10]. Ren H., *et al.*, *AMRTO: Automated CAD model reconstruction of topology optimization result*, Computer Methods in Applied Mechanics and Engineering, vol. 435, article 117673, 2025.

[11]. Nazir A., *et al.*, *A state-of-the-art review on types, design, optimization, and additive manufacturing of cellular structures*, The International Journal of Advanced Manufacturing Technology, vol. 104, p. 3489-3510, 2019.

[12]. Chen L.-Y., *et al.*, *Additive manufacturing of metallic lattice structures: Unconstrained design, accurate fabrication, fascinated performances, and challenges*, Materials Science and Engineering: R: Reports, vol. 146, article 100648, 2021.

[13]. Liu R., *et al.*, *A Review on Factors Affecting the Mechanical Properties of Additively-Manufactured Lattice Structures*, Journal of Materials Engineering and Performance, vol. 33, p. 4685-4711, 2023.

[14]. Yang J., *et al.*, *Additive Manufacturing and Influencing Factors of Lattice Structures: A Review*, Materials, vol. 18, no. 7, article 1397, 2025.

[15]. Miao X., *et al.*, *Review on mechanical properties of metal lattice structures*, Composite Structures, vol. 342, article 118267, 2024.

THE ANNALS OF "DUNAREA DE JOS" UNIVERSITY OF GALATI
FASCICLE IX. METALLURGY AND MATERIALS SCIENCE
N°. 3 - 2026, ISSN 2668-4748; e-ISSN 2668-4756
Article DOI: https://doi.org/10.35219/mms.2026.3.03

THE IMPACT OF ATMOSPHERIC POLLUTION GENERATED BY INTERNAL COMBUSTION ENGINES ON HUMAN HEALTH

Mariana LUPCHIAN
"Dunarea de Jos" University of Galati, Romania
e-mail: mariana.lupchian@ugal.ro

ABSTRACT

This paper addresses the issue of emissions generated by vehicle engines and their impact on human health. The study aims to analyse the levels of major pollutants resulting from fuel combustion, such as carbon monoxide, nitrogen oxides, hydrocarbons, and particulate matter. The analysis emphasizes the impact of exposure to emitted pollutants on human health, identifying increased risks of respiratory and cardiovascular diseases. The study highlights the need to adopt effective measures to reduce pollutant emissions through the development of environmentally friendly technologies and the implementation of sustainable policies, to protect the environment and public health.

KEYWORDS: motor vehicle emissions, air pollution, human health, particulate matter, emission levels, engine technology, environmental impact

1. Introduction

Exposure to atmospheric pollutants is associated with increased risks of premature mortality, adverse effects on child development, and heightened susceptibility to infectious diseases.

Exhaust emissions contain a complex mixture of toxic compounds, including carbon monoxide (CO), nitrogen oxides (NO_x), particulate matter (PM), and hydrocarbons (HC), which exert detrimental effects on human health. Furthermore, pollutants originating from exhaust gases can negatively influence plant physiology, inhibit growth processes and contribute to the degradation of agricultural crops.

Fine particulate matter ($PM_{2.5}$ and PM_{10}) penetrates deeply into the pulmonary system and can enter the bloodstream, while nitrogen oxides (NO_x) induce inflammatory responses and oxidative stress. Polycyclic aromatic hydrocarbons (PAHs) and sulphur dioxide (SO_2) act as respiratory and cardiovascular irritants. These pollutants can also stimulate bone marrow activity, leading to increased production of inflammatory cells.

Air pollution adversely affects human health by increasing the risk of respiratory diseases (such as asthma and bronchitis), cardiovascular disorders, and lung cancer, as well as by causing irritation of the eyes and skin.

The European Parliament and the Council establish the need to reduce pollution to levels that minimize harmful effects on human health, with particular attention given to sensitive population groups and the environment [1].

To protect human health, it is essential to identify and implement the most efficient emission reduction measures. Emissions of harmful atmospheric pollutants should be prevented, controlled, or reduced, and appropriate ambient air quality objectives should be established, considering the standards and guidelines of the World Health Organization [2].

It is necessary to adopt detailed mechanisms for the transmission of information regarding ambient air quality [3].

Data quality objectives have been established, and these objectives need to be updated to ensure a higher degree of accuracy and clarity. Reference methods for the assessment of pollutant concentrations have also been defined, and these methods should be periodically revised to reflect the evolution of relevant standards [4].

Furthermore, provisions have been established regarding reference methods, data validation, and the siting of sampling points for the assessment of ambient air quality [5].

Within the framework of efforts to reduce CO_2 emissions and to achieve climate neutrality by 2050, it is necessary to reduce greenhouse gas emissions from the transport sector by 90% compared to 1990 levels.

THE ANNALS OF "DUNAREA DE JOS" UNIVERSITY OF GALATI
FASCICLE IX. METALLURGY AND MATERIALS SCIENCE
Nº. 3 - 2026, ISSN 2668-4748; e-ISSN 2668-4756
Article DOI: https://doi.org/10.35219/mms.2026.3.03

To reduce emissions from road transport, the European Union intends to complement the CO_2 targets for cars and vans with additional measures [6]. These include the introduction of a new emissions trading scheme for road transport and buildings, increasing the share of renewable fuels in transportation, and phasing out fiscal advantages for fossil fuels [7].

2. Case study analysis on the impact of emissions on human health

A gradual decrease in emissions can be observed, from approximately 820 million tonnes in 2015 to 660 million tonnes in 2025. This trend reflects the increased adoption of electric and hybrid vehicles, the implementation of stricter emission regulations, and improvements in the efficiency of internal combustion engines.

The comparative chart showing the evolution of CO_2, NO_x, and PM emissions from thermal engines between 2015 and 2025.

Transport accounted for approximately one quarter of total CO_2 emissions in the European Union in 2019. Of these, 71.7% originated from road transport, according to a report by the European Environment Agency. There are two main approaches to reducing CO_2 emissions from vehicles: improving their efficiency or changing the type of fuel used.

In 2019, most of the road transport in Europe relied on diesel (66.7%), followed by gasoline (24.55%). However, electric vehicles are gaining significant ground. They represented 17.8% of all newly registered vehicles in 2021, a considerable increase from 10.7% in 2020. Sales of electric vehicles (fully electric and plug-in hybrid) have grown substantially since 2017 and tripled in 2020, when the current CO_2 targets began to apply. Electric vans accounted for 3.1% of the newly registered van market in 2021.

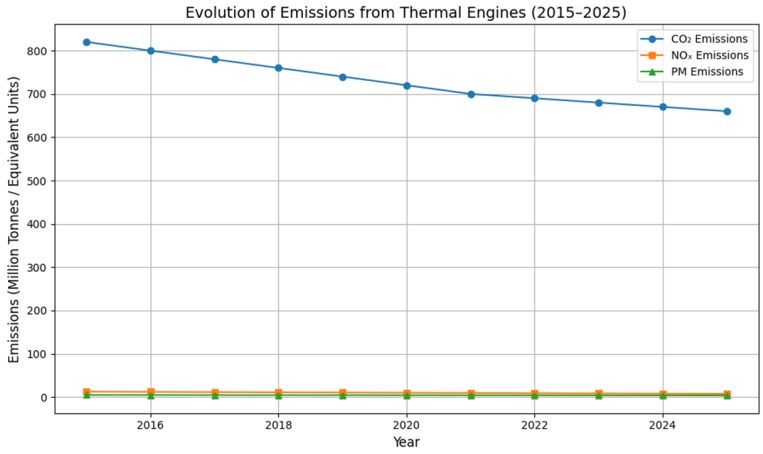

Fig. 1. *Assessment of Emission Trends from Internal Combustion Engines during 2015-2025*

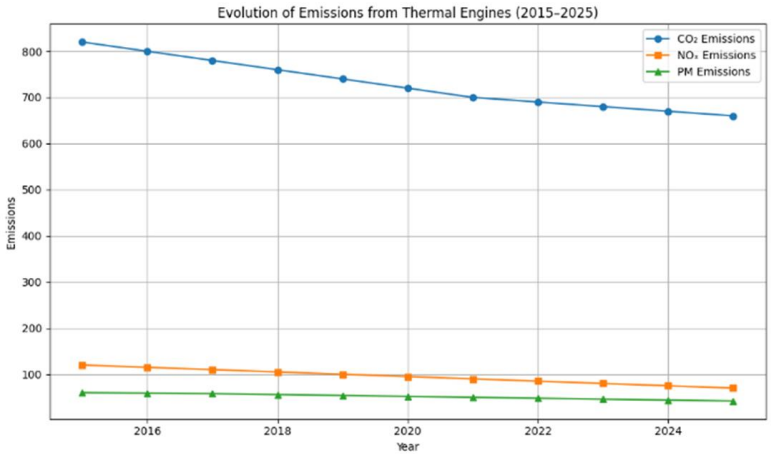

Fig. 2. *Evolution of CO_2, NO_x and PM emissions from internal combustion engines between 2015 and 2025*

THE ANNALS OF "DUNAREA DE JOS" UNIVERSITY OF GALATI
FASCICLE IX. METALLURGY AND MATERIALS SCIENCE
N°. 3 - 2026, ISSN 2668-4748; e-ISSN 2668-4756
Article DOI: https://doi.org/10.35219/mms.2026.3.03

When assessing the amount of CO_2 emissions generated by a vehicle, it is essential to consider not only the emissions produced during its operation, but also those associated with its manufacturing and end-of-life disposal.

Studies have shown that individuals exposed to elevated levels of $PM_{2.5}$ exhibit increased bone marrow activity and arterial inflammation, which consequently lead to a higher risk of myocardial infarction and stroke.

2.1. Impact of pollutant emissions on human health

According to recent studies, fine particulate matter can penetrate the bloodstream and induce systemic inflammation, thereby increasing the risk of arterial hypertension, atherosclerosis (arterial thickening), and blood clot formation-leading to an elevated risk of deep vein thrombosis and pulmonary embolism, myocardial infarction, and stroke. Nitrogen oxides are also associated with increased hospitalization rates for cardiovascular conditions.

Inhalation of air pollutants causes irritation of the respiratory tract, resulting in coughing, wheezing, shortness of breath, and exacerbation of asthma.

Exposure to fine particulate matter ($PM_{2.5}$, PM_{10}) and toxic gases such as nitrogen dioxide (NO_2) can trigger or aggravate asthma, chronic bronchitis, and other pulmonary diseases.

Air pollution is further associated with an increased risk of hypertension, cardiac arrhythmias, physiological stress, myocardial infarction, and cerebrovascular accidents.

Approximately 99% of the global population breathes air that exceeds safe limits, according to the World Health Organization (WHO).

Furthermore, approximately 22% of deaths due to myocardial infarction and 15% of deaths caused by stroke are associated with exposure to air pollution.

An increase in the concentration of fine particulate matter ($PM_{2.5}$) is associated with a progressive rise in:

- arterial blood pressure;
- the risk of myocardial infarction;
- the risk of stroke.

An increase in the concentration of fine particulate matter ($PM_{2.5}$) is associated with a progressive elevation in arterial blood pressure, as well as a higher risk of myocardial infarction and cerebrovascular events. This relationship is primarily attributed to the induction of systemic inflammation, oxidative stress, and endothelial dysfunction, which collectively contribute to the development and progression of cardiovascular diseases.

Biological Mechanisms Involved:

- Chronic inflammation: the body responds to pollutants in a manner similar to an infectious process.
- Oxidative stress: adversely affects endothelial cells lining the blood vessels.
- Vascular dysfunction: arteries become stiffer, leading to increased arterial blood pressure.

2.2. Quantified risks associated with $PM_{2.5}$ exposure

Evidence indicates a clear association between increased concentrations of fine particulate matter ($PM_{2.5}$) and an elevated risk of cerebrovascular events.

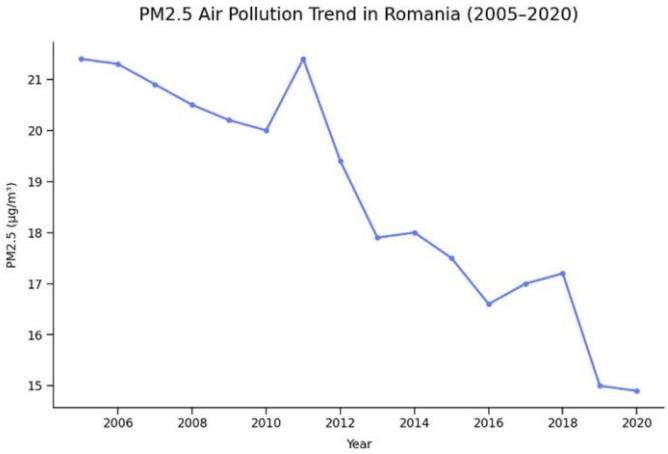

Fig. 3. *$PM_{2.5}$ emissions*

THE ANNALS OF "DUNAREA DE JOS" UNIVERSITY OF GALATI
FASCICLE IX. METALLURGY AND MATERIALS SCIENCE
N°. 3 - 2026, ISSN 2668-4748; e-ISSN 2668-4756
Article DOI: https://doi.org/10.35219/mms.2026.3.03

Specifically, an increase of +1 μg/m³ in $PM_{2.5}$ levels has been shown to correspond to a rise of approximately 0.7–2.2% in the incidence of certain types of strokes. This finding underscores the sensitivity of cerebrovascular outcomes to even minor variations in ambient air pollution levels.

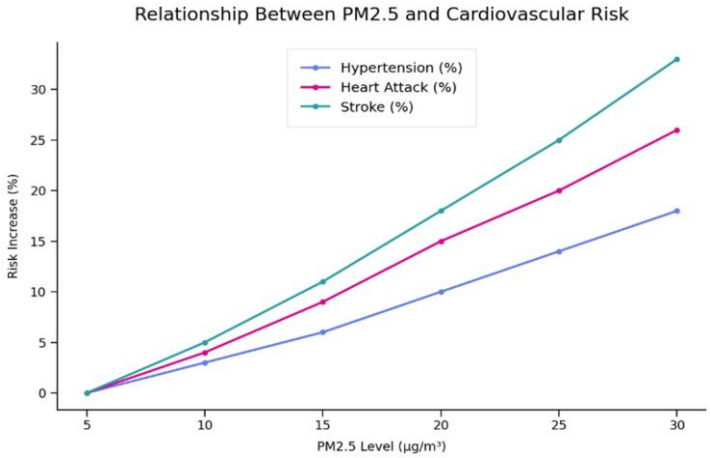

Fig.4. *Mortality associated with air pollution*

Moreover, moderate elevations in $PM_{2.5}$ concentrations are associated with a significant increase approximately 11–12% in hospitalization rates due to stroke. This suggests that population-level exposure to particulate matter not only contributes to disease onset but also exerts a measurable burden on healthcare systems.

Short-term exposure to elevated concentrations of $PM_{2.5}$ further exacerbates clinical outcomes, being linked to increased severity of stroke manifestations, including more pronounced neurological deficits and complications. These effects are primarily mediated by acute inflammatory responses, endothelial dysfunction, and alterations in cerebral blood flow.

Collectively, these findings emphasize the critical role of air quality in influencing both the incidence and severity of cerebrovascular diseases, highlighting the importance of effective environmental and public health interventions aimed at reducing exposure to fine particulate matter.

Deaths due to air pollution: Cardiovascular diseases ~70%; respiratory diseases ~20%; cancer and other causes ~10%.

Figure 5 presents the temporal evolution of $PM_{2.5}$ emissions in Romania during the period 2005-2020.

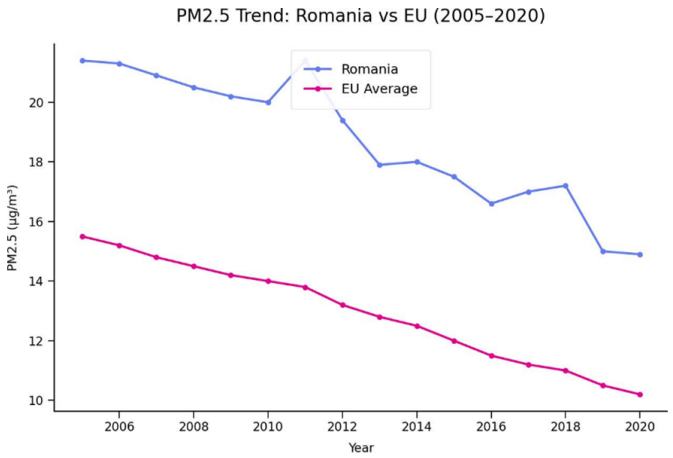

Fig. 5. *Comparative Analysis between Romania and the European Union*

The figure shows that both curves exhibit a decreasing trend, indicating an improvement in air quality. The European Union experienced a more consistent and rapid decline.

THE ANNALS OF "DUNAREA DE JOS" UNIVERSITY OF GALATI
FASCICLE IX. METALLURGY AND MATERIALS SCIENCE
No. 3 - 2026, ISSN 2668-4748; e-ISSN 2668-4756
Article DOI: https://doi.org/10.35219/mms.2026.3.03

Chemical substances present in the atmosphere can cause skin irritation and aggravate pre-existing dermatological conditions. Certain pollutants may also contribute to headaches, migraines, and even an increased risk of neurodegenerative conditions, including intracranial cysts, brain tumours, Alzheimer's disease, and Parkinson's disease.

Short-term and long-term exposure to air pollution represents a major cause of premature mortality, particularly due to cardiovascular and pulmonary diseases.

Exposure to air pollution during childhood can impair lung development, leading to reduced pulmonary function and an increased susceptibility to infections.

Poor air quality generates increased healthcare costs and reduces productivity, exerting a significant economic impact.

Vulnerability to the effects of air pollution varies, being higher among elderly individuals, those with pre-existing medical conditions, and children.

The resulting systemic inflammation affects arterial walls, promoting the formation of atherosclerotic plaques. Studies indicate that approximately 29% of the cardiovascular risk associated with air pollution is explained by this mechanism. Arterial wall thickness increases proportionally with the concentration of fine particulate matter in the air.

Fuel vapours contain toxic substances such as benzene, toluene, xylene, ethylbenzene, and volatile organic compounds. Inhalation of these compounds, even in small quantities, may cause irritation of the eyes, nose, and throat; dizziness, headaches, and nausea; breathing difficulties or fatigue; and, in severe cases (for example, in confined spaces), loss of consciousness.

Long-term exposure may lead to chronic respiratory conditions, such as bronchitis and asthma, as well as liver and kidney disorders and dysfunctions of the nervous system. It also increases the risk of cancer, particularly due to benzene, which is a well-established carcinogen.

When fuel vapours are released into the atmosphere, they contribute significantly to air pollution, including the formation of photochemical smog, the enhancement of the greenhouse effect and climate change, as well as the contamination of soil and water resources.

3. Conclusion

Although arterial wall damage is often attributed to associated conditions such as diabetes, growing evidence suggests that air pollution may represent a major underlying contributing factor. The inhalation of vapours originating from diesel fuel and motor oil can adversely affect multiple physiological systems, particularly the respiratory and cardiovascular systems.

Exposure to diesel emissions and used motor oil poses significant health risks, primarily due to the presence of toxic compounds such as polycyclic aromatic hydrocarbons, which are known for their carcinogenic potential and long-term adverse effects. In addition to inhalation risks, direct contact with these substances may lead to various health complications, while inadequate waste management practices can further amplify environmental contamination and public health risks at the community level.

These findings highlight the critical importance of reducing pollutant emissions, improving fuel handling practices, and implementing effective environmental regulations. The adoption of cleaner technologies, proper waste management, and increased public awareness are essential measures for minimizing exposure and protecting both human health and the environment.

References

[1]. ***, https://eur-lex.europa.eu/LexUriServ/LexUriServ.do?uri=OJ, Directive 2004/107/EC of the European Parliament and of the Council of 15 December 2004.
[2]. ***, https://eur-lex.europa.eu/legal-content/RO/TXT/HTML/?uri=CELEX:32008L0050, Directiva 2008/50/CE a Parlamentului European și a Consiliului din 21 mai 2008 privind calitatea aerului înconjurător și un aer mai curat pentru Europa.
[3]. ***, https://eur-lex.europa.eu/legal-content/EN/TXT/HTML/?uri=CELEX:52022PC0542, Directive of the European Parliament and of the Council on ambient air quality and cleaner air for Europe.
[4]. ***, https://eur-lex.europa.eu/legal-content/RO/TXT/PDF/?uri=CELEX:32015L1480, Commission Directive (EU) 2015/1480 of 28 August 2015, Directiva (UE) 2015/1480 A COMISIEI din 28 august 2015 de modificare a mai multor anexe la Directivele 2004/107/CE și 2008/50/CE ale Parlamentului European și ale Comisiei prin care se stabilesc normele privind metodele de referință, validarea datelor și amplasarea punctelor de prelevare pentru evaluarea calității aerului înconjurător.
[5]. ***, https://www.europarl.europa.eu/topics/ro/article/20190313STO31218/emisiile-de-co2-de-la-autovehicule-date-si-cifre-infografic.
[6]. Ileana Negrea, *Cercetări Privind Impactul Sistemelor de Transport Asupra Mediului*, Universitatea Politehnica Tmișoara, Facultatea de Mecanică, 2009.
[7]. ***, https://www.calitateaer.ro/export/sites/default/.galleries/Legislation/european/decizia-2011_850_ue.pdf_2063068895.pdf, Decizia de punere în aplicare a Comisiei din 12 decembrie 2011 de stabilire a normelor pentru Directivele 2004/107/CE și 2008/50/CE ale Parlamentului European și ale Consiliului în ceea ce privește schimbul reciproc de informații și raportarea privind calitatea aerului înconjurător.

THE ANNALS OF "DUNAREA DE JOS" UNIVERSITY OF GALATI
FASCICLE IX. METALLURGY AND MATERIALS SCIENCE
N°. 3 - 2026, ISSN 2668-4748; e-ISSN 2668-4756
Article DOI: https://doi.org/10.35219/mms.2026.3.04

COMPARATIVE ANALYSIS OF METALLIC OXIDES AND NANOSTRUCTURED MATERIALS FOR AIR PURIFICATION APPLICATIONS

Omar AHMED[1], Adriana-Gabriela SCHIOPU[1,2], Mihai OPROESCU[3]
[1] Science and Materials Engineering Doctoral School, National University of Science and Technology POLITEHNICA Bucharest, Romania
[2] Faculty of Mechanics and Technology, National University of Science and Technology POLITEHNICA Bucharest - Pitești University Centre, Romania
[3] Faculty of Electronics, Communication and Computers, National University of Science and Technology POLITEHNICA Bucharest- Pitești University Centre, Romania
e-mail: omaralsaadi@yahoo.com; gabriela.schiopu@upb.ro; mihai.oproescu@upb.ro

ABSTRACT

Air pollution represents one of the major environmental and public health challenges worldwide, generating an increasing demand for efficient air purification technologies. Nanostructured materials have attracted significant attention due to their high surface area, enhanced reactivity, and multifunctional pollutant removal mechanisms. This paper presents a comparative analysis of metallic oxides employed in air purification applications, focusing on titanium dioxide (TiO_2), zinc oxide (ZnO), copper oxide (CuO), nickel oxide (NiO), and magnesium oxide (MgO). The fundamental purification mechanisms, including heterogeneous photocatalysis, reactive oxygen species generation, gas adsorption, and chemisorption processes, are discussed in relation to the structural and electronic properties of each material. The study evaluates the advantages and limitations of these oxides in removing volatile organic compounds, nitrogen oxides, sulphur oxides, and biological contaminants. Furthermore, the performance of metallic oxides is compared with that of carbon-based nanomaterials and metal-organic frameworks, highlighting the benefits of hybrid nanocomposite systems. Attention is given to practical implementation challenges, such as charge carrier recombination, photocorrosion, catalyst deactivation, mass transfer limitations, formation of toxic by-products, and nanoparticle immobilization requirements. The analysis indicates that no single material can provide a universal solution for air purification; instead, future developments should focus on engineered heterojunctions and multifunctional hybrid systems capable of combining adsorption, photocatalytic degradation, and long-term operational stability. These approaches offer promising perspectives for the development of next-generation sustainable air purification technologies.

KEYWORDS: air purification, mechanism, comparative analysis, environmental applications, metallic oxides application, air quality

1. Introduction

In Romania, the monitoring and evaluation of ambient air quality are strictly regulated, being fully aligned with European Union legislation. The main legal framework in Romania is represented by Law no. 104/2011 on ambient air quality, which directly transposes the European Directive 2008/50/EC (Framework Directive on ambient air quality for cleaner air in Europe) and Directive 2004/107/EC [1].

From a technical and legal point of view, there are no differences between the limit values imposed in Romania and those in the rest of Europe, as all EU member states must comply with the same thresholds. However, major differences arise at the level of implementation, effective monitoring and penalties (infringement procedures) [2].

THE ANNALS OF "DUNAREA DE JOS" UNIVERSITY OF GALATI
FASCICLE IX. METALLURGY AND MATERIALS SCIENCE
N°. 3 - 2026, ISSN 2668-4748; e-ISSN 2668-4756
Article DOI: https://doi.org/10.35219/mms.2026.3.04

The efficiency of nanomaterials such as ZnO, TiO_2, graphene, metal-organic frameworks (MOFs) or carbon nanotubes in the gas phase is due to clear physical laws. As the particle size decreases below 100 nm, the percentage of atoms exposed to the surface increases exponentially. For air purification, this means high density of active adsorption sites and reaction sites per unit mass. The modification of the structure of the energy bands (widening of the forbidden band to very small sizes or the generation of surface defect states, such as oxygen vacancies in ZnO) allows for a more efficient generation of reactive oxygen species (ROS:•OH,•O2−). Nanomaterials can operate simultaneously through three mechanisms: physical/chemical adsorption (storage of the pollutant), heterogeneous photocatalysis (destruction of the pollutant under the action of light) and antimicrobial activity (destruction of bioaerosols and bacteria) [3].

The performance of nanomaterials employed in air purification technologies is strongly governed by their structural and physicochemical characteristics. At the nanoscale, the reduction of particle dimensions results in a substantial increase in the surface-to-volume ratio, leading to a higher density of active sites available for adsorption and catalytic reactions. Consequently, nanostructured materials exhibit significantly enhanced interaction with gaseous pollutants compared to their bulk counterparts [4].

Surface morphology represents a critical parameter influencing pollutant capture efficiency. Nanorods, nanowires, nanosheets, hollow spheres, and hierarchical porous structures provide different diffusion pathways and adsorption capacities. Materials exhibiting interconnected mesoporous networks facilitate rapid mass transfer and improved accessibility of active sites, thereby increasing the degradation rate of volatile organic compounds (VOCs), nitrogen oxides (NOx), sulphur oxides (SOx), and biological contaminants [5-8].

Defect engineering has emerged as a powerful strategy for improving the environmental performance of metal oxide nanomaterials. Structural defects such as oxygen vacancies, cation vacancies, grain boundaries, and surface disorder introduce localized electronic states that enhance charge separation and promote the formation of reactive oxygen species (ROS). These species, including hydroxyl radicals (•OH), superoxide radicals (•O2−), and singlet oxygen, play a fundamental role in the oxidation and mineralization of airborne contaminants [8].

Furthermore, crystal phase composition directly influences photocatalytic efficiency. Highly crystalline structures generally facilitate charge carrier transport and reduce recombination losses, whereas controlled defect concentrations can create additional active centres without excessively increasing electron-hole recombination rates. Therefore, optimization of morphology, porosity, crystallinity, and defect density remains essential for the rational design of advanced air purification nanomaterials.

2. Comparative analysis of metallic oxides used for air purification

Nanomaterials used in air purification can be broadly classified into semiconductor metal oxides, carbon-based nanomaterials, metal-organic frameworks (MOFs), and hybrid nanocomposites. Each class exhibits distinct advantages and limitations that determine its suitability for specific environmental applications.

Semiconductor metal oxides such as TiO_2, ZnO, CuO, NiO, and WO_3 remain the most extensively investigated materials due to their photocatalytic properties, chemical stability, and relatively low production costs. TiO_2 is considered the benchmark photocatalyst because of its excellent photostability and oxidation capability; however, its wide band gap restricts activation primarily to ultraviolet radiation. ZnO exhibits comparable photocatalytic activity while additionally possessing intrinsic antibacterial properties [9-12]. Nevertheless, ZnO may suffer from photocorrosion under prolonged operating conditions [13].

Carbon-based nanomaterials, including graphene, graphene oxide, reduced graphene oxide, carbon nanotubes, and activated carbon nanostructures, primarily contribute through adsorption mechanisms. Their exceptionally high specific surface area facilitates efficient capture of volatile organic compounds and particulate matter. Moreover, their high electrical conductivity enhances charge transport when integrated into photocatalytic heterostructures [14, 15].

Metal-organic frameworks represent a rapidly growing class of porous crystalline materials characterized by unprecedented surface areas and tuneable chemical functionality. MOFs exhibit remarkable selectivity toward specific pollutants, particularly carbon dioxide, ammonia, and volatile organic compounds. However, long-term stability under humid atmospheric conditions remains a significant challenge for practical implementation [16, 17].

Hybrid nanocomposites combine the advantages of multiple material classes. Systems such as TiO_2/graphene, ZnO/CuO, TiO_2/MOF, and ZnO/carbon nanotube composites exhibit improved charge separation, broader light absorption ranges, enhanced adsorption capacity, and superior

THE ANNALS OF "DUNAREA DE JOS" UNIVERSITY OF GALATI
FASCICLE IX. METALLURGY AND MATERIALS SCIENCE
Nº. 3 - 2026, ISSN 2668-4748; e-ISSN 2668-4756
Article DOI: https://doi.org/10.35219/mms.2026.3.04

photocatalytic efficiency. Consequently, hybrid nanostructures currently represent one of the most promising directions for next-generation air purification technologies.

Despite laboratory performance (where pollutant degradation rates of over 95% are often reported), transfer to real-world applications faces several critical barriers [18].

Table 1. *Comparative analysis of metallic oxides for air purification*

Metal oxide	Semiconductor Type	Band Gap (Eg)	Activation spectrum	Main mechanism in purification	Major advantage	Major limitation
TiO_2	n	≈3.2 eV (Anatase)	UV (λ< 387nm)	Heterogeneous photocatalysis (generate ·OH and·O_2)	Chemical stability, standard in photocatalysis	Inactive under visible light; relatively fast recombination
ZnO	n	≈3.37 eV	UV (λ< 368nm)	Heterogeneous photocatalysis; intrinsic antibacterial activity	Morphological versatility, low cost, biocompatible	Susceptible to photocorrosion in aqueous/acidic media.
CuO	p	1.2 - 1.7 eV	Visible/Near IR	Co-catalyst (heterojunctions); Catalytic decomposition	It absorbs strongly in the visible spectrum.	Extremely fast recombination of carriers when used alone.
NiO	p	≈3.6 - 4.0 eV	UV	Gas adsorption; co-catalyst in NOx decomposition	Excellent hole mobility (h^+).	Higher toxicity; Very wide Eg
MgO	Insulator / Wide semiconductor	≈6.0 eV	Primarily non-photocatalytic; active mainly under UV-C irradiation	Acid-base chemical adsorption (chemisorption) of toxic gases	Strong basic surface, excellent for retaining CO, SO_x, NO_x	Lack of photocatalytic activity under sunlight/indoors.

For the removal and neutralization of inorganic pollutants from the air, a category dominated by nitrogen oxides (NOx, especially NO and NO_2, sulphur dioxide (SO_2), carbon monoxide (CO) and tropospheric ozone (O_3) – metal oxides act through completely different mechanisms than those used for volatile organic compounds (VOC) [19].

Unlike VOCs, which are degraded to CO_2 and H_2O by complete mineralization, inorganic pollutants are cleaned up by two major pathways:

A. Selective photocatalytic oxidation: On the surface of n-type semiconductors (ZnO, TiO_2), nitric oxide (NO) is successively oxidized by hydroxyl radicals (•OH) and superoxide (•O_2) generated under the action of light. The goal is to transform a highly toxic gas into a stable and much safer species (nitrogen ion, NO_3^-):

$$NO \rightarrow NO_2 \rightarrow HNO_3 \rightarrow NO_3^-$$

If the photocatalyst is not active enough, the reaction can stop halfway, releasing NO_2, which is about 10 times more toxic than NO. ZnO often exhibits higher selectivity than TiO_2, favouring direct conversion to NO_3^-, blocking intermediate NO_2 desorption.

B. Acid-base chemisorption and reactive adsorption: Nitrogen and sulphur oxides are gases with an acidic character. Metal oxides with a pronounced basic character (especially MgO) interact with them extremely strongly electrostatically and chemically, fixing them on the surface in the form of sulphites/sulphates or nitrites/nitrates, without necessarily requiring light activation:

$$MgO + SO_2 \rightarrow MgSO_3$$
$$MgO + 2NO_2 \rightarrow Mg(NO_3)_2 + NO\uparrow$$

Semiconductor metal oxides (ZnO, TiO_2) are stable and inexpensive, but they suffer from rapid recombination of charge carriers and often require UV energy. For indoor air, where the light is LED (visible), their photocatalytic efficiency becomes significantly reduced if they are not doped with noble metals (Ag, Pt) or associated in heterojunctions (e.g. ZnO/CuO) [20-23]. A comparative analysis of the behavior of metal oxides is presented in Table 1.

Carbon-based nanomaterials (Graphene, Graphene Oxide - GO) have an exceptional physical adsorption capacity for VOCs due to π-π interactions. However, they do not have their own high catalytic activity of destroying gaseous inorganic pollutants, functioning optimally only as conductive carriers for metal oxides.

Metal-Organic Frameworks (MOFs) represent one of the most promising classes of materials

THE ANNALS OF "DUNAREA DE JOS" UNIVERSITY OF GALATI
FASCICLE IX. METALLURGY AND MATERIALS SCIENCE
Nº. 3 - 2026, ISSN 2668-4748; e-ISSN 2668-4756
Article DOI: https://doi.org/10.35219/mms.2026.3.04

currently investigated for air purification. Their major limitations, however, remain their low thermal and hydrothermal stability (many MOF structures structurally collapse under conditions of high atmospheric humidity) and the prohibitive cost of production.

3. Carbon-Based Nanomaterials for Air Purification Applications

Carbon-based nanomaterials have emerged as one of the most promising classes of advanced materials for air purification applications due to their exceptional physicochemical properties, including high specific surface area, tuneable pore structure, superior electrical conductivity, chemical stability, and versatile surface functionalization capability [15, 24]. Unlike semiconductor metal oxides, whose primary mechanism relies on photocatalytic degradation, carbon nanomaterials predominantly operate through adsorption processes, although recent studies have demonstrated their ability to participate actively in catalytic and photocatalytic reactions when integrated into hybrid nanostructures.

The remarkable adsorption capacity of carbon nanomaterials originates from their highly developed surface area and the presence of extensive π-electron systems. These characteristics promote strong interactions with gaseous pollutants through van der Waals forces, π–π stacking interactions, electrostatic attraction, and surface complexation mechanisms. Consequently, carbon-based materials have demonstrated high efficiency in the removal of volatile organic compounds (VOCs), polycyclic aromatic hydrocarbons (PAHs), nitrogen-containing pollutants, sulphur compounds, and ultrafine particulate matter.

Among the various carbon nanomaterials investigated for environmental remediation, graphene and graphene oxide have attracted considerable attention [25]. Graphene consists of a single atomic layer of sp^2-hybridized carbon atoms arranged in a two-dimensional honeycomb lattice. This unique structure provides an exceptionally large theoretical specific surface area exceeding 2600 $m^2\ g^{-1}$, facilitating efficient adsorption of gaseous contaminants. Furthermore, graphene exhibits excellent electrical conductivity, which promotes rapid electron transport and suppresses charge carrier recombination when incorporated into photocatalytic systems.

Graphene oxide (GO) represents an oxidized derivative of graphene containing abundant oxygen-containing functional groups, including hydroxyl, epoxy, carbonyl, and carboxyl moieties. These functional groups significantly increase the hydrophilicity and chemical reactivity of the material, enabling enhanced interactions with polar gaseous pollutants such as ammonia, formaldehyde, nitrogen oxides, and sulphur dioxide. Moreover, the oxygenated surface provides anchoring sites for metallic nanoparticles and semiconductor oxides, facilitating the fabrication of multifunctional composite materials with improved environmental performance [14].

Reduced graphene oxide (rGO) combines the advantages of graphene and graphene oxide by partially restoring the conjugated carbon network while retaining a fraction of the oxygen-containing functional groups. As a result, rGO exhibits improved electrical conductivity compared to GO while maintaining sufficient chemical activity for pollutant adsorption and catalyst immobilization. Numerous studies have reported that TiO_2/rGO and ZnO/rGO heterostructures display substantially enhanced photocatalytic activity under both ultraviolet and visible light irradiation due to improved charge separation and electron transport efficiency [20, 23, 26, 27].

A comparative analysis of carbon nanomaterials used for air purification is presented in Table 2.

Table 2. *Comparative analysis of carbon-based nanomaterials for air purification application*

Carbon nanomaterial	Specific surface area (m^2/g)	Main mechanism	Target pollutants	Major limitation
Graphene	2000–2600	Adsorption, electron transport	VOCs, NOx	Agglomeration
Graphene Oxide (GO)	500–1500	Adsorption, surface functionalization	NH_3, HCHO, NOx	Lower conductivity
Reduced Graphene Oxide	800–1800	Adsorption + photocatalytic support	VOCs, NOx	Cost of reduction
SWCNTs (single wall carbon nanotube)/ MWCNTs (multiwall carbon nanotubes)	200–1200	Adsorption, conductive support	VOCs, aromatic compounds	Difficult large-scale production
Activated Carbon	500–2500	Physical adsorption	VOCs, odors	Saturation of active sites

THE ANNALS OF "DUNAREA DE JOS" UNIVERSITY OF GALATI
FASCICLE IX. METALLURGY AND MATERIALS SCIENCE
Nº. 3 - 2026, ISSN 2668-4748; e-ISSN 2668-4756
Article DOI: https://doi.org/10.35219/mms.2026.3.04

Carbon nanotubes (CNTs) constitute another important category of carbon-based nanomaterials employed in air purification technologies. Depending on their structure, carbon nanotubes may be classified as single-walled (SWCNTs) or multi-walled (MWCNTs). Their cylindrical geometry, high aspect ratio, and hollow internal structure provide multiple adsorption pathways for gaseous contaminants. In addition, carbon nanotubes exhibit excellent mechanical strength and thermal stability, making them suitable candidates for incorporation into filtration membranes and multifunctional air-cleaning systems.

The adsorption performance of carbon nanotubes is strongly influenced by their diameter, surface functionalization, defect concentration, and degree of graphitization. Functionalized CNTs containing oxygen- or nitrogen-containing groups have demonstrated enhanced affinity toward acidic and polar pollutants, while pristine nanotubes exhibit superior adsorption of aromatic volatile organic compounds through π–π interactions. Furthermore, CNTs can serve as conductive support for metal oxide nanoparticles, improving photocatalytic efficiency by facilitating interfacial electron transfer [28-30].

Activated carbon nanostructures remain among the most widely implemented commercial materials for air purification. Their hierarchical pore network, consisting of micro-, meso-, and macropores, enables simultaneous adsorption of molecules of different sizes. Although activated carbon generally lacks intrinsic photocatalytic activity, its low cost, high adsorption capacity, and industrial scalability continue to make it a key component of commercial filtration systems. Recent developments focus on combining activated carbon with photocatalytic nanoparticles to create self-regenerating filters capable of degrading adsorbed pollutants.

Despite their numerous advantages, carbon-based nanomaterials also present several limitations. Adsorption sites may become saturated during prolonged operation, leading to reduced pollutant removal efficiency. Additionally, regeneration processes often require thermal treatment, chemical oxidation, or ultraviolet irradiation, which may increase operational costs. Concerns related to nanomaterial release, environmental persistence, and potential respiratory toxicity have also stimulated research toward safer immobilization strategies and sustainable composite structures.

Current research trends increasingly focus on the development of hybrid carbon-based nanocomposites integrating graphene, carbon nanotubes, activated carbon, metal oxides, and metal-organic frameworks. Such multifunctional systems combine high adsorption capacity with photocatalytic degradation, antimicrobial activity, and improved structural stability. These synergistic effects offer significant potential for the design of next-generation air purification technologies capable of simultaneously removing gaseous pollutants, particulate matter, and airborne microorganisms under realistic environmental conditions.

4. The limitations and technical challenges

A. Mass transfer and gas-phase kinetics: Unlike water decontamination, where pollutants are in intimate and prolonged contact with the catalyst, in air purification we are dealing with high dynamic flow (the air passes quickly through the filter) and typically below 1 ppm.

Many nanostructured photocatalysts have too slow reaction kinetics. The residence time of the gas molecule (e.g. NO or formaldehyde) on the surface of the nanomaterial is often in the order of milliseconds, insufficient for the redox reaction to take place completely.

B. Risk of by-products more toxic than the original pollutant: This is one of the biggest safety issues in air photocatalysis. If the mineralization of a volatile organic compound (VOC) is not complete due to low light intensity or deactivation of active sites, partial degradation of a benign pollutant can generate much more dangerous intermediates. For example, the partial photodegradation of some alcohols or hydrocarbons on TiO_2 or ZnO nanostructures can release formaldehyde or acetaldehyde into the airstream. In the case of NOx, incomplete oxidation releases NO_2, a gas considerably more toxic than NO initially.

C. Deactivation of the catalyst ("poisoning" of active sites): Real air contains a multitude of compounds, including variable humidity, sulphur compounds (SO_2, H_2S), or organic compounds with a high molecular weight. Nanostructured metal oxides tend to irreversibly adsorb sulphate species or heavy carbonic compounds. They block ("poison") the active sites of the nanomaterial, dramatically decreasing its efficiency after just a few tens of hours of operation, making filter regeneration difficult and expensive.

D. The problem of immobilization and ecotoxicity (Nanodusting): The use of free nano powders is excluded in air purification due to the risk that the nanomaterials will be entrained by airflow and inhaled by humans, causing cellular oxidative stress and severe lung toxicity. Therefore, their immobilization on supports (textiles, geopolymers, glass) is mandatory. However, immobilization techniques (using polymer binders or silanes) bring a massive compromise: they partially encapsulate the

THE ANNALS OF "DUNAREA DE JOS" UNIVERSITY OF GALATI
FASCICLE IX. METALLURGY AND MATERIALS SCIENCE
N°. 3 - 2026, ISSN 2668-4748; e-ISSN 2668-4756
Article DOI: https://doi.org/10.35219/mms.2026.3.04

nanomaterial, reducing the active surface area accessible to gases by up to 40-60%.

5. Conclusions and future perspectives

Nanomaterials should not be regarded as a standalone solution but as a high-performance component that must be integrated into hybrid systems. For nanomaterial-based air purification technologies to become viable on a large scale, the scientific community needs to shift its attention from simply reporting "degradation rates under ideal conditions" to:

• the design of dynamic reactors capable of ensuring an optimal contact time without generating high pressure losses (pressure drop) in ventilation systems;

• in-situ green synthesis of heterojunctions (such as ZnO/CuO or ZnO/C), ensuring a strong covalent bond with the filter material to completely eliminate the risk of nanoparticle detachment;

• systematic study of the selectivity of the mechanisms, guaranteeing that the reaction by-products are strictly benign (CO_2, H_2O and immobilized NO_3^- ions).

References

[1]. Ahmed O., *et al.*, *Necessity of emergent materials development for air filtration to increase air quality*, 16th International Conference on Electronics, Computers and Artificial Intelligence (ECAI), IEEE, p. 1-5, Jun. 2024.

[2]. Oproescu M., *et al.*, *Trends and Advantages in Using Nanomaterials for Air Filtration*, 15th International Conference on Electronics, Computers and Artificial Intelligence (ECAI), IEEE, p. 1-6, Jun. 2023.

[3]. Biloshchytskyi A., *et al.*, *Reducing Outdoor Air Pollutants through a Moss-Based Biotechnological Purification Filter in Kazakhstan*, Urban Science, vol. 7, no. 4, Dec. 2023.

[4]. Kaliva M., Vamvakaki M., *Nanomaterials characterization*, Polymer Science and Nanotechnology: Fundamentals and Applications, p. 401-433, Jan. 2020.

[5]. Sha R., *et al.*, *ZnO nano-structured based devices for chemical and optical sensing applications*, Sensors and Actuators Reports, vol. 4, p. 100098, Nov. 2022.

[6]. Liu B., Liu J., *Sensors and biosensors based on metal oxide nanomaterials*, TrAC Trends in Analytical Chemistry, vol. 121, p. 115690, Dec. 2019.

[7]. Ur Rehman F., *et al.*, *Synthesis of Zinc Oxide Nanoparticles, Characterization and Biomedical Applications in Medicinal Sciences*, Characterization and Biomedical Applications in Medicinal Sciences Article in Journal of Materials Science and Surface Engineering, 2022.

[8]. Kaur A., *et al.*, *A review on template assisted synthesis of multi-functional metal oxide nanostructures: Status and prospects*, Materials Science and Engineering: B, vol. 286, p. 116005, Dec. 2022.

[9]. Rahman M., *et al.*, *Conversion of n-type to p-type conductivity in ZnO by incorporation of Ag and Ag-Li*, Mater. Today Commun., vol. 33, p. 104278, Dec. 2022.

[10]. Miquel-Jeanjean C., *et al.*, *Penetration Study of Formulated Nanosized Titanium Dioxide in Models of Damaged and Sun-Irradiated Skins*, DOI: 10.1111.

[11]. Kong Y., *et al.*, *SnO_2 nanostructured materials used as gas sensors for the detection of hazardous and flammable gases: A review*, Nano Materials Sc., vol. 4, no. 4, p. 339-350, Dec. 2022.

[12]. Yang B., *et al.*, *Enhancing gas sensing performance of tungsten trioxide (WO3) nanofibers through diameter and crystallinity control*, Sens. and Act. Rep., vol. 7, p. 100182, 2024.

[13]. Modan E. M., *et al.*, *Ultrasound and microwave assisted hydrolysis of nanostructured magnesium oxide for impregnation of polyester fibre filters*, Bull., Series B, vol. 86, p. 2024.

[14]. Mohamed E. F., *Nanotechnology: Future of Environmental Air Pollution Control*, Environmental Management and Sustainable Development, vol. 6, no. 2, p. 429, 2017.

[15]. Garg N., *et al.*, *Exploring the Potential of Carbon Based Materials in Air Purification*, MatSci Express, vol. 2, no. 1, p. 29-57, 2025.

[16]. Yan Y., *et al.*, *Novel Nanomaterials for Indoor Air Chemical Purification: A Review*, Inorganics, vol. 14, no. 4, p. 111, 2026.

[17]. Soni A., *Nanotechnology and Its Implications for Controlling Air Pollution: A Mini Review*, Nanomedicine & Nanotechnology Open Access, vol. 9, no. 4, p. 1-6, 2024.

[18]. Haruta M., *et al.*, *Gold catalysts prepared by coprecipitation for low-temperature oxidation of hydrogen and of carbon monoxide*, J. Catal., vol. 115, no. 2, p. 301-309, 1989.

[19]. Mo J., *et al.*, *Photocatalytic purification of volatile organic compounds in indoor air: A literature review*, Atmos. Environ., vol. 43, no. 14, p. 2229-2246, 2009.

[20]. Li X., *et al.*, *Exploring the photocatalytic conversion mechanism of gaseous formaldehyde degradation on TiO2–x-OV surface*, J. Hazard. Mater., vol. 424, p. 127217, 2022.

[21]. Ayappan C., *et al.*, *TiO_2-based photocatalysts for emerging gaseous pollutants removal: From photocatalysts to reactors design*, Coord. Chem. Rev., vol. 515, 2024.

[22]. Kuk S. K., *et al.*, *Singlet-oxygen-driven photocatalytic degradation of gaseous formaldehyde and its mechanistic study*, Appl. Catal. B, vol. 328, 2023.

[23]. Lahiri J., Batzill M., *Surface Functionalization of ZnO Photocatalysts with Monolayer ZnS*, The Journal of Physical Chemistry C, vol. 112, no. 11, p. 4304-4307, 2008.

[24]. Ren X., *et al.*, *Carbon nanotubes as adsorbents in environmental pollution management: A review*, Chemical Engineering Journal, vol. 170, no. 2-3, p. 395-410, 2011.

[25]. hsin Shih Y., syue Li M., *Adsorption of selected volatile organic vapors on multiwall carbon nanotubes*, J. Hazard. Mater., vol. 154, no. 1-3, p. 21-28, 2008.

[26]. Wu C.-M., *et al.*, *Sulfur Dioxide Adsorption on ZnO Nanoparticles and Nanorods*, The Journal of Physical Chemistry C, vol. 115, no. 20, p. 10164-10172, 2011.

[27]. Li X., *et al.*, *H_2O_2-assisted hydrothermal synthesis of TiO2-SiO_2 and its enhanced photocatalytic-adsorptive desulfurization performance for model fuel*, Fuel, vol. 226, p. 527-535, 2018.

[28]. Gupta V. K., Saleh T. A., *Sorption of pollutants by porous carbon, carbon nanotubes and fullerene - An overview*, Environmental Science and Pollution Research, vol. 20, no. 5, p. 2828-2843, 2013.

[29]. Pan B., Xing B., *Adsorption mechanisms of organic chemicals on carbon nanotubes*, Environ. Sci. Technol., vol. 42, no. 24, p. 9005-9013, 2008.

[30]. Zhang X., *et al.*, *Adsorption of VOCs onto engineered carbon materials: A review*, J. Hazard. Mater., vol. 338, p. 102-123, 2017.

THE ANNALS OF "DUNAREA DE JOS" UNIVERSITY OF GALATI
FASCICLE IX. METALLURGY AND MATERIALS SCIENCE
No. 3 - 2026, ISSN 2668-4748; e-ISSN 2668-4756
Article DOI: https://doi.org/10.35219/mms.2026.3.05

STUDIES AND RESEARCH ON THE CORROSION BEHAVIOR IN K_2SO_4 OF SOME LASER DEPOSITED COATINGS

Simona BOICIUC
"Dunarea de Jos" University of Galati, Romania
e-mail: simona_boiciuc@yahoo.com

ABSTRACT

The paper presents a series of experimental investigations regarding the corrosion behavior in a K_2SO_4 – 0.5M solution of laser-deposited layers using a Ni-Cr-B-Fe-Al alloy, compared to the substrate material made of 1C45 steel. Corrosion resistance can be influenced by the deposition parameters, which determine the stress state, chemical inhomogeneity, defects, and discontinuities within the surface layer, as well as subsequent processing.

KEYWORDS: injected powder laser cladding, continuous wave laser, corrosion resistance

1. Introduction

Concerns regarding increasing the durability of carbon and alloy steel components, while also reducing energy consumption, labour, and materials, have led to the development of unconventional technologies for the surface treatment of active zones. These involve the use of concentrated energy beams (laser radiation, electrons, plasma).

The use of lasers in surface treatments offers a series of advantages [1]:

- It allows for the precise localization of the areas to be processed, regardless of their configuration, and the exact focusing of laser radiation through beam delivery and component positioning systems.
- It enables precisely controllable processing within very short time intervals, with minimal heat-affected zones (adjacent to the processing zone).
- It ensures the reduction of deformations, internal stresses, oxidation, and decarburization of components.
- It allows processing to be carried out within electrical or magnetic fields, or vacuum chambers.
- It provides a wide spectrum of properties to the processed surfaces by increasing hardness, wear resistance, fatigue resistance, and corrosion resistance.
- It enables full automation of the workflow.

In laser cladding, the interaction of the laser radiation with the workpiece can be achieved in the presence of a filler material that is either injected or pre-deposited in the laser-material interaction zone.

Evaluating the possibilities of laser cladding requires characterizing the involved elements: the processed material, the laser beam, and the working environment.

Thus, it is important to know the physical-mechanical characteristics of the processed material, along with the shape, dimensions, and precision required for the process.

The laser generator and the beam power density are selected depending on the absorption rate of the material and the transformations that occur.

The effects of the laser beam-material interaction depend on the actual distribution of energy across the processed surface.

Experimental determination of the laser beam dimensions and the spatial distribution of power density constitute a necessary condition for evaluating results and controlling the process.

Qualitative indicators of the laser-processed zone during the cladding process - such as the height of the deposited layer, its hardness, wear resistance, and corrosion resistance - are influenced by the processing parameters, namely power density, feed rate, powder feed rate, and laser action duration.

Thus, small changes in laser radiation absorption can lead to significant changes in the size of the molten pool formed on the processed surface.

Variations in the filler material feed rate can cause fluctuations in the geometry and microstructure of the deposited layer.

Consequently, by varying the processing parameters, the complex physical-mechanical characteristics of the deposited layers can be controlled.

THE ANNALS OF "DUNAREA DE JOS" UNIVERSITY OF GALATI
FASCICLE IX. METALLURGY AND MATERIALS SCIENCE
No. 3 - 2026, ISSN 2668-4748; e-ISSN 2668-4756
Article DOI: https://doi.org/10.35219/mms.2026.3.05

Laser cladding can be used in industry for hardening turbine blades in aircraft engines, valve seats in automotive engines, and lathe tools.

Through multi-layer deposition, the reconstruction of worn parts such as turbines, aircraft turbine shafts, and dies in the automotive industry can be achieved, thereby reducing material consumption, processing time, and the cost of subsequent machining [2-4].

Laser cladding with nickel-based alloys is utilized for components operating under high mechanical and thermal loads in aggressive environments.

They are resistant to atmospheric corrosion, water, alkaline solutions, salts, organic acids, and dry gases containing hydrochloric acid, hydrofluoric acid, and chlorine up to approximately 500 °C.

The aim of this paper is to characterize the corrosion behavior, in a K_2SO_4 – 0.5M, solution, of some laser-deposited layers using a Ni-Cr-B-Fe-Al, alloy, compared to the substrate material made of 1C45 steel.

2. Experimental conditions

The powder used for laser cladding is spherical, obtained by gas atomization, and presents the following chemical composition 8.9 %Cr; 4.5 %Fe; 5.1 %B; 2.4 %Al; 0.6 %Cu; and the rest Ni. The powder particle size ranged between 0.045-0.1 mm, and the hardness was HV0.1 = 12046 MPa [5].

The base material used in the experimental research is 1C45 steel in a quenched and tempered state. This material is widely used across many industrial sectors.

The laser cladding was performed in a single stage, with the powder being introduced directly into the laser-material interaction zone.

The implemented method involved lateral powder feeding because it is suitable for components of any shape.

It was observed that when the direction of the powder flow matches the direction of the component's movement, higher deposition efficiency is recorded, the melting depth is easier to control, and the occurrence of pores is less likely.

For the experimental depositions, a continuous-wave gas active medium system was used, specifically a Laser GT 1400W model.

The operating parameters used for the laser cladding of the Ni-Cr-B-Fe-Al alloy are presented in Table 1.

Metallographic analysis of the used samples was carried out using a Neophot 2 microscope with computerized data acquisition.

Microhardness determination was performed using a PMT-3 microhardness tester with a 100 g load.

Table 1. *Operating parameters used for laser cladding*

Processing Parameters	Sample 1	Sample 2 – with substrate preheating to 60 °C
Filler material feed rate, [mg/s]	105	63.9
Number of overlapping passes	4	4
Laser radiation power, [W]	1150	1150
Laser beam scanning speed across the processed surface, [mm/s]	11	11
Laser beam diameter, [mm]	1.8	1.8
Feed step, [mm]	1.5	1.5
Layer thickness, [mm]	0.59	0.42
Vickers microhardness, [MPa]	12500	6500

EDX analyses performed on the corroded samples were carried out using a Quanta 200 electronic microscope with a resolution of 30 nm, equipped with an AMETEK spectrometer.

Prior to the corrosion tests, the samples were mechanically ground and polished to limit contamination caused by previous processing. They were then connected to a copper wire and insulated with an epoxy resin.

Electrochemical studies were conducted using a PGP 201 Potentiostat/Galvanostat system, and data acquisition was carried out using VoltaMaster 4 software, version 7.10. The electrochemical cell used was a classic three-electrode setup: the working electrode (the studied material), the reference electrode (Hg/Hg_2SO_4 in a saturated K_2SO_4, solution, with a potential of +651 mV vs. NHE), to which all measured potentials were reported, and the auxiliary electrode (a pure platinum electrode). The active surface area of the samples was 1 $cm^2 \pm 0.3$ cm^2.

The electrolyte used (K_2SO_4 - 0.5 M) was prepared in the laboratory using analytical grade (p.a.) chemical reagents purchased from Sigma-Aldrich. The tests were conducted at room temperature 25 °C ± 1 °C. The electrochemical parameters of the studied electrolyte are shown in Table 2 below.

THE ANNALS OF "DUNAREA DE JOS" UNIVERSITY OF GALATI
FASCICLE IX. METALLURGY AND MATERIALS SCIENCE
No. 3 - 2026, ISSN 2668-4748; e-ISSN 2668-4756
Article DOI: https://doi.org/10.35219/mms.2026.3.05

Table 2. *Electrochemical parameters of the studied electrolyte*

pH	Electrical Conductivity [mS/cm]	Salinity [g/L]	TDS (Total Dissolved Salts) [ppt]
7.28	73.4	30.2	52.1

The applied electrochemical protocol was as follows:

- Evaluation of the free open circuit potential (OCP) for 3 hours, with a measuring period of 1.8 s.
- Potentiodynamic polarization (PD), general corrosion Rp and corrozion rate Vcorr; scan rate 1 mV/s; overvoltage 40 mV; OCP duration 1 min; determined measure 50 Rp; step duration 0.6 s; step amplitude 3 mV; total time 149 min; and initial scan cathodic.

3. Results and discussions

3.1. Metallographic Analysis of Samples Tested for Corrosion in K_2SO_4 – 0.5M Solution

To highlight the corrosion behavior of the tested samples, a series of investigations were carried out using a Neophot 2 optical microscope, with computerized data acquisition, at a magnification power of 50x.

The obtained results are presented in Figure 1.

Figure 1.a, corresponding to sample P1, highlights localized corrosion in certain areas of the surface.

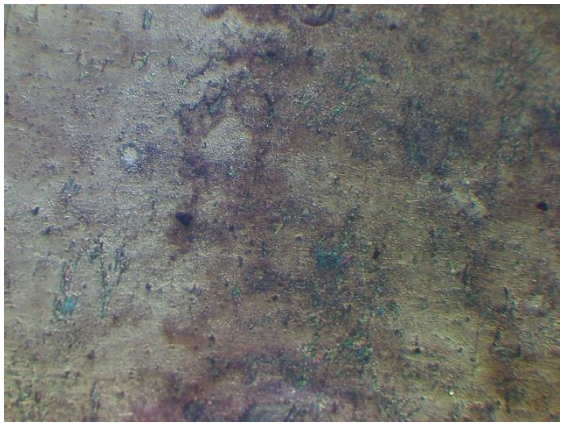

a) sample P1

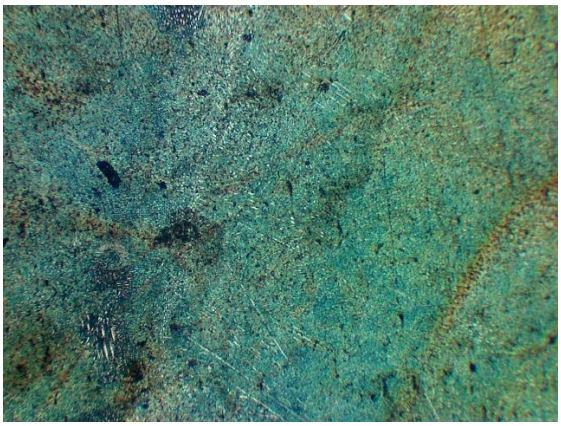

b) sample P2

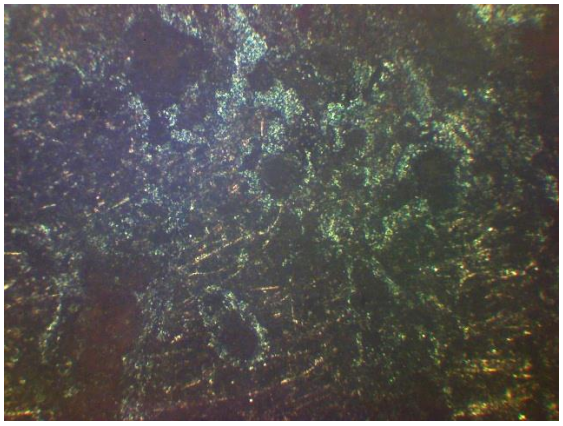

c) base material - sample P3

Fig. 1. *Metallographic analysis of the samples tested for corrosion in the K_2SO_4 – 0.5M solution, 50x*

Figure 1.b, corresponding to sample P2, which was prepared with substrate preheating, highlights reduced corrosion.

Figure 1.c, corresponding to sample P3 (the base material), highlights severe, uniform corrosion across the entire surface.

THE ANNALS OF "DUNAREA DE JOS" UNIVERSITY OF GALATI
FASCICLE IX. METALLURGY AND MATERIALS SCIENCE
Nº. 3 - 2026, ISSN 2668-4748; e-ISSN 2668-4756
Article DOI: https://doi.org/10.35219/mms.2026.3.05

Nevertheless, it can be observed that both samples produced by laser cladding with the Ni-Cr-B-Fe-Al alloy (P1 and P2) exhibit superior corrosion behavior compared to the 1C45 steel substrate.

3.2. EDX Microanalysis of Samples Tested for Corrosion in K_2SO_4 – 0.5M solution

EDX investigations carried out on the corroded samples were performed using a Quanta 200 electron microscope with a resolution of 30 nm, equipped with an AMETEK spectrometer.

Figure 2 shows the EDX microanalysis for sample P1 tested for corrosion in the in K_2SO_4 – 0.5M solution.

Analysing Figure 2 corresponding to sample P1, it can be observed that localized corrosion occurs in the form of pitting and spots. This typically manifests around defects such as pores, discontinuities, cracks, or inclusions.

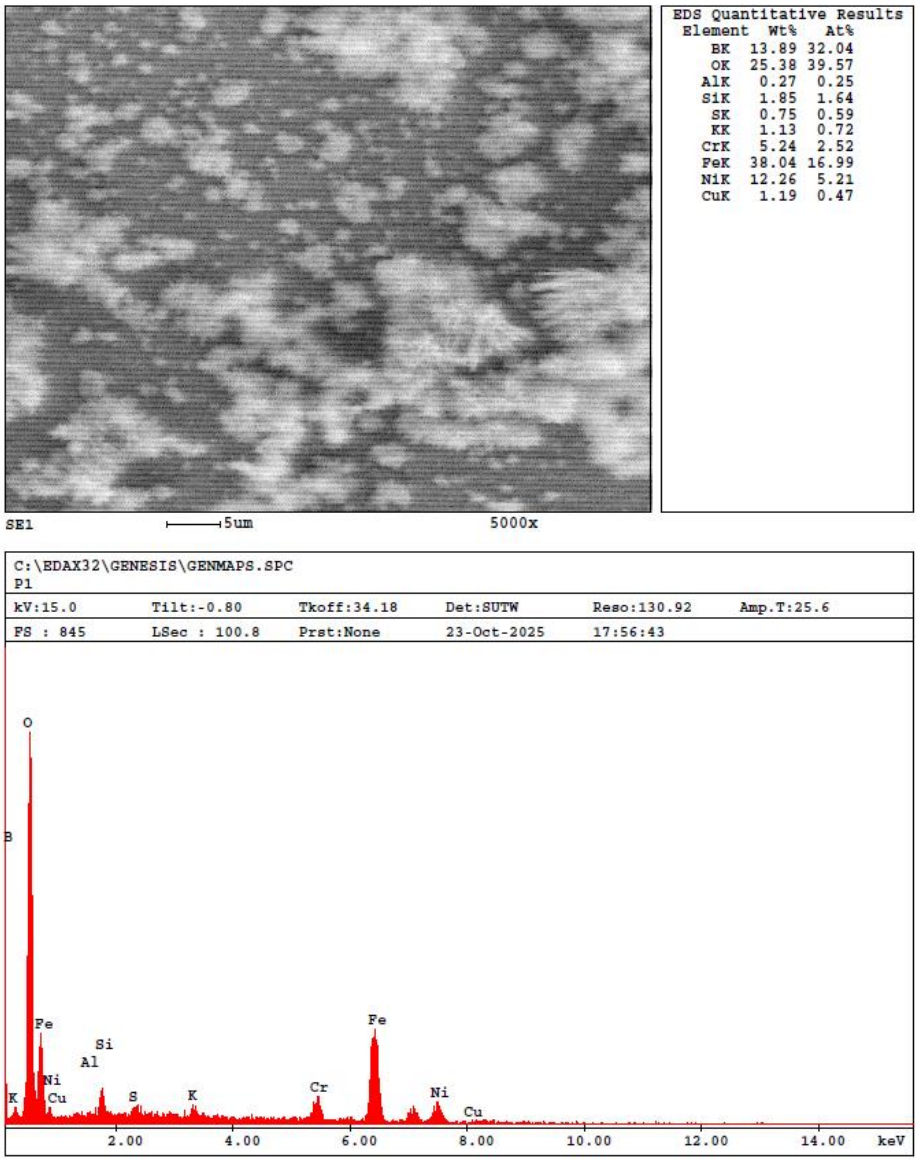

***Fig. 2.** EDX microanalysis for sample P1*

Figure 3 presents the EDX microanalysis for sample P2, prepared with substrate preheating at 60 ºC, tested for corrosion in the K_2SO_4 – 0.5M. A lower degree of corrosion can be observed compared to sample P1. This behavior is determined by the reduction in the cracking tendency of the deposited layer.

THE ANNALS OF "DUNAREA DE JOS" UNIVERSITY OF GALATI
FASCICLE IX. METALLURGY AND MATERIALS SCIENCE
No. 3 - 2026, ISSN 2668-4748; e-ISSN 2668-4756
Article DOI: https://doi.org/10.35219/mms.2026.3.05

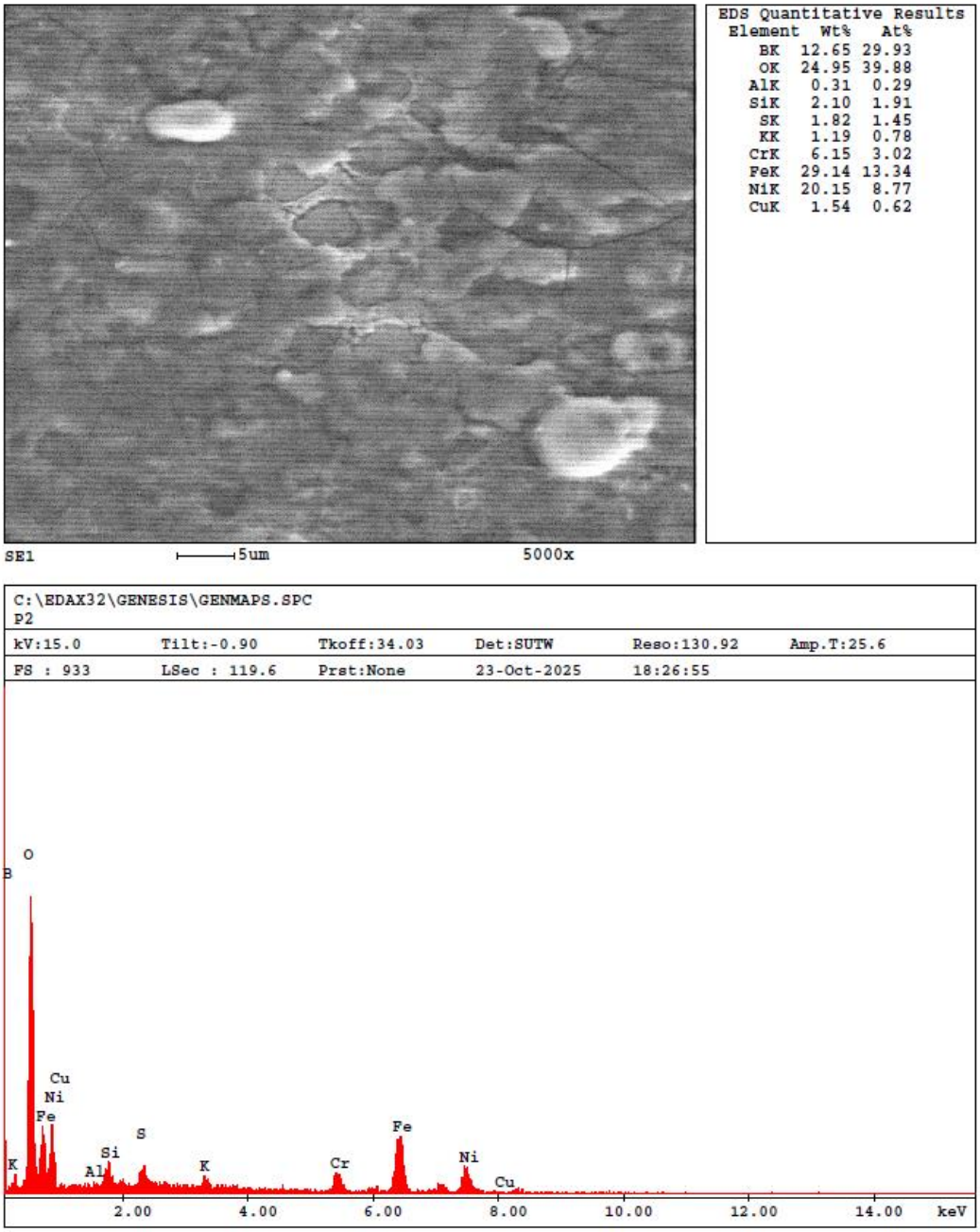

Fig. 3. *EDX microanalysis for sample P2, performed with substrate preheating*

Figure 4 corresponding to the EDX microanalysis for sample P3 (the base material), highlights generalized corrosion, characterized by the presence of corrosion products across the entire surface.

Analysing Figures. 2, 3, and 4, it can be concluded that the presence of chromium and aluminium in nickel-based alloys improves corrosion behavior. The formation of nickel, chromium, and aluminium oxides plays an important role in maintaining their passivity.

THE ANNALS OF "DUNAREA DE JOS" UNIVERSITY OF GALATI
FASCICLE IX. METALLURGY AND MATERIALS SCIENCE
Nº. 3 - 2026, ISSN 2668-4748; e-ISSN 2668-4756
Article DOI: https://doi.org/10.35219/mms.2026.3.05

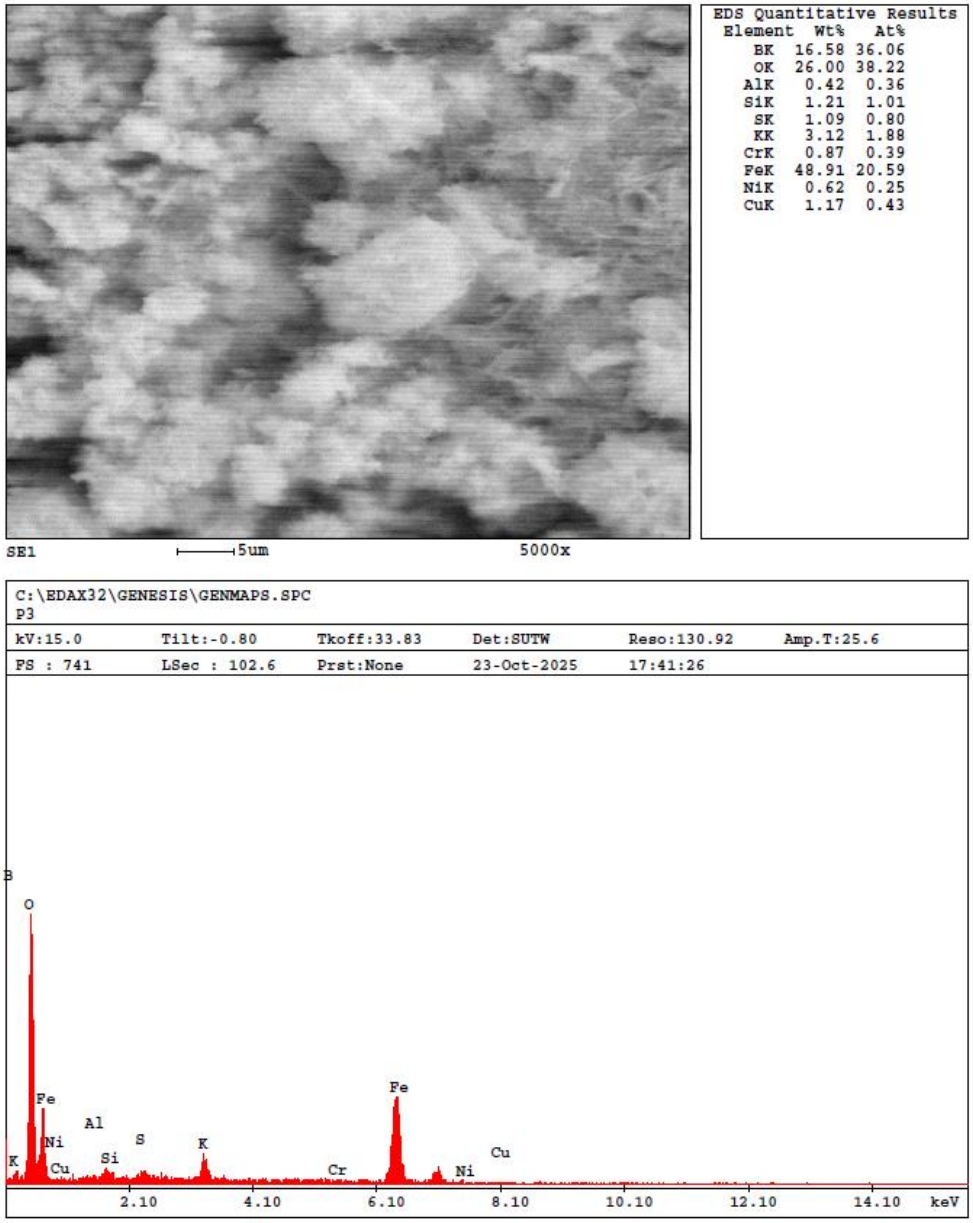

Fig. 4. *EDX microanalysis for sample P3, the base material*

Thus, the EDX investigations carried out on the corroded samples highlight the formation of corrosion products.

This aspect is confirmed by the appearance of oxygen in the resulting spectra. It can be observed that the oxygen percentage reaches its highest value in the base material, where corrosion was most intense.

Furthermore, the percentage of nickel, chromium, and aluminium decreases in sample P1 compared to sample P2 (prepared with substrate preheating), which confirms the appearance of oxides on their surfaces and a differing resistance to corrosion.

3.3. Evaluation of Free Potential (OCP) or Open Circuit Potential

Testing for each sample began with monitoring the free open circuit potential (OCP) after immersion in the K_2SO_4 – 0.5M, solution, aiming to observe their interaction with the corrosive solution. OCP monitoring was performed until a stationary value was reached.

Figure 5 shows the time evolution of the free OCP potential for the analysed samples.

THE ANNALS OF "DUNAREA DE JOS" UNIVERSITY OF GALATI
FASCICLE IX. METALLURGY AND MATERIALS SCIENCE
No. 3 - 2026, ISSN 2668-4748; e-ISSN 2668-4756
Article DOI: https://doi.org/10.35219/mms.2026.3.05

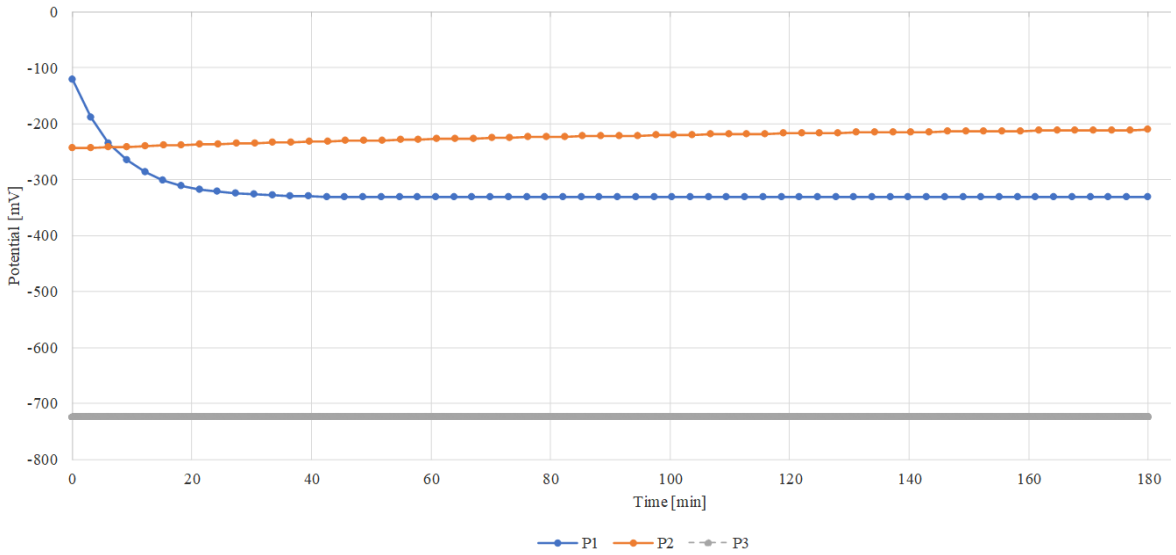

Fig. 5. *Time evolution of the free potential (OCP)*

Analysing Figure 5 regarding the time evolution of the free OCP potential, it can be observed that for sample P2, the corrosion potential stabilizes after approximately 150 minutes from immersion. Its more positive value, ranging between – 243.929 mV and – 210.913 mV indicates a greater tendency toward passivation, which reduces the corrosion process in the 0.5M K_2SO_4 solution, compared to the potential ranging between – 121.61 mV and – 331 mV for sample P1, and – 724 mV for sample P3.

3.4. Potentiodynamic method

This is used to study the kinetics of corrosion processes to determine the passivation range of a material after immersion in a corrosive electrolyte. From the analysis of the polarization curves, the mechanism and rate of the occurring corrosion reactions can be characterized [6, 7].

Figure 6 shows the evolution of polarization resistance over time.

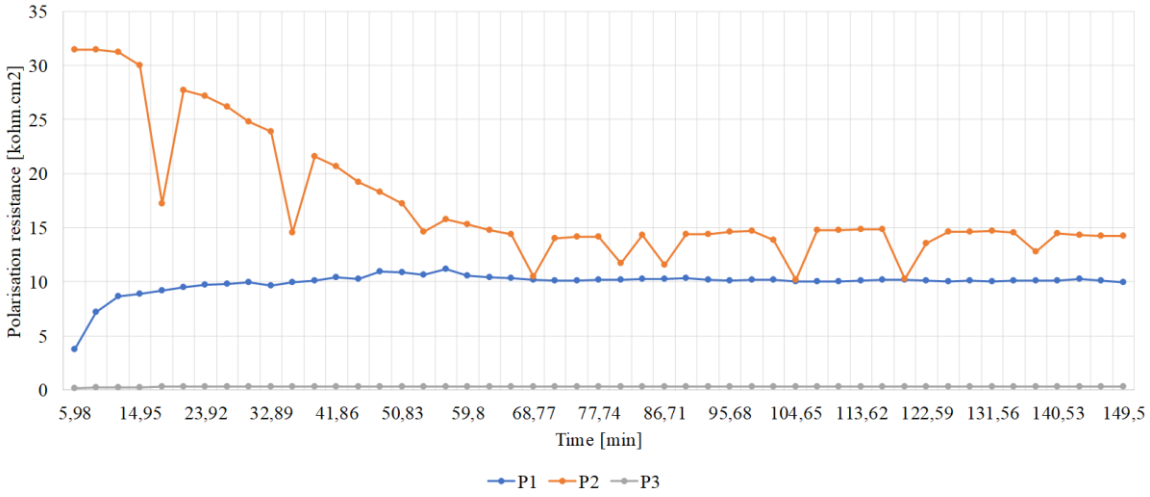

Fig. 6. *Evolution of polarization resistance over time*

Analysing Figure 6, it can be noted that for sample P1, the polarization resistance ranges between 3.77736÷9.9695 KΩcm^2, for sample P2 it varies between 31.4795÷14.2099 KΩcm^2, and for sample P3 it ranges between 0.136786÷0.312298 KΩcm^2. Thus, it can be concluded that sample P2, where the polarization resistance exhibits the highest values, presents the best corrosion resistance.

In the laser cladding process, depending on the parameters used, residual stresses can form between the substrate and the deposited material. These can influence the corrosion behavior. Compressive

THE ANNALS OF "DUNAREA DE JOS" UNIVERSITY OF GALATI
FASCICLE IX. METALLURGY AND MATERIALS SCIENCE
No. 3 - 2026, ISSN 2668-4748; e-ISSN 2668-4756
Article DOI: https://doi.org/10.35219/mms.2026.3.05

stresses appear within the deposited material, while tensile stresses form in the heat-affected zone.

These stresses are generated by the difference in the thermal expansion coefficient between the substrate and the deposition material, as well as by the temperature gradient that occurs during solidification. If the value of these stresses exceeds the ultimate strength of the material, it can lead to crack formation, thereby influencing corrosion behavior.

Thermal stresses can also lead to crack formation.

One way to avoid these shortcomings is to preheat the samples in a furnace, with a flame, or via induction. This leads to a reduction in the temperature gradient between the deposition material and the base material during cooling, and increases melting and deposition rates. Consequently, the productivity of the process is also improved. A larger dilution zone can occur in this case. This aspect can be limited by increasing the deposition speed.

Stresses can also be regulated by establishing and controlling the absorbed power, the track formation speed, and the feed rate.

Sample P2, produced with substrate preheating, is characterized by a lower stress state, which led to better corrosion behavior.

In the case of sample P1, where deposition was carried out without substrate preheating, the corrosive attack occurred along the cracks caused by the presence of residual stresses.

Nevertheless, it can be observed that both samples produced by laser cladding with the Ni-Cr-B-Fe-Al alloy (P1 and P2) exhibit superior corrosion behavior compared to the 1C45 steel substrate.

Figure 7 shows the evolution of the corrosion rate over time.

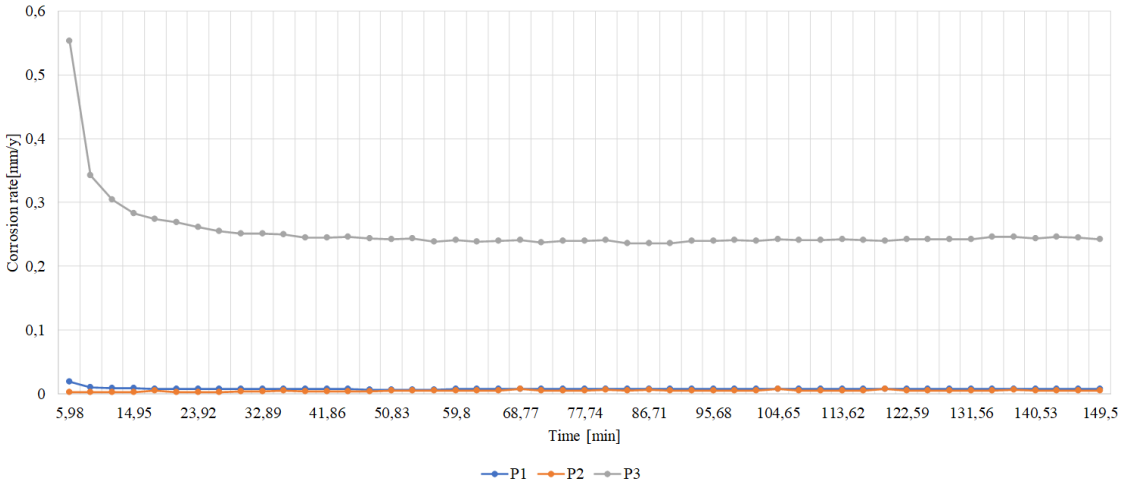

Fig. 7. *Evolution of corrosion rate over time*

Analysing Figure 7, it can be observed that the corrosion rate for sample P1 is between 0.018604÷0.007049 mm/year, for sample P2 it varies between 0.002232÷0.004945 mm/year, and for sample P3 it is between 0.552533÷0.242009 mm/year. Thus, sample P2 exhibits the best corrosion resistance in the 0.5M K_2SO_4.

The laser-deposited samples P1 and P2 exhibit a much lower corrosion rate compared to the substrate material.

Corrosion behavior can be influenced by the existence of pores and cracks within the deposited layer.

The presence of non-metallic inclusions, undispersed hard phase particles, and structural changes induced by laser cladding (imperfections such as dislocations or twins, which influence the stress state) can also affect corrosion behavior.

Table 3 presents the parameters of the solution after corrosion.

Table 3. *Electrochemical parameters of the electrolyte after corrosion*

Sample Code	pH	Electrical Conductivity [mS/cm]	Salinity [g/L]	TDS (Total Dissolved Salts) [ppt]
Initial	7.28	73.4	30.2	52.1
P1	8.02	75.4	21	53.6
P2	7.82	75.2	21.9	53.4
P3	7.75	75.7	19.9	53.8

THE ANNALS OF "DUNAREA DE JOS" UNIVERSITY OF GALATI
FASCICLE IX. METALLURGY AND MATERIALS SCIENCE
Nº. 3 - 2026, ISSN 2668-4748; e-ISSN 2668-4756
Article DOI: https://doi.org/10.35219/mms.2026.3.05

Analysing Table 3, an increase in the pH of the solution after corrosion can be observed. An increase in TDS can also be noticed as a result of the dissolution of the surfaces subjected to corrosion in the aggressive environment. Sparingly soluble compounds may form, which, by accumulating on the surface of the samples, can influence corrosion behavior. Thus, if the deposited film is compact, the surface is protected; if it is porous and permeable, it becomes corroded. In the case of sample P2, the total dissolved salts have the lowest value. An increase in electrical conductivity and a decrease in solution salinity after corrosion are also recorded.

4. Conclusions

The research conducted led to the formulation of the following conclusions:

- Laser cladding constitutes a more efficient alternative for modifying the properties of surface layers than conventional treatment methods (thermal spraying, welding, electrochemical deposition, electrical discharge in gases) because it ensures precisely controllable processing of parts with any configuration, under conditions of low filler material consumption, while achieving a strong metallurgical bond with the substrate, without deformations, and with reduced subsequent machining expenses.

- By controlling the processing parameters, the required physical and mechanical properties for service conditions can be imparted to the surface layer of components; the thickness of the laser-deposited layer must be correlated with the stresses arising from operation under specific known or foreseeable conditions; complex interactions may occur under static or cyclic loading, in corrosive environments, or at elevated temperatures.

- When the feed rate of the filler material is increased to 105mg/s for sample P1, the energy available for melting the substrate decreases, leading to an increase in the thickness and hardness of the deposited layer, as well as a reduction in dilution; residual stresses develop, resulting in the formation of cracks in the deposited layer, which in turn leads to a decrease in corrosion resistance.

- Preheating the substrate to 60 °C in the case of sample P2 and reducing the powder feed rate to 63.9 mg/s results in a reduction of the deposited layer thickness, a decrease in hardness, and a reduction in residual stresses, which leads to better corrosion behavior in the 0.5M K_2SO_4 solution. The dilution zone is larger in this case.

- Since the laser beam provides the energy required to melt the filler material, it is useful to correlate the scanning speed with the filler material feed rate; this, the higher the feed rate, the more the scanning speed should be reduced.

- Laser-deposited samples P1 and P2 with the Ni – Cr – B – Fe – Al alloy exhibit a much better corrosion behavior compared to the substrate material made of 1C45 steel.

- With an increase in the concentration of chromium, nickel, and silicon within the deposited layer, corrosion resistance improves.

- Corrosion can be exacerbated by the lack of chemical or physical homogeneity on the surface, by defects caused by the deposition parameters (pores, discontinuities, cracks), or by subsequent processing methods (which influence roughness and the stress state).

References

[1]. Donțu O., *Laser processing technologies*, Technical Publishing House, Bucureşti, 1985, (Tehnologii de prelucrare cu laser, Editura tehnică, Bucureşti, 1985).
[2]. Schneider M. F., *Laser cladding with powder*, Ph. D. Thesis University of Twente, Enschede, Netherlands, 1998.
[3]. Gedda H., *Laser surface cladding - a literature survey*, Lulea University of Technology, Division of Materials Processing, 2000.
[4]. Toyserkani E., *et al.*, *Laser Cladding*, U.S.A, 2005.
[5]. Boiciuc S., *Research on laser cladding with injected powder*, PhD thesis, Galaţi 2010, (Cercetări privind depunerea laser cu pulbere injectată, teză de doctorat, Galaţi 2010).
[6]. Dumitraşcu V. M., *Functional surfaces obtained by electrochemical methods and their characterization*, Galaţi 2018, (Suprafețe funcționale obținute prin metode electrochimice și caracterizarea acestora, Galaţi 2018).
[7]. Cârâc G., Stefan C., *Electrochemistry – fundamental principles and applications* (Electrochimie – principii fundamentale și aplicații), Editura GUP, 2012).

THE ANNALS OF "DUNAREA DE JOS" UNIVERSITY OF GALATI
FASCICLE IX. METALLURGY AND MATERIALS SCIENCE
N°. 3 - 2026, ISSN 2668-4748; e-ISSN 2668-4756
Article DOI: https://doi.org/10.35219/mms.2026.3.06

END-OF-LIFE VEHICLE RECYCLING IN THE CONTEXT OF THE CIRCULAR ECONOMY

Lizica Simona PARASCHIV, Mihaela Alexandra GHEORGHICA, Spiru PARASCHIV
"Dunarea de Jos" University of Galati, Romania
e-mail: sparaschiv@ugal.ro

ABSTRACT

This paper synthesises, from an industrial engineering management perspective, the recycling of end-of-life vehicles (ELVs) within the European transition towards a circular economy. The study integrates three levels of analysis: the theoretical foundations of Life Cycle Assessment (LCA) under ISO 14040 and ISO 14044, the European and Romanian legal and institutional framework built around Directive 2000/53/EC and its national transposition and an applied case study carried out at an authorised ELV collection and treatment centre in Romania, where the complete technological flow — reception, de-pollution, dismantling, sorting and recovery — is analysed for a representative vehicle (Volkswagen Golf IV). The results show that a properly organised treatment centre can reach recovery rates above 90%, approaching the EU target of 95% set by Directive 2000/53/EC. The application of quality-management tools allows critical points of the technological flow to be identified and corrective measures to be substantiated, leading to reduced hazardous-liquid losses, improved traceability of reusable parts, and shorter average vehicle processing time. The paper also offers a comparative view of emerging challenges — automotive shredder residue (ASR) and electric-vehicle battery recycling and puts forward recommendations for digitalising traceability and optimising sorting processes.

KEYWORDS: end-of-life vehicles, circular economy, life cycle assessment, automotive recycling, quality management, environmental pollution

1. Introduction

End-of-life vehicle (ELV) recycling has become a fundamental component of the global sustainable development strategy, particularly in the context of a continuously expanding automotive industry that generates substantial volumes of waste and places considerable pressure on natural resources. Each year, approximately 12–15 million vehicles reach the end of their service life within the European Union alone [8], representing not only a significant waste stream but also an important secondary source of recoverable and recyclable materials - including steel, aluminium, copper, glass, and plastics - which can be reintroduced into the economic cycle. This process contributes to reducing the consumption of virgin raw materials and mitigating environmental impacts.

From a management perspective, ELV recycling is closely aligned with the principles of the circular economy, which promote efficient resource utilization, product life extension, and the minimization of waste disposal. The implementation of efficient collection, treatment, and recovery systems contributes not only to environmental protection but also to the development of a more resource-efficient and sustainable industrial model. This perspective is increasingly supported by recent international literature, which recognizes ELV management as an emerging research field situated at the intersection of industrial engineering, waste management, and environmental policy [10, 14].

Romania has aligned its national legislative framework with European Union regulations through the transposition of Directive 2000/53/EC on End-of-Life Vehicles [3]. The directive establishes clear responsibilities for vehicle manufacturers and economic operators involved in the collection and treatment of ELVs, imposing strict environmental, safety, and traceability requirements. Consequently, automotive recycling can no longer be regarded

THE ANNALS OF "DUNAREA DE JOS" UNIVERSITY OF GALATI
FASCICLE IX. METALLURGY AND MATERIALS SCIENCE
N°. 3 - 2026, ISSN 2668-4748; e-ISSN 2668-4756
Article DOI: https://doi.org/10.35219/mms.2026.3.06

solely as a waste disposal activity, but rather as a complex industrial process requiring rigorous planning, substantial infrastructure investments, and compliance with well-defined technical and organizational standards.

The present study aims to analyse the recycling process of end-of-life vehicles from the perspective of industrial engineering management, focusing on:

- the theoretical foundations of Life Cycle Assessment (LCA) and circular economy principles applied to the automotive sector;
- the European and Romanian legal and institutional framework governing ELV management;
- the organization and technological workflow of authorized collection and treatment facilities;
- an applied case study illustrating how these principles are implemented in the day-to-day activities of an authorized recycling operator. The primary objective is to highlight opportunities for improving both the operational efficiency and environmental performance of ELV recycling processes, thereby contributing to the achievement of national and European recycling targets.

2. Theoretical Framework of End-of-Life Vehicle Recycling

2.1. Life Cycle Assessment (LCA) According to ISO 14040 and ISO 14044 Standards

Life Cycle Assessment (LCA) is one of the most widely recognized methodologies for evaluating the environmental impacts associated with products, processes, and services throughout their entire life cycle, from raw material extraction to final disposal ("cradle-to-grave"). The methodological framework for LCA is internationally standardized through ISO 14040, which establishes the principles and general framework, and ISO 14044, which specifies the technical requirements and methodological guidelines for conducting LCA studies, emphasizing transparency, consistency, and comparability of results [1, 2].

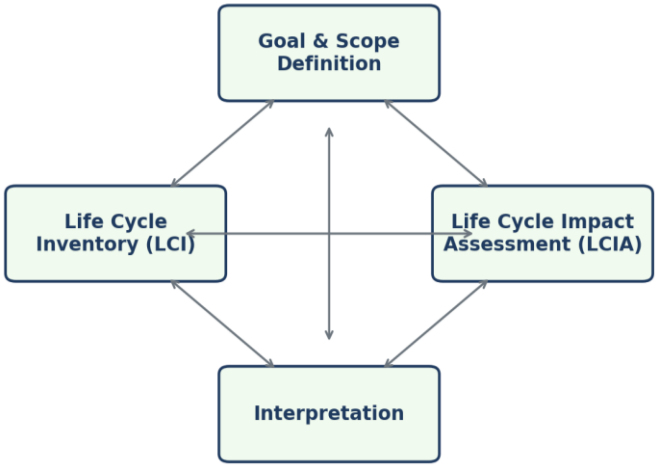

Fig. 1. *Methodological Framework of Life Cycle Assessment According to ISO 14040 and ISO 14044*

A standard LCA study comprises four interrelated phases: goal and scope definition, life cycle inventory (LCI) analysis, involving the quantification of input and output flows, life cycle impact assessment (LCIA), and interpretation of the results [1, 2]. These four phases are not strictly sequential but are connected through an iterative interpretation process, as illustrated in Figure 1.

In the automotive industry, the application of Life Cycle Assessment (LCA) is essential because vehicles are complex products characterized by high consumption of materials, energy, and natural resources. Their environmental impact is not limited to the use phase but also extends to the stages of raw material extraction, manufacturing, maintenance, and end-of-life management. Consequently, validated LCA studies are increasingly regarded as a "market passport" for automotive manufacturers, providing transparent, standardized, and comparable information on the environmental performance of vehicles throughout their entire life cycle [1, 2].

By applying the LCA methodology, different technological scenarios and design alternatives can be systematically evaluated, ranging from material selection and manufacturing processes to end-of-life vehicle (ELV) treatment and recycling strategies. This approach provides an objective scientific basis for environmental management decisions, sustainable product development, and the formulation of circular economy and sustainability policies.

THE ANNALS OF "DUNAREA DE JOS" UNIVERSITY OF GALATI
FASCICLE IX. METALLURGY AND MATERIALS SCIENCE
N°. 3 - 2026, ISSN 2668-4748; e-ISSN 2668-4756
Article DOI: https://doi.org/10.35219/mms.2026.3.06

2.2. Vehicle Life Cycle

The life cycle of a vehicle encompasses all stages through which it passes, beginning with design and manufacturing, continuing through the use and maintenance phases, and concluding with end-of-life management and recycling (Figure 2). Decisions made during the design stage have a direct influence on the vehicle's recyclability, production costs, and long-term environmental impact. This principle is widely recognized in the scientific literature as Design for Recycling (DfR) or Eco-design, emphasizing the integration of environmental considerations into product development from the earliest design phases [13].

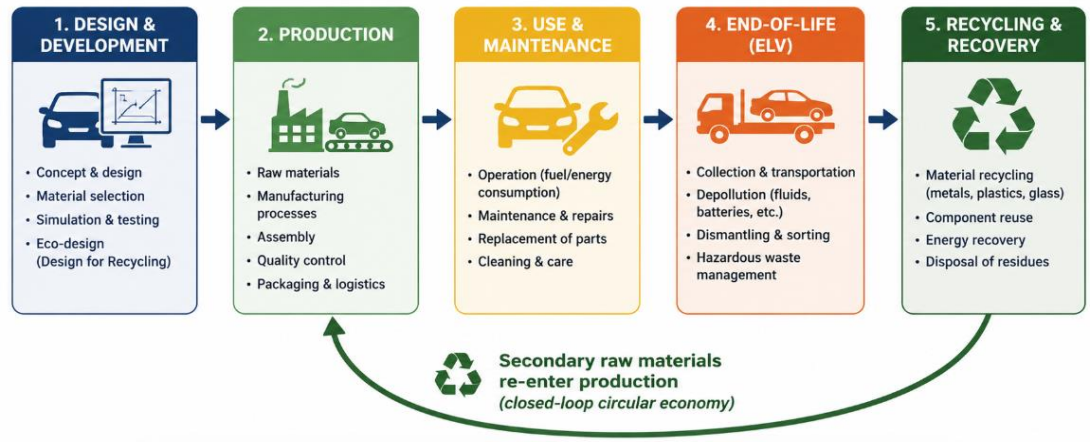

Fig. 2. *Life Cycle Stages of a Motor Vehicle, Including the Closed-Loop Reintegration of Secondary Raw Materials into the Production Process.*

The vehicle life cycle comprises the following stages:

• Design and development – during this stage, the vehicle's structural characteristics, material selection, and technological solutions are defined. Decisions made at this phase have a direct influence on the vehicle's future recyclability, resource efficiency, and overall environmental performance.

• Production – involves complex industrial manufacturing processes characterized by significant consumption of energy and raw materials, as well as the generation of emissions and industrial waste.

• Use and maintenance – the longest phase of the vehicle life cycle, encompassing fuel or energy consumption, pollutant emissions, routine maintenance, and the replacement of worn or damaged components.

• End-of-life (ELV) – the stage at which the vehicle is no longer functional or economically viable for continued operation. The vehicle is transferred to an authorized treatment facility, where a Certificate of Destruction (CoD) is issued in accordance with the applicable regulatory requirements.

• Recycling and recovery – the final stage of the life cycle, during which the vehicle undergoes depollution, dismantling, and material separation. Recoverable materials are recycled and reintroduced into the production cycle as secondary raw materials. According to European legislation, at least 95% of the average vehicle weight must be recovered, of which a minimum of 85% must be achieved through material recycling [3].

2.3. Circular Economy Applied to the Automotive Industry

The circular economy is a sustainable development model that aims to keep materials and resources in productive use for as long as possible through reuse, recycling, remanufacturing, and recovery, thereby minimizing waste generation and reducing pressure on natural resources. Unlike the traditional linear economic model ("take–make–consume–dispose"), the circular economy promotes the closing of product life cycle loops by reintegrating secondary materials into economic and industrial processes, thus improving resource efficiency and supporting long-term sustainability (Figure 3) [7, 9].

At the European Union level, the Second Circular Economy Action Plan (CEAP), adopted in March 2020 as a key component of the European Green Deal, identifies the automotive sector as one of the priority value chains, alongside electronics, batteries, packaging, textiles, and construction, owing to its significant potential for circularity [7, 9]. This strategic direction has recently been reinforced through a provisional agreement between the

THE ANNALS OF "DUNAREA DE JOS" UNIVERSITY OF GALATI
FASCICLE IX. METALLURGY AND MATERIALS SCIENCE
Nº. 3 - 2026, ISSN 2668-4748; e-ISSN 2668-4756
Article DOI: https://doi.org/10.35219/mms.2026.3.06

European Parliament and the Council on a new regulation governing the circularity of vehicle design, manufacturing, and end-of-life vehicle (ELV) management. The proposed regulation introduces mandatory targets for recycled plastic content in new vehicles - at least 15% within six years and 25% within ten years after its entry into force - as well as design requirements aimed at facilitating component dismantling by authorized treatment facilities [8].

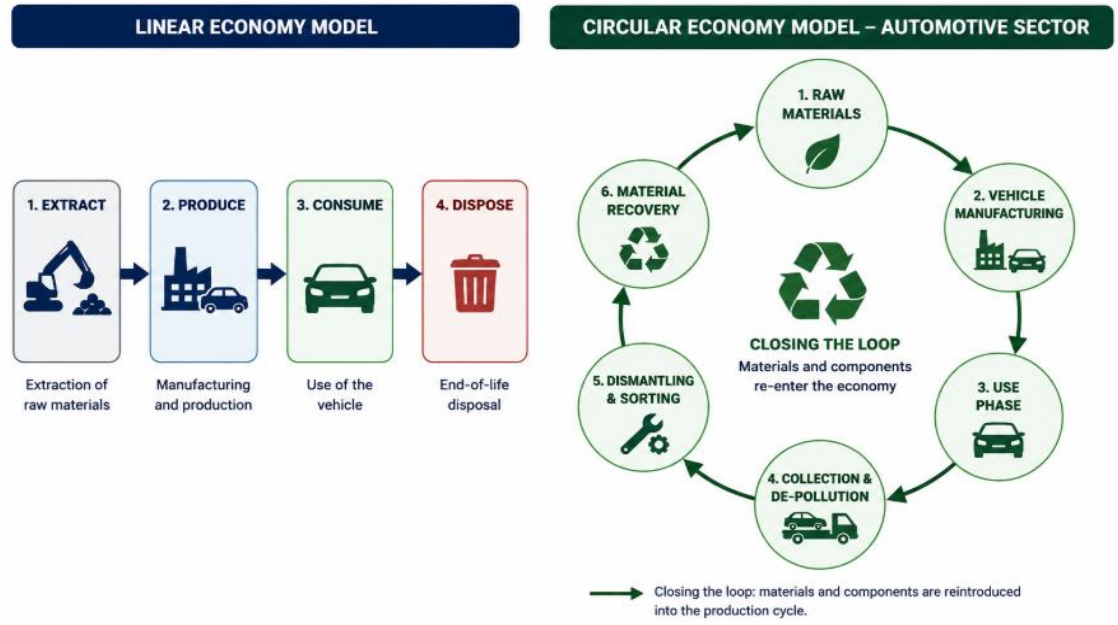

***Fig. 3**. Comparison between the Linear Economy Model and the Circular Economy Model Applied to the Automotive Industry*

End-of-life vehicles (ELVs) constitute an important source of recoverable secondary raw materials. The average material composition of a passenger vehicle (Figure 4) shows that ferrous metals account for the largest proportion of the total vehicle mass, followed by plastics, non-ferrous metals, rubber, glass, and a heterogeneous residual fraction known as Automotive Shredder Residue (ASR) [17-18, 22]. The environmental impacts associated with these materials differ considerably. In particular, the recycling of ferrous and non-ferrous metals provides substantial energy savings compared with the production of primary metals, thereby significantly reducing the climate impact and resource consumption of the automotive sector [29, 30, 32].

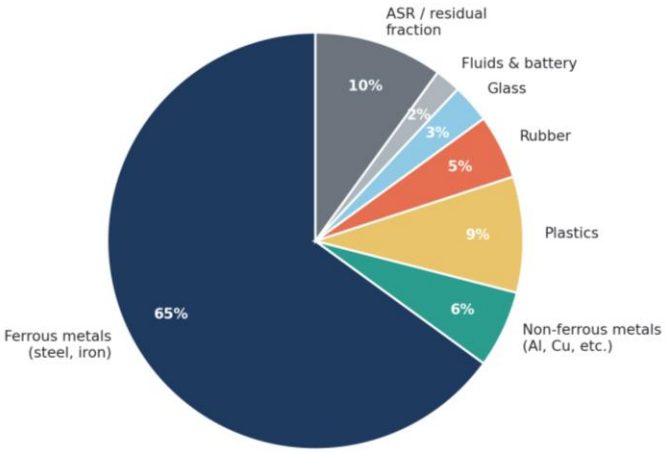

***Fig. 4.** Estimated Average Material Composition of an End-of-Life Vehicle, Expressed as a Percentage of Total Vehicle Weight*

THE ANNALS OF "DUNAREA DE JOS" UNIVERSITY OF GALATI
FASCICLE IX. METALLURGY AND MATERIALS SCIENCE
Nº. 3 - 2026, ISSN 2668-4748; e-ISSN 2668-4756
Article DOI: https://doi.org/10.35219/mms.2026.3.06

A clear definition of the terminology used in the field is essential for a rigorous analysis. Recycling refers to the process of converting waste materials into secondary raw materials that can be used in the manufacture of new products. Reuse involves the direct use of products or functional components without substantial industrial processing. Recovery encompasses both material recycling and energy recovery from non-recyclable waste, while treatment refers to the complete set of operations including depollution, dismantling, sorting, and preparation of materials for recycling or environmentally sound disposal [3, 4].

A comprehensive understanding of the vehicle life cycle, combined with the principles of the circular economy and the application of the ISO 14040 and ISO 14044 Life Cycle Assessment (LCA) standards, provides the theoretical foundation for end-of-life vehicle (ELV) recycling. The integration of these concepts enables the reduction of environmental impacts, improves resource and economic efficiency, and supports the transition toward a more sustainable and circular automotive sector.

3. Legal and Institutional Framework in Romania and the European Union

The collection, treatment, and recycling of end-of-life vehicles (ELVs) are governed by a comprehensive legal framework established at both the European Union and national levels. This regulatory framework aims to prevent the adverse environmental impacts associated with end-of-life vehicles, promote the efficient use of natural resources, and clearly define the responsibilities of all stakeholders involved in the management of vehicles reaching the end of their service life.

3.1. European Legislation

Directive 2000/53/EC on End-of-Life Vehicles constitutes the principal European legislative instrument governing the management of ELVs [3]. Its primary objective is to prevent waste generation from vehicles while promoting the reuse, recycling, and recovery of vehicle components and materials. Among its key provisions are restrictions on the use of hazardous substances in vehicle manufacturing - including lead, mercury, cadmium, and hexavalent chromium, except in specifically regulated applications - the obligation for vehicle manufacturers to ensure the free take-back of end-of-life vehicles, and the establishment of quantitative targets for reuse, recycling, and recovery.

The final target, applicable since 1 January 2015, requires a minimum reuse and recovery rate of 95% of the average vehicle weight, of which at least 85% must be achieved through reuse and material recycling, while the remaining fraction may be fulfilled through energy recovery [3, 17, 18, 22].

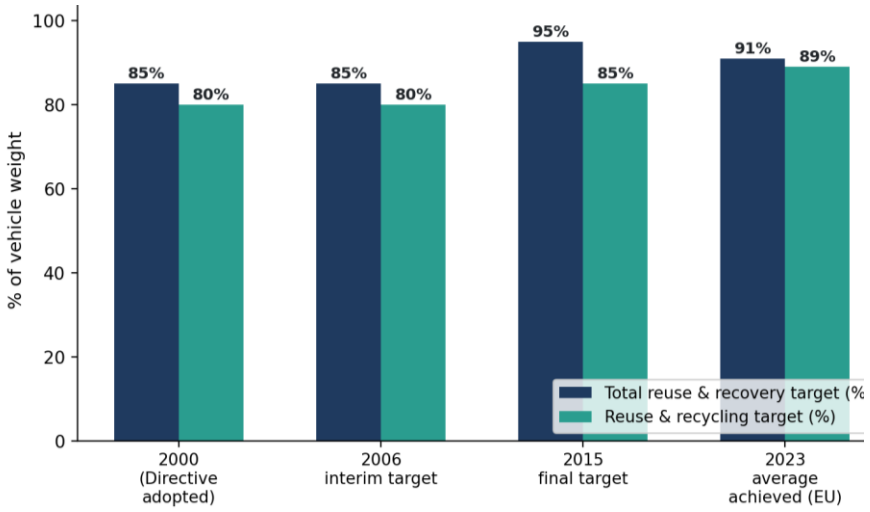

Fig. 5. *Evolution of European End-of-Life Vehicle (ELV) Recovery and Recycling Targets Compared with the Average Recovery Rate Achieved*

The evolution of these regulatory targets, together with the average recovery rates achieved across the European Union, is presented in Figure 5. As illustrated, a persistent gap exists between the mandatory 95% recovery target and the actual average recovery performance, estimated at approximately 89–91%. According to the scientific literature, this discrepancy is primarily attributed to the difficulty of recovering the Automotive Shredder Residue (ASR) fraction, a heterogeneous waste stream that continues to be disposed of predominantly in landfills due to the limited availability of

THE ANNALS OF "DUNAREA DE JOS" UNIVERSITY OF GALATI
FASCICLE IX. METALLURGY AND MATERIALS SCIENCE
N°. 3 - 2026, ISSN 2668-4748; e-ISSN 2668-4756
Article DOI: https://doi.org/10.35219/mms.2026.3.06

economically and technically viable recovery technologies [17, 18, 21].

The European regulatory framework has been substantially strengthened in recent years through the Second Circular Economy Action Plan (CEAP, 2020) [7, 9] and, more recently, through a provisional agreement (2025) between the European Parliament and the Council of the European Union on a new Regulation on Vehicle Circularity. This regulation will progressively replace Directive 2000/53/EC and introduce design requirements aimed at improving vehicle dismantlability, mandatory recycled-content targets for plastics, steel, and aluminium, as well as a strengthened Extended Producer Responsibility (EPR) framework [8].

In addition, Regulation (EC) No. 1907/2006 (REACH) governs the Registration, Evaluation, Authorisation and Restriction of Chemicals used in automotive components. The REACH Regulation has direct implications for vehicle depollution operations and the management of hazardous waste generated during the treatment of end-of-life vehicles, ensuring a higher level of environmental and human health protection throughout the recycling process [6].

3.2. National Legislation

Romania has transposed the European regulatory requirements through Law No. 212/2015 on the Management of Vehicles and End-of-Life Vehicles (ELVs) [4] and Government Emergency Ordinance No. 92/2021 on Waste Management [5]. These legislative acts establish the responsibilities of vehicle owners, manufacturers, and economic operators involved in the collection, treatment, recovery, and recycling of end-of-life vehicles, while also defining the minimum technical requirements applicable to authorized collection and treatment facilities.

The national legislation further specifies the requirements regarding the location and infrastructure of authorized treatment facilities, the mandatory equipment necessary for depollution and dismantling operations, the documentation required upon vehicle handover - including the Certificate of Destruction (CoD), the Vehicle Registration Certificate, and the Vehicle Handover Report - as well as the reporting obligations imposed on operators with respect to the competent environmental authorities.

3.3. Authorities Responsible for the Authorization and Supervision of ELV Recycling Facilities

The legal operation of an authorized end-of-life vehicle (ELV) collection and treatment facility requires the involvement of several public authorities, each exercising specific regulatory, authorization, monitoring, and enforcement responsibilities. The main institutions and their respective roles are summarized in Table 1.

From the perspective of industrial engineering management, the systematic planning of the authorization process is essential for optimizing the time, costs, and resources required to establish an end-of-life vehicle (ELV) collection and treatment facility. Each of the authorities listed in Table 1 requires specific documentation and compliance inspections, while the logical sequence of obtaining the necessary permits—urban planning approval → RAR technical authorization → environmental permit → water management permit (where applicable) → operating authorization—has a direct influence on the overall duration and efficiency of the investment project.

Table 1. *The main institutions and their respective roles in authorization and supervision of ELV Recycling Facilities*

Authority	Main Responsibilities	Issued Document / Authorization
Romanian Automotive Registry (RAR)	Technical authorization of vehicle dismantling and treatment activities	ELV Treatment Authorization issued by RAR
Environmental Protection Agency (EPA)	Assessment of environmental impacts and verification of environmental protection infrastructure	Environmental Permit (typically valid for five years)
Romanian Waters National Administration – ANAR	Regulation of water resource use and wastewater discharge	Water Management Permit
Inspectorate for Emergency Situations (ISU)	Verification of compliance with fire prevention and fire safety regulations	Fire Safety Approval / Fire Safety Permit
Local Municipality / Local Public Administration	Verification of compliance with urban planning regulations and issuance of the operating approval	Urban Planning Certificate and Operating Approval

THE ANNALS OF "DUNAREA DE JOS" UNIVERSITY OF GALATI
FASCICLE IX. METALLURGY AND MATERIALS SCIENCE
Nº. 3 - 2026, ISSN 2668-4748; e-ISSN 2668-4756
Article DOI: https://doi.org/10.35219/mms.2026.3.06

4. Organization of Automotive Recycling Facilities and Technological Workflow

4.1. Site Selection and Minimum Infrastructure Requirements

The selection of an appropriate site for an end-of-life vehicle (ELV) collection and treatment facility must consider several technical and regulatory factors, including accessibility for heavy vehicles, the minimum distance from residential areas, the availability of essential utilities (water supply, sewerage, and three-phase electrical power), the required site area (typically 1.000–2.000 m², depending on the treatment capacity), and the applicable urban planning and land-use regulations. Furthermore, the facility should not be in flood-prone areas, protected environmental zones, or in the vicinity of drinking water sources.

The minimum mandatory infrastructure includes an impermeable reinforced concrete platform resistant to aggressive chemical substances, a hazardous liquid collection system for waste oils, fuels, brake fluid, antifreeze, refrigerants, and battery acids, dedicated storage areas for untreated and depolluted ELVs, reusable components, and non-recoverable waste, as well as the technical equipment required for dismantling operations, such as vehicle lifts or ramps, fluid extraction systems, dismantling tools, and containers for the separate collection of recyclable materials.

5. Technological Workflow for End-of-Life Vehicle Recycling

The technological workflow of end-of-life vehicle (ELV) recycling comprises the sequence of organized operations through which a vehicle is received, treated, and recovered in accordance with safety regulations and applicable legal requirements.

Fig. 6. *Technological Workflow of an Authorized End-of-Life Vehicle (ELV) Treatment Facility*

The process includes successive stages of collection, storage, depollution, dismantling, material sorting, and resource recovery (Figure 6), with the primary objectives of minimizing environmental impacts, maximizing resource efficiency, and achieving the recycling and recovery targets established by European and national legislation.

5.1. Collection and Traceability of End-of-Life Vehicles

The collection of end-of-life vehicles (ELVs) may be carried out through several channels, including direct handover by the vehicle owner (the most common method, in exchange for a Certificate of Destruction), government incentive schemes promoting vehicle fleet renewal (e.g., the "Rabla" scrappage program), partnerships with automotive repair workshops and dealerships, or vehicle collection services for non-operational vehicles directly from the owner's premises.

Upon delivery, the vehicle owner is required to provide an identity document, the vehicle registration certificate, the vehicle identification document, and a vehicle handover protocol. In return, the authorized treatment facility issues a Certificate of Destruction (CoD), which is a mandatory document for the deregistration of the vehicle from the records of the Romanian Automotive Registry (RAR) and the Directorate for Driving Licences and Vehicle Registration (DRPCIV).

Traceability - the process through which the movement and treatment of a vehicle are monitored and documented from its reception until the completion of all treatment operations - is essential for preventing the illegal abandonment of vehicles, ensuring accurate reporting of recycled quantities, and fulfilling the obligations established under the Extended Producer Responsibility (EPR) framework. An increasing number of authorized treatment

THE ANNALS OF "DUNAREA DE JOS" UNIVERSITY OF GALATI
FASCICLE IX. METALLURGY AND MATERIALS SCIENCE
N°. 3 - 2026, ISSN 2668-4748; e-ISSN 2668-4756
Article DOI: https://doi.org/10.35219/mms.2026.3.06

facilities are implementing digital traceability systems, enabling the electronic registration of each vehicle, the integration of supporting documentation, and the automatic generation of reports required by public authorities. These systems improve operational efficiency while ensuring regulatory compliance.

5.2. Depollution, Dismantling, and Material Sorting

Depollution constitutes the first mandatory stage of the treatment process. It involves the removal of all hazardous substances and fluids, including the remaining fuel in the tank, engine oil, transmission oil, brake fluid, power steering fluid, and engine coolant, as well as the recovery of refrigerants from air-conditioning systems. In addition, the battery - which contains sulfuric acid and lead - together with airbags, seatbelt pretensioners, filters, and other potentially hazardous components, must be safely removed before further processing. All extracted fluids are required to be stored in properly labelled, leak-proof containers in accordance with environmental regulations.

The dismantling stage aims primarily at recovering reusable components, such as engines, alternators, mirrors, windows, and alloy wheels, which can subsequently be marketed as second-hand spare parts, thereby reducing the demand for newly manufactured components produced from virgin raw materials. Components that cannot be reused are subsequently sorted according to material type - including ferrous and non-ferrous metals, plastics, rubber, glass, and electrical cables - to facilitate their efficient recycling and recovery.

5.3. Material and Energy Recovery: The Challenge of Automotive Shredder Residue (ASR)

Following the sorting process, the recovered materials are delivered to authorized recycling facilities. Ferrous and non-ferrous metals are transported to specialized smelters, plastics are processed by polymer recycling facilities, while rubber and glass are directed to dedicated recycling or recovery streams.

Metal recycling provides substantial energy savings compared with primary production from virgin raw materials. Aluminium recycling can reduce energy consumption by up to 95% compared with primary aluminium production from bauxite, copper recycling saves approximately 85%, while steel recycling typically reduces energy requirements by 60–75%, depending on the recycling technology employed (Figure 7) [29-30, 32].

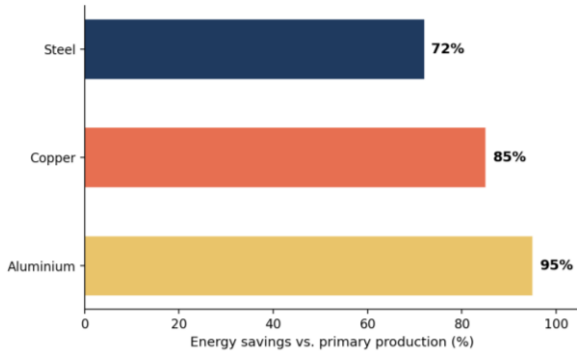

Fig. 7. *Energy Savings Achieved through the Recycling of Metals Recovered from End-of-Life Vehicles Compared with Production from Primary Raw Materials*

The fraction that cannot be recovered through mechanical sorting—Automotive Shredder Residue (ASR)—accounts, according to the scientific literature, for approximately 20–25% of the mass of a vehicle and represents the main barrier to achieving the 95% recovery target established by Directive 2000/53/EC [17, 18, 21, 22]. ASR has a heterogeneous composition, consisting of plastics, rubber, glass, textiles, foams, and metallic dust, which makes its separation and recovery using conventional technologies difficult [24, 33]. Consequently, it is currently disposed of predominantly in landfills [18, 22]. Post-shredder technologies (PSTs), based either on additional mechanical separation or on thermal treatment for energy recovery, are considered in the scientific literature to be the main solution for closing this recovery gap [17, 21].

5.4. An Emerging Challenge: Recycling of Electric Vehicle Batteries

The expansion of the electric vehicle fleet is generating a new category of waste that affects the conventional technological workflow of automotive recycling: lithium-ion batteries. Recent studies indicate that the current recycling rate of these batteries remains low, estimated at 5–10% worldwide, mainly due to the lack of standardized methods for assessing battery condition, the high costs associated with collection and transportation (since batteries are classified as hazardous waste), and the fragmented regulatory framework [23-27]. The materials recovered through battery recycling, including lithium, cobalt, nickel, and manganese, can reduce the carbon footprint of new batteries by up to 40% while decreasing dependence on critical primary raw materials, whose extraction is often associated with significant environmental and geopolitical risks

THE ANNALS OF "DUNAREA DE JOS" UNIVERSITY OF GALATI
FASCICLE IX. METALLURGY AND MATERIALS SCIENCE
N°. 3 - 2026, ISSN 2668-4748; e-ISSN 2668-4756
Article DOI: https://doi.org/10.35219/mms.2026.3.06

[28]. The new European Batteries Regulation establishes mandatory recycled-content targets (at least 6% lithium and nickel and 16% cobalt by 2031) [28], which will require authorized ELV treatment facilities to progressively develop specific expertise and procedures for the safe dismantling of traction batteries, separate from the conventional depollution process.

6. Case Study: Recycling Centre

To illustrate how the theoretical principles and legal requirements presented above are implemented in practice, an end-of-life vehicle (ELV) collection and treatment centre in Romania was analysed. The facility operates in the field of waste collection and recovery, including recyclable materials originating from end-of-life vehicles. The site benefits from convenient access to the road transport network, facilitating the collection and transportation of vehicles from private individuals, economic operators, and other entities.

6.1. Application of the ELV Guideline Stages

The analysed centre implements each stage specified in the ELV Best Practice Guidelines. Vehicle collection is carried out either directly at the facility or through the company's own fleet. Each vehicle is registered in the record system and its documentation is verified before the Certificate of Destruction is issued. Depollution is performed on an impermeable platform equipped with a leakage collection system and an oil separator, where all hazardous fluids are removed and batteries and airbags are dismantled. Dismantling and material sorting are carried out by qualified personnel using dedicated equipment, including vehicle lifts, presses, and power tools. Reusable components are cleaned, labelled, and stored in a covered area, while non-reusable components are sorted according to material type. The sorted materials are delivered to authorized recycling companies, and hazardous waste is periodically transferred to specialized operators for neutralization and disposal.

Through this organization, the centre achieves a recovery rate exceeding 92%, which is reported annually to the Environmental Protection Agency, approaching the European target of 95% [3].

6.2. Practical Example: Workflow of a Volkswagen Golf IV

To illustrate the application of the ELV guideline at the individual vehicle level, the treatment process of a Volkswagen Golf IV, equipped with a 1.4-1.6 L gasoline engine complying with the Euro 3 emission standard, was analysed. The vehicle had an unladen weight of approximately 1.150 kg, was more than 20 years old, in non-operational condition due to major engine failure and severe body corrosion and did not have a valid periodic technical inspection.

Upon reception, the owner's documents and the vehicle documentation were verified, after which the centre issued the Certificate of Destruction. The depollution process consisted of removing the residual fuel, lubricating oils, and technical fluids, together with the battery and pyrotechnic components. During dismantling, several components in good condition - including the engine, radiator, and alloy wheels - were recovered for resale as second-hand spare parts, while other components, such as the windshield, side windows, and interior upholstery, were separated for glass recycling and textile/composite recycling streams, respectively. Non-ferrous metals and end-of-life tyres were also separated for dedicated recovery processes. The overall treatment of this individual vehicle confirmed that a recovery rate exceeding 90% can be achieved through the combination of complete depollution, dismantling focused on component reuse, and appropriate material sorting.

6.3. Quality Management in the ELV Treatment Process

To identify and correct operational deficiencies, the analysed centre applies the PDCA (Plan–Do–Check–Act) continuous improvement cycle.

The risks associated with the main operations of the technological workflow - depollution, dismantling, sorting, and storage - were evaluated based on the criteria of severity, probability of occurrence, and defect detectability. Among the risks identified as having high priority were the incomplete removal of brake fluid, the accidental mixing of plastic and metallic materials during the sorting process, and the improper storage of used batteries.

The causes of the identified non-conformities were determined, making it possible to move from the simple identification of symptoms (for example, hazardous liquid leaks) to the identification of their underlying causes (such as the absence of standardized inspection procedures). Based on this analysis, solutions, devices, and procedures for error prevention by design were proposed, including liquid presence sensors in collection containers, colour-coded trays for the visual sorting of plastic and metal components, and labelled containers with lockable lids for the storage of used batteries.

THE ANNALS OF "DUNAREA DE JOS" UNIVERSITY OF GALATI
FASCICLE IX. METALLURGY AND MATERIALS SCIENCE
Nº. 3 - 2026, ISSN 2668-4748; e-ISSN 2668-4756
Article DOI: https://doi.org/10.35219/mms.2026.3.06

Table 2. *Quality Management in the ELV Treatment Process*

Process Stage / Identified Risk	Observed Non-conformity	Proposed Solution	Type of Control
Fluid removal (depollution)	Incomplete removal of brake fluid	Liquid presence sensor in the collection container	Automatic detection
Component sorting	Accidental mixing of plastic and metal components	Colour-coded trays according to material type	Visual guidance
Storage of used batteries	Improper or non-sealed storage	Labelled containers with lockable lids	Physical and visual inspection

6.4. Recommendations and Evaluation of the Impact of the Proposed Improvements

Based on the analysis performed, the following recommendations were formulated to optimize the process: the introduction of QR codes on reusable components, connected to a centralized database, in order to improve traceability; periodic training of personnel regarding dismantling and sorting procedures; equipping the facility with automatic optical systems for the accurate sorting of materials; the complete digitalization of the traceability system, including the automatic generation of reports for the competent authorities; and the definition of key performance indicators (KPIs) specific to each stage of the process, including processing time, recovery rate, hazardous liquid loss rate, and reusable component traceability.

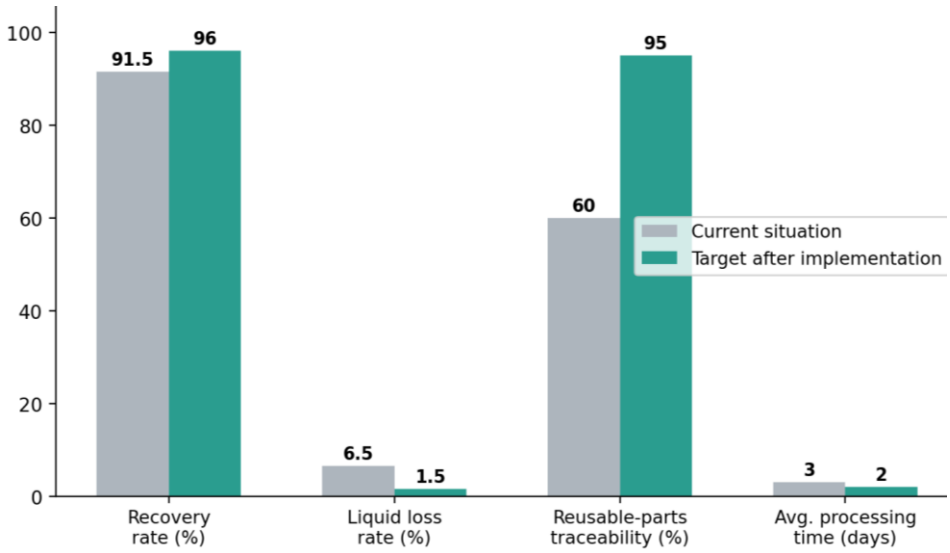

Fig. 8. *Key performance indicators of the case study before and after the implementation of the proposed improvement measures*

The evaluation of the impact of these measures, summarized in Figure 8, indicates the potential to increase the recovery rate from 91–92% to more than 95%, reduce the hazardous liquid loss rate from 5–8% to below 2%, improve the traceability of reusable components from approximately 60% to 95%, and reduce the average processing time per vehicle from 3 days to 2 days.

These results confirm that an integrated quality management approach can lead to sustainable long-term performance from economic, environmental, and operational safety perspectives.

7. Discussion: An International Comparative Perspective

Placing the Romanian case study within a broader international context reveals both common features and significant differences compared with other markets. Within the European Union, the gap between the regulated recovery target of 95% and the

THE ANNALS OF "DUNAREA DE JOS" UNIVERSITY OF GALATI
FASCICLE IX. METALLURGY AND MATERIALS SCIENCE
N°. 3 - 2026, ISSN 2668-4748; e-ISSN 2668-4756
Article DOI: https://doi.org/10.35219/mms.2026.3.06

actual average recovery rate achieved (89–91%) is mainly attributed to the difficulty of recovering Automotive Shredder Residue (ASR), a finding confirmed by studies conducted in the United Kingdom and the Netherlands, where investments in post-shredder technologies (PSTs) remain essential for achieving the final recovery target [17-18, 21].

In Asia, a comparative analysis of China and Japan shows an expected increase in recycling rates from approximately 90% to 98% over the coming years, supported by a combination of strict regulations, technological advances, and increased public awareness regarding resource recovery [13]. In emerging economies, such as India, Malaysia, and other developing countries, the literature identifies structural barriers - including the informality of the recycling sector, ambiguous legislation concerning vehicle deregistration, and the lack of authorized treatment infrastructure - as the main obstacles to the development of a functional circular economy in the automotive sector [10-12, 16]. These findings support the idea that the success of ELV recycling depends not only on the existence of an appropriate legal framework but also on the institutional capacity to implement and consistently enforce it.

Compared with these contexts, the case study conducted at the Romanian recycling centre indicates a level of compliance and operational performance comparable to European best practices, with a recovery rate exceeding 92%, significantly above the minimum legal threshold of 85% and approaching the European target of 95%. This performance supports the argument that the rigorous implementation of legal requirements, combined with quality management tools, can partially compensate for the technological limitations associated with the recovery of the ASR fraction by maximizing reuse and material recycling in the stages preceding shredding.

One area of research and industrial practice that will become increasingly important during the next decade is the recycling of electric vehicle batteries, a field in which the current recovery rate remains considerably below its technical potential due to the technological, economic, and regulatory barriers identified in the recent literature [23-27]. In the future, authorized ELV treatment centres will need to integrate specific procedures for the safe dismantling of traction batteries, separate from the conventional depollution process applied to internal combustion engine vehicles. This development will require additional investments in equipment, personnel training, and specific authorizations.

8. Conclusions and recommendations

The recycling of end-of-life vehicles (ELVs) represents an essential component of the transition towards a circular economy and a sustainable automotive sector, playing a major role in reducing environmental impacts, conserving natural resources, and improving economic efficiency. In the context of the continuous growth of the vehicle fleet and the increasing number of vehicles reaching the end of their service life, their proper management has become a priority at both the European and national levels.

The analysis carried out in this study highlighted the following main aspects:

• ISO 14040 and ISO 14044 provide the methodological framework for Life Cycle Assessment (LCA), enabling the identification of the stages with the greatest environmental impact and supporting the adoption of technical and organizational solutions aimed at reducing resource consumption and pollutant emissions.

• The legal and institutional framework in Romania is harmonized with the requirements of the European Union, particularly through the transposition of Directive 2000/53/EC, which establishes clear recycling and recovery targets, as well as specific responsibilities for economic operators, public authorities, and vehicle manufacturers.

• The technological workflow of an authorized treatment facility - including collection, depollution, dismantling, sorting, and recovery - makes it possible to recover a significant proportion of the vehicle mass, particularly ferrous and non-ferrous metals, thereby reducing the demand for primary raw materials and the climate impact associated with industrial production processes.

• The case study conducted at the recycling centre demonstrated the practical implementation of the ELV guidelines in an authorized facility, showing that, through complete depollution, dismantling focused on reuse, and appropriate material sorting, a recovery rate exceeding 90% can be achieved, approaching the European target.

• The integration of quality management tools into the management of the ELV treatment process contributes to the continuous improvement of performance, the reduction of environmental risks, and the enhancement of operational efficiency.

• The emerging challenges facing the sector - the recovery of Automotive Shredder Residue (ASR) and the recycling of electric vehicle batteries - remain the principal technological and regulatory barriers to achieving full circularity targets, requiring additional investments in post-shredder technologies and traction battery recycling infrastructure.

The recommendations formulated in this study focus on optimizing material sorting through automatic optical systems, fully digitalizing traceability using QR codes and centralized

databases, and increasing the reuse of components through the systematic cataloguing and commercialization of recovered parts. The implementation of these measures can generate multiple benefits, including reduced operating costs, increased revenues from the recovery of materials and reusable components, and improved compliance with environmental requirements.

In conclusion, the recycling of end-of-life vehicles represents not only a legal obligation but also a strategic opportunity for the development of a more efficient, responsible, and sustainable automotive sector. Through the integrated application of Life Cycle Assessment (LCA) standards, circular economy principles, and appropriate technical and quality management practices, recycling centres can make a significant contribution to environmental protection, resource conservation, and the sustainable development of the automotive industry, both in Romania and throughout the European Union.

References

[1]. ***, *ISO 14040:2006. Environmental management — Life cycle assessment — Principles and framework*, International Organization for Standardization, Geneva.
[2]. ***, *ISO 14044:2006. Environmental management — Life cycle assessment — Requirements and guidelines*, International Organization for Standardization, Geneva.
[3]. ***, *Directiva 2000/53/CE a Parlamentului European și a Consiliului din 18 septembrie 2000 privind vehiculele scoase din uz*, Jurnalul Oficial al Uniunii Europene, L 269, 21.10.2000.
[4]. ***, *Legea nr. 212/2015 privind modalitatea de gestionare a vehiculelor și a vehiculelor scoase din uz*, Monitorul Oficial al României.
[5]. ***, *Ordonanța de urgență a Guvernului nr. 92/2021 privind regimul deșeurilor*, Monitorul Oficial al României.
[6]. ***, *Regulamentul (CE) nr. 1907/2006 al Parlamentului European și al Consiliului din 18 decembrie 2006 privind înregistrarea, evaluarea, autorizarea și restricționarea substanțelor chimice (REACH)*, Jurnalul Oficial al Uniunii Europene, L 396, 30.12.2006.
[7]. ***, *European Commission. Communication COM(2020) 98 final — A New Circular Economy Action Plan for a Cleaner and More Competitive Europe*, Brussels, 2020.
[8]. ***, *European Parliament. Circular economy: deal on new EU rules for the automotive sector. Press release*, December 2025.
[9]. ***, *The EU's Circular Economy Action Plan (case study)*, Ellen MacArthur Foundation, Disponibil online.
[10]. Aggarwal A., *et al.*, *A global review of end-of-life vehicle management: India as a model for circular economy in automotive sector*, Journal of Environmental Management, 394, 127386, 2025.
[11]. ***, *A Review of Challenges and Opportunities for End-of-Life Vehicle Recycling in Developing Countries and Emerging Economies: A SWOT Analysis. Sustainability*, 13(9), 4918, 2021.
[12]. ***, *Insights into end-of-life vehicle recycling and its quality assessment systems in Malaysia reveals the need for a new stakeholder-centric approach for vehicle waste management*, Waste Management & Research, 2023.
[13]. Wang J., *et al.*, *Institutional, technology, and policies of end-of-life vehicle recycling industry and its indication on the circular economy — comparative analysis between China and Japan*, Frontiers in Sustainability, 2, 645843, 2021.
[14]. ***, *End-of-life vehicle management: a comprehensive review*, Journal of Material Cycles and Waste Management, Springer, 2019.
[15]. ***, *End-of-life vehicles (Netherlands recycling system case study, book chapter)*, ScienceDirect, 2024.
[16]. ***, *Evaluation of end-of-life vehicle recycling system in India in responding to the sustainability paradigm: an explorative study*, Scientific Reports, 13, 2023.
[17]. ***, *Strategies for the enhancement of automobile shredder residues (ASR) recycling: Results and cost assessment*, Waste Management, ScienceDirect, 2013.
[18]. ***, *Challenges around automotive shredder residue production and disposal*, Waste Management, ScienceDirect, 2017.
[19]. ***, *Material recycling for manufacturing aggregates using melting slag of automobile shredder residues*, PMC, 2023.
[20]. ***, *LIFE 3.0 project — Aim to realise 95% ELV recycling in the Netherlands by means of post-shredder technology*, European Commission LIFE Programme.
[21]. ***, *Automotive industry challenges in meeting EU 2015 environmental standard*, Resources, Conservation and Recycling, ScienceDirect, 2012.
[22]. Inglezakis V. J., Zorpas A. A., *Automotive shredder residue (ASR): a rapidly increasing waste stream waiting for a sustainable response*, WIT Transactions on Ecology and the Environment.
[23]. ***, *Robotic removal and collection of screws in collaborative disassembly of end-of-life electric vehicle batteries*, PMC, 2025.
[24]. Daniela Spasova, *et al.*, *Comparative Analysis of the Mechanical Properties of Polymer Matrix Composites Reinforced with Fiberglass Fabric*, TEM Journal, vol. 10, issue 4, p. 1745-1750, 2021.
[25]. ***, *Moving towards a circular economy: a systematic review of barriers to electric vehicle battery recycling*, Journal of Cleaner Production / ScienceDirect, 2025.
[26]. ***, *Barriers to electric vehicle battery recycling in a circular economy: an interpretive structural modeling*, ScienceDirect, 2024.
[27]. ***, *Progress, challenges and opportunities in recycling electric vehicle batteries: a systematic review*, Recycling (MDPI), 11(6), 230, 2025.
[28]. ***, *IDDRI. Aligning decarbonization, circularity and competitiveness in Europe's automotive industry*, 2025.
[29]. ***, *International Aluminium Institute. Aluminium recycling saves 95% of the energy needed for primary aluminium production*, 2024.
[30]. ***, *Stena Recycling. The value of recycling metals for sustainability*, 2025.
[31]. Daniela Spasova, *et al.*, *Analysis of failure causes of S135 drill pipe*, Materials Today: Proceedings, 59, 3, p. 1719-1725, 2022.
[32]. ***, *U.S. Energy Information Administration. Recycling is the primary energy efficiency technology for aluminum and steel manufacturing*, 2014.
[33]. ***, *European Parliament - Legislative Train Schedule. New circular economy action plan (vehicle circularity regulation)*, 2025.

THE ANNALS OF "DUNAREA DE JOS" UNIVERSITY OF GALATI
FASCICLE IX. METALLURGY AND MATERIALS SCIENCE
N°. 3 - 2026, ISSN 2668-4748; e-ISSN 2668-4756
Article DOI: https://doi.org/10.35219/mms.2026.3.07

STUDIES AND RESEARCH ON THE INFLUENCE OF CLEANING PRODUCTS ON THE SURFACE QUALITY OF OCULAR PROSTHESES

Antonia DINESCU, Beatrice TUDOR
"Dunarea de Jos" University of Galati, Romania
e-mail: beatrice.tudor@ugal.ro

ABSTRACT

The paper presents a study on the influence of different cleaning products on the quality of ocular prostheses. For cleaning, tap water, still water, chlorhexidine and artificial tears were used. The pH of the cleaning solutions was determined and a microscopic analysis of the surface of the samples was performed to observe how the solution used and the method of drying the prosthesis, respectively, air drying or wiping with a napkin, influenced the quality of its surface.

KEYWORDS: ocular prosthesis, cleaning solutions, surface quality

1. Introduction

Ocular prosthesis is a preferred method in cases where one eye has lost its natural appearance. The ocular prosthesis is custom-made, based on the colour of the person's other eye [1, 4].

Proper care of the ocular prosthesis ensures a healthy cavity and increases the lifespan of the prosthesis.

Ocular prostheses require special maintenance because they are in direct contact with the patient's anatomical areas and bodily fluids. The maintenance of such a prosthesis requires very rigorous hygiene because the patient is exposed to daily atmospheric pollution [2].

Over time, the surface of the ocular prosthesis collects proteins and impurities. Proper care ensures a healthy orbit and increases the lifespan of the prosthesis.

2. Experimental procedure

Several cleaning solutions, plain water, tap water, chlorhexidine and artificial tears were studied and their pH was measured (Figure 1).

The data obtained for the pH of cleaning solutions are presented in Table 1.

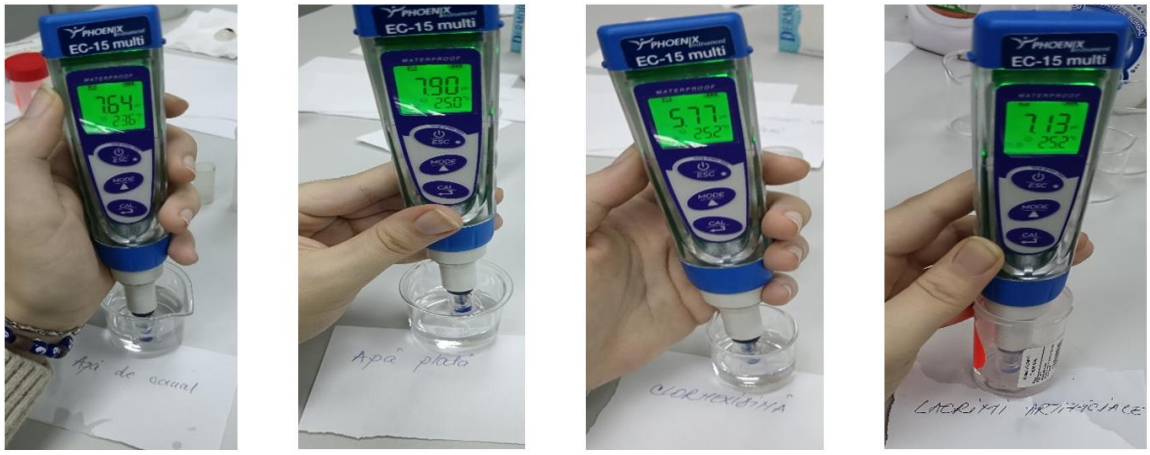

a b c d

Fig. 1. *pH determination: a) tap water, b) still water, c) chlorhexidine, d) artificial tears*

THE ANNALS OF "DUNAREA DE JOS" UNIVERSITY OF GALATI
FASCICLE IX. METALLURGY AND MATERIALS SCIENCE
No. 3 - 2026, ISSN 2668-4748; e-ISSN 2668-4756
Article DOI: https://doi.org/10.35219/mms.2026.3.07

Table 1. *Physical properties of cleaning solutions used in experimentation*

Determinations	Tap water	Still water	Chlorhexidine	Artificial tears
pH	7.6	7.9	5.7	7.1
Conductivity	-39.7 mV	-62.0 mV	-71.2 mV	-11 mV
Salinity	608 mg/L	142,4mg/L	3,3 g/L	7 mg/L

Chlorhexidine, compared to other solutions, has an acidic pH. In this case, it is used for cleaning, which can damage the acrylic layer, and is recommended only if the eye cavity presents certain inflammations and requires a deeper cleaning [3].

The highest pH was found in tap water, as it is considered strongly alkaline, due to the presence of bicarbonate ions in the aquifer.

Tap water has a pH of 7.64 and a salinity of 608 mg/L, which makes it not recommended.

The most effective and neutral cleaning solution is artificial tears.

The use of alcohol and abrasive detergents can cause permanent and irreparable damage to the surface [5].

3. Microscopic study of the surface quality of ocular prostheses

The microscopic analysis of the surface of the prostheses was performed using the KERN optical microscope assembly, consisting of a computer and a monitor (Figure 2).

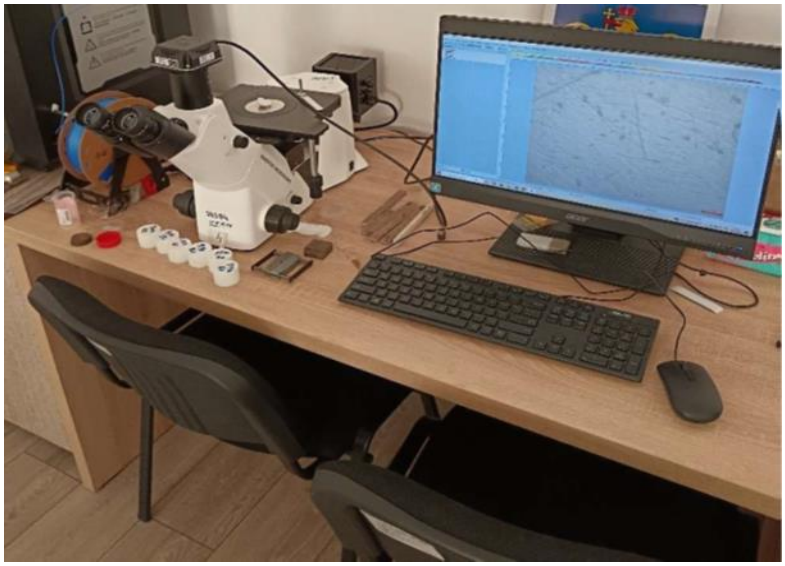

Fig. 2. *The optical microscope, model KERN*

The 50 W halogen unit ensures optimal illumination of the samples.

The technical data of the KERN optical microscope are:

- Infinite optical system;
- Five-position relay;
- 30° inclined viewing position;
- Diopter compensation on both eyepieces;
- Dimensions: L×W×H: 747×271×379 mm;
- Net weight approx. 12.968 kg.

The surfaces of the samples, including the control sample, the sample after air drying, and the sample dried with a napkin, were analysed under a microscope.

The image obtained under the optical microscope of the ocular prosthesis surface, before being subjected to research, is presented in Figure 3.

The sample after using the cleaning solution was dried and studied under the optical microscope.

First, the sample was dried in air, then analysed under the microscope, (Figure 4a). The sample for which a napkin was used for drying is shown in Figure 4b.

THE ANNALS OF "DUNAREA DE JOS" UNIVERSITY OF GALATI
FASCICLE IX. METALLURGY AND MATERIALS SCIENCE
N°. 3 - 2026, ISSN 2668-4748; e-ISSN 2668-4756
Article DOI: https://doi.org/10.35219/mms.2026.3.07

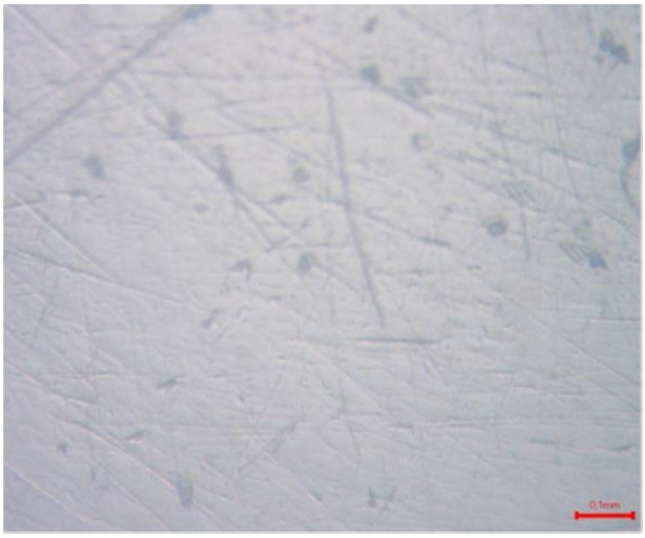

Fig. 3. *Surface of the initial sample, 100x magnification*

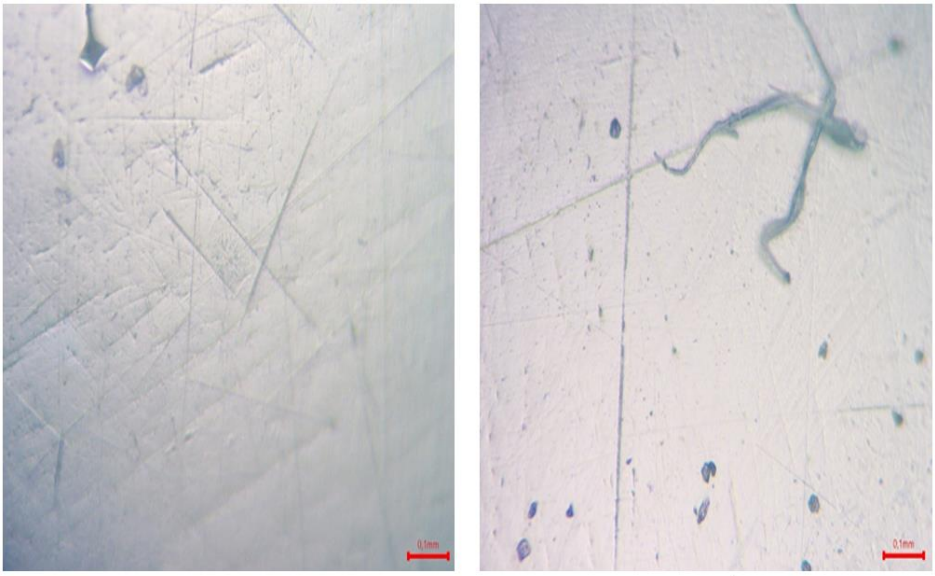

a b

Fig. 4. *a) Air-dried sample, b) Tissue-dried sample*

From the point of view of surface quality, it is observed that the air-dried sample shows fewer scratches on the surface, while the sample dried with a napkin showed a more pronounced deterioration in surface quality, as well as adhesions of cellulose fibres on the surface of the prosthesis.

Following this study, artificial tears and air-drying are recommended for cleaning the ocular prosthesis.

4. Results and Discussion

Studies and recommendations on ocular prosthesis maintenance solutions have also been conducted by Osborn and Hettler. According to them, the recommended cleaning agents are mild soap, baby shampoo, and a hard contact lens cleaner.

In this paper, the study was based on measuring the pH of the cleaning solutions and performing a microscopic analysis of the ocular prosthesis surface to assess the quality of its surface after the use of these solutions.

The prosthesis surface was also analysed microscopically based on the drying method used after cleaning - specifically, drying with a tissue versus air drying.

Regular tap water should be avoided, as it is a potential source of contamination. Alcohol and

THE ANNALS OF "DUNAREA DE JOS" UNIVERSITY OF GALATI
FASCICLE IX. METALLURGY AND MATERIALS SCIENCE
Nº. 3 - 2026, ISSN 2668-4748; e-ISSN 2668-4756
Article DOI: https://doi.org/10.35219/mms.2026.3.07

abrasive cleaning products should not be used, as they can cause permanent and irreparable damage to the prosthesis surface [5].

5. Conclusions

The study of the influence of cleaning products on the quality of ocular prostheses, as well as their maintenance method, was done by determining the pH of some products for cleaning and maintaining prostheses, namely plain water, tap water, chlorhexidine and artificial tears.

The highest pH was obtained with still water, because it is considered strongly alkaline, due to the presence of bicarbonate ions in the aquifer.

Tap water has a pH of 7.64 and a salinity of 608 mg/L, which does not make it recommended.

The most effective and neutral cleaning solution is artificial tears.

The use of alcohol and abrasive detergents can cause permanent and irreparable damage to the surface of the prosthesis.

The microscopic analysis of the surface of the ocular prosthesis was performed using a KERN optical microscope in order to observe changes in the quality of the surface following the use of cleaning products.

After microscopic analysis, in terms of surface quality, we observe that the air-dried sample obtained a less scratched surface, while the tissue-dried sample showed a more pronounced deterioration in surface quality and adhesion of fibres from the tissue to the surface of the prosthesis.

It is recommended to dry the ocular prosthesis outdoors.

The longevity of such a prosthesis can last from 2 to 6 years, depending on the patient's age, occupation (job) and care for it.

References

[1]. Francesco Baino, *Biomaterials for orbital implants and ocular prostheses: Overview and future prospects*, Acta Biomaterialia, p. 24, 2014.

[2]. Alexander C. Rokohl, *Prosthetic eye care – The current state of the art*, Progress in Retinal and Eye Research, p. 32, 2025.

[3]. Sergio Bonaque-Gonzáleza, *Recommendations for post-adaption care of an ocular prosthesis: A Review*, Contact Lens and Anterior Eye, p. 5, 2015.

[4]. ***, https://www.kern-sohn.com/shop/en/products/optical-instruments/fluorescence-microscopes/tobn-142-a/.

[5]. Osborn K. L., Hettler D., *A survey of recommendations on the care of ocular prostheses*, Optometry 81, p. 142-145, 2010.

THE ANNALS OF "DUNAREA DE JOS" UNIVERSITY OF GALATI
FASCICLE IX. METALLURGY AND MATERIALS SCIENCE
Nº. 3 - 2026, ISSN 2668-4748; e-ISSN 2668-4756
Article DOI: https://doi.org/10.35219/mms.2026.3.08

THE INFLUENCE OF HUMIDITY ON THE HARDNESS OF ACRYLIC OCULAR PROSTHESES

Antonia DINESCU, Beatrice TUDOR
"Dunarea de Jos" University of Galati, Romania
e-mail: beatrice.tudor@ugal.ro

ABSTRACT

The paper presents a study on the influence of humidity on the hardness of ocular prostheses made of acrylic material. To carry out this study, a determination of the hardness of the ocular prosthesis was made after immersion in artificial tears for seven weeks, performing several determinations of the hardness values of the acrylic material. Since the ocular prosthesis is subject to the humidity of the ocular cavity and external atmospheric factors, the study also focused on determining the humidity of the acrylic material from which the prosthesis is made.

KEYWORDS: ocular prosthesis, hardness, humidity, acrylic material

1. Introduction

An ocular prosthesis is a device that occupies the anterior part of an orbit, and is designed to aesthetically repair an eye lost due to trauma, congenital anomalies, irreparable injuries, or tumours.

The ocular prosthesis is used in cases where an eye has lost its functionality and natural appearance or even in the congenital absence of the eye. The ocular prosthesis is custom-made for each patient, depending on the colour of the person's other eye [1].

Humidity plays a key role in the wear and maintenance of ocular prostheses. The ocular cavity must be kept properly lubricated to prevent irritation and discomfort, while the prosthesis itself should not be allowed to dry out excessively when not worn, as the material may deteriorate.

Because the ocular prosthesis is subject to the moisture of the ocular cavity and external atmospheric factors, there are changes in the properties of the prosthesis [7].

Hardness is a physical property of a material that indicates its resistance to permanent deformation or scratching under the action of an external force.

This can be measured by various methods, such as penetration or indentation measurement, and is important in assessing the quality and performance of materials in a wide range of industrial and engineering applications.

Hardness determination is the process of evaluating a material's resistance to permanent deformation, especially breaking or scratching, under the action of an external force.

The hardness of ocular prostheses refers to their resistance to scratches and other forms of damage.

A scratched or damaged surface can affect the patient's health and quality of life. Factors that influence the quality of the ocular prosthesis are: the material from which the prosthesis is made, the covering with the protective material, humidity and last but not least, care and handling [8, 9].

2. Materials and methods

The production of ocular prostheses underwent a great development with the introduction of polymethylmethacrylate (PMMA) implants 75 years ago.

PMMA stands for polymethyl methacrylate. It is a synthetic polymer that is widely used because it is transparent, lightweight, and has good mechanical properties.

Prostheses made of polymethylmethacrylate (PMMA), are a polymerized product of a mixture of acrylic powder (mainly PMMA) and liquid monomer (mainly methyl acrylate (MMA)) [7].

For the use of the material in ocular prostheses, polymerization must be carried out for a long enough time to prevent residual monomer, which is toxic and can cause adverse reactions, but polymerization for too long can change its colour.

There are two types of orbital implants, porous and non-porous. In the past, non-porous implants were made of glass, rubber, and metals such as steel, gold, or silver, but nowadays the most commonly

THE ANNALS OF "DUNAREA DE JOS" UNIVERSITY OF GALATI
FASCICLE IX. METALLURGY AND MATERIALS SCIENCE
N°. 3 - 2026, ISSN 2668-4748; e-ISSN 2668-4756
Article DOI: https://doi.org/10.35219/mms.2026.3.08

used materials are silicone, acrylic, and polymethyl methacrylate (PMMA).

Due to its biocompatibility, processability, and durability, PMMA is the standard material for plastic ophthalmic prostheses [8].

3. Determination of ocular prosthesis hardness after immersion in artificial tears

To simulate a real natural environment, namely the placement of a prosthesis in the ocular cavity, and to study the behavior of the acrylic material and how humidity can influence the hardness of the prosthesis, a prosthesis was immersed in artificial tears (purified water, sodium borate, sodium chloride) for a period of 7 weeks.

The determination of the prosthesis hardness was performed at 2, 5 and 7 weeks, with the automatic digital Micro-Vickers HDT-VS1D INSIZE device, from the laboratory of the Faculty of Engineering (Figure 1).

The technical specifications of the device are: load 0.5 (kg), replacement time 10 (s), objective at 40x, brightness of 4 [2].

The stages of carrying out the determinations consist of:

- placing the prosthesis on the device support;
- fixing the specifications used for all determinations;
- focusing the area and marking the length and width;
- data generation, for the control sample (before immersion) and the determinations after 2, 5 and 7 weeks (Figure 2).

Fig. 1. *Micro-Vickers HDT-VS1D INSIZE hardness tester*

The data obtained from determining the hardness of the prosthesis were summarized in Table 1 and graphically represented in Figure 3.

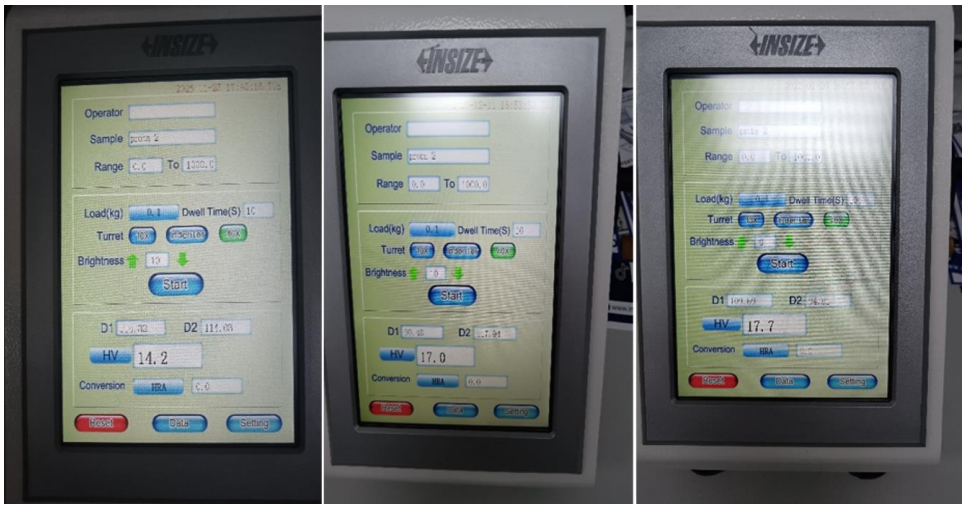

Fig. 2. *Data generated by the device during the research*

Table 1. *Ocular prosthesis hardness*

Weekly	D1 (distance 1)	D2 (distance 2)	HV (hardness)
Initial	114.32	114.03	14.2
2 weeks	90.48	117.94	17
5 weeks	105.3	118.4	17.7
7 weeks	109.69	94.81	17.7

THE ANNALS OF "DUNAREA DE JOS" UNIVERSITY OF GALATI
FASCICLE IX. METALLURGY AND MATERIALS SCIENCE
N°. 3 - 2026, ISSN 2668-4748; e-ISSN 2668-4756
Article DOI: https://doi.org/10.35219/mms.2026.3.08

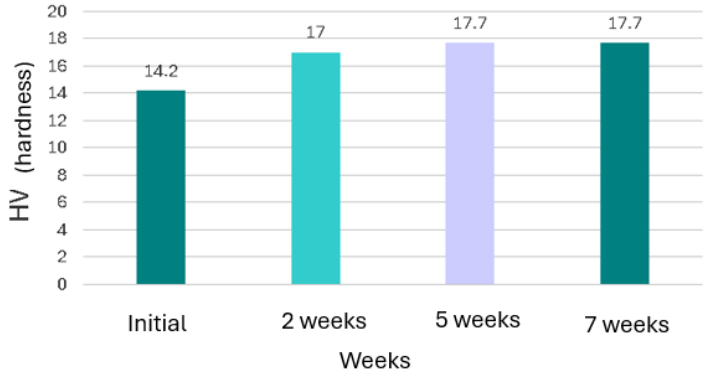

Fig. 3. *Evolution of hardness as a function of immersion time*

Following these determinations, we found that the hardness values increased with the immersion time of the ocular prosthesis in the artificial tear solution. The hardness value remained constant after five weeks of immersion, obtaining the same hardness values in the seventh week of immersion.

The increase in hardness compared to the initial un-immersed sample is due to the capillary channels existing in the ceramic powder used to make the prosthesis being filled with the liquid absorbed by the material [3].

After the capillaries were filled, the material became saturated and the hardness increased, remaining constant after week 5. Therefore, in the final determinations, in week 7, the hardness values remained identical to those measured in week 5.

4. Determining the humidity content of acrylic material

Humidity can have a significant impact on PMMA, causing physical and chemical changes, which can affect the performance and appearance of the ocular prosthesis.

Humidity can have different effects on PMMA. One of the most noticeable things is absorption. PMMA is a hydrophilic polymer, which means it can absorb water from the environment.

Since during the research, it was found that the ocular prosthesis immersed in artificial tears absorbed some of the liquid, the moisture content of the sample was calculated.

Swelling capacity is the property of a material to absorb water or a solvent and consequently, to increase its volume, an essential property for evaluating the hydration behavior of polymers, hydrogels and paint films.

The initial dry sample was weighed, and then after the sample was immersed in artificial tears, several weightings were made over the course of 7 weeks, until it was found that the mass of the sample remained constant.

Fig. 4. *Weighing the sample*

The humidity content of the sample was calculated with the formula:

$$U = \frac{M_f - M_i}{M_i} * 100\ [\%]$$

where: M_f -final mass; M_i - initial mass; U – humidity.

$$U = \frac{2{,}814 - 2{,}554}{2{,}554} * 100 = 10.18\ \%$$

After weighing the sample, it was found that at the beginning of the prosthesis immersion in artificial tears, the mass of the sample increased, and after five weeks of immersion it remained constant.

Due to water absorption, the release of residual monomer may increase, this leads to continued polymerization of the resin and higher microhardness values [1].

For the sample immersed in artificial tears, a microscopic analysis of the surface was also performed, on which the solution drops and the trace left by the hardness determination device can be observed (Figure 5).

THE ANNALS OF "DUNAREA DE JOS" UNIVERSITY OF GALATI
FASCICLE IX. METALLURGY AND MATERIALS SCIENCE
No. 3 - 2026, ISSN 2668-4748; e-ISSN 2668-4756
Article DOI: https://doi.org/10.35219/mms.2026.3.08

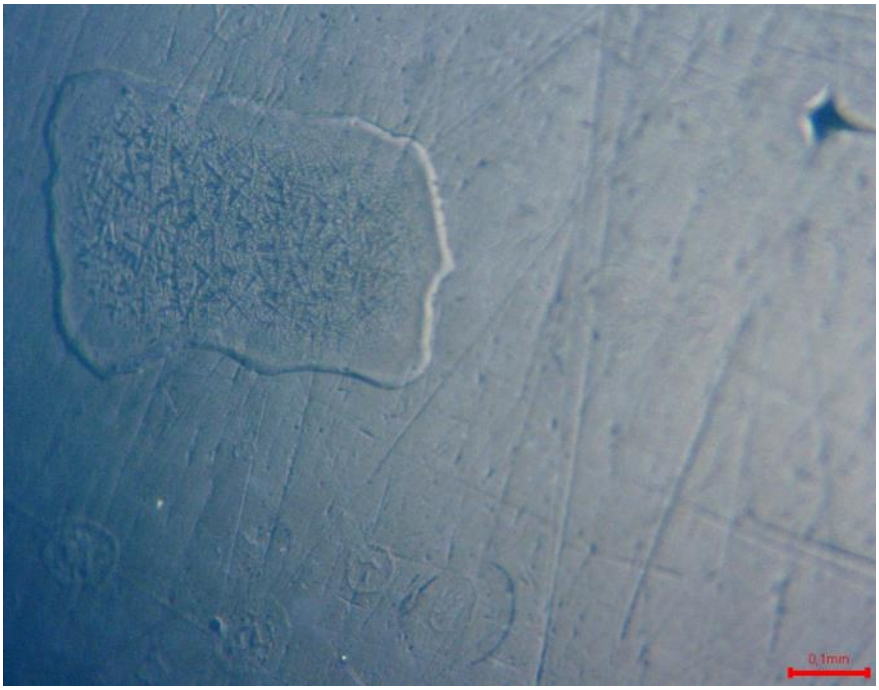

Fig. 5. *Sample surface immersed in artificial tears*

5. Results and discussion

The lifespan of an ocular prosthesis is between 2 and 6 years in an adult, depending on the patient's age, occupation, care of the prosthesis, and the materials it is made of.

Any rough or scratched surfaces can be easily removed by polishing. These aspects make the PMMA ocular prosthesis a very durable prosthesis.

A PMMA prosthesis has the advantage that it can be adjusted at any stage of the manufacturing process, both in terms of colour and shape. If an incorrect estimate has been made, the shape can be adjusted later [7].

This property makes the production of acrylic ocular prostheses easily accessible for fine-tuning. If minor adjustments to the shape are necessary over time, additional material can be pressed or the model can be locally planned to adapt to the new situation of the socket.

Despite these advantages, a disadvantage of PMMA is that it is hydrophobic. Water tends to adhere in droplets rather than form a smooth tear film that would evenly wet the surface of the prosthesis, as would the natural eye.

Once the PMMA implant has absorbed moisture, this can lead to physical changes, such as dimensional change. The prosthesis may swell as water molecules take up space in the polymer structure [9].

Water absorption can affect the mechanical properties, dimensional stability, and overall durability of the material.

Studies are being conducted to increase the wettability (hydrophilicity) of the artificial eye. Among the promising options is adjusting the proportion of ethylene glycol dimethacrylate (EGDMA) already available in the liquid monomer of the PMMA mixture. The addition of polyethylene glycol makes the surface more hydrophilic and reduces bacterial adhesion [8].

6. Conclusions

The influence of humidity on the hardness of acrylic ocular prostheses was determined out after immersing the sample in artificial tears.

The study revealed that the hardness values of the ocular prosthesis immersed in artificial tears increased with immersion time, from 14.2 HV initially, to 17.7 HV in the fifth week, after which the hardness value remained constant until the end of the experiment, namely seven weeks.

The capillary channels existing in the ceramic powder used to make the prosthesis were filled with the liquid absorbed by the material, which led to an increase in hardness compared to the initial un-immersed sample.

After filling the capillaries, the material became saturated and the hardness increased, remaining constant after the fifth week. Therefore, in the final determinations, in the seventh week, the hardness

values remained identical to those measured in the fifth week.

For the sample immersed in artificial tears, the moisture content was calculated, obtaining a moisture content of 10.18%, which led to higher microhardness values, due to water absorption. The release of residual monomer leads to the continuous polymerization of the resin, resulting in increased hardness.

References

[1]. Alexander C. Rokohl, *Prosthetic eye care – The current state of the art*, Progress in Retinal and Eye Research, p. 32, 2025.
[2]. *,** https://insize.co.id/beli/insize-hdt-vs1d-micro-vickers-hardness-tester-iso-6507-motor-driven-magnification-400x/.
[3]. Francesco Baino, *Biomaterials for orbital implants and ocular prostheses: Overview and future prospects*, Acta Biomaterialia, p. 24, 2014.
[4]. Emanuele de Oliveira, *Properties of Acrylic Resin For CAD/CAM: A Systematic Review and Meta-Analysis of In Vitro Studies*, Prosthodontics, p. 9, 2021.
[5]. Sergio Bonaque-Gonzáleza, *Recommendations for post-adaption care of an ocular prosthesis: A Review*, Contact Lens and Anterior Eye, p. 5, 2015.
[6]. Tamara Mladenovic, *Application of Silicone in Ophthalmology: A Review*, materials, p. 27, 2024.
[7]. Parr G. R., *et al.*, *Surgical considerations in the prosthetic treatment of ocular and orbital defects*, J. Prosthet. Dent. 49, p. 379-385, 1983.
[8]. Pine K. R., *et al.*, *The response of the anophthalmic socket to prosthetic eye wear*, Clin. Exp. Optom., 96, p. 388-393, 2013.
[9]. Laiseca J., *et al.*, *Prótesis oculares cirugía reconstructiva de cavidades*, Madrid. Ed. Prensa Hispanoamericana, 1991.

MANUSCRISELE, CĂRŢILE ŞI REVISTELE PENTRU SCHIMB, PRECUM ŞI ORICE CORESPONDENŢE SE VOR TRIMITE PE ADRESA:

MANUSCRIPTS, REVIEWS AND BOOKS FOR EXCHANGE COOPERATION, AS WELL AS ANY CORRESPONDANCE WILL BE MAILED TO:

LES MANUSCRIPTS, LES REVUES ET LES LIVRES POUR L'ECHANGE, TOUT AUSSI QUE LA CORRESPONDANCE SERONT ENVOYES A L'ADRESSE:

MANUSCKRIPTEN, ZIETSCHRITFTEN UND BUCHER FUR AUSTAUCH SOWIE DIE KORRESPONDENZ SID AN FOLGENDE ANSCHRIFT ZU SEDEN:

After the latest evaluation of the journals by the National Center for Science Policy and Scientometrics (**CENAPOSS**), in recognition of its quality and impact at national level, the journal will be included in the B^+ category, 215 code (http://cncsis.gov.ro/userfiles/file/CENAPOSS/Bplus_2011.pdf).

The journal is already indexed in:
DOAJ: https://doaj.org/
SCIPIO-RO: http://www.scipio.ro/web/182206
EBSCO: http://www.ebscohost.com/titleLists/a9h-journals.pdf
Google Academic: https://scholar.google.ro
Index Copernicus: https://journals.indexcopernicus.com
Crossref: https://search.crossref.org/

The papers published in this journal can be viewed on the website: http://www.gup.ugal.ro/ugaljournals/index.php/mms

Name and Address of Publisher:
Contact person: Prof. Dr. Eng. Elena MEREUȚĂ
Galati University Press - GUP
47 Domneasca St., 800008 - Galati, Romania
Phone: +40 336 130139
Fax: +40 236 461353
Email: gup@ugal.ro

Name and Address of Editor:
Ș. L. Dr. Eng. Marius BODOR
"Dunarea de Jos" University of Galati, Faculty of Engineering
111 Domneasca St., 800201 - Galati, Romania
Phone: +40 336 130208
Phone/Fax: +40 336 130283
Email: marius.bodor@ugal.ro

AFFILIATED WITH:

- THE ROMANIAN SOCIETY FOR METALLURGY
- THE ROMANIAN SOCIETY FOR CHEMISTRY
- THE ROMANIAN SOCIETY FOR BIOMATERIALS
- THE ROMANIAN TECHNICAL FOUNDRY SOCIETY
- THE MATERIALS INFORMATION SOCIETY (ASM INTERNATIONAL)

Edited under the care of the FACULTY OF ENGINEERING

Annual subscription (4 issues per year)

Fascicle DOI: https://doi.org/10.35219/mms

Volume DOI: https://doi.org/10.35219/mms.2026.3

Editing date: 15.09.2026
Number of issues: 200
Printed by Galati University Press (accredited by CNCSIS)
47 Domneasca Street, 800008, Galati, Romania